# ASSESSMENT OF THE SOURCES AND BIODEGRADATION POTENTIAL OF HYDROCARBONS AND NAPHTHENIC ACIDS IN AN OIL SAND END PIT LAKE

# ASSESSMENT OF THE SOURCES AND BIODEGRADATION POTENTIAL OF HYDROCARBONS AND NAPHTHENIC ACIDS IN AN OIL SAND END PIT LAKE

By: Mohamed El-Waraky, B.Sc., M.Sc.

A Thesis Submitted to the School of Graduate Studies in Partial Fulfillment of the Requirements for the Degree Doctor of Philosophy

McMaster University

Doctor of Philosophy (2021) McMaster University, Hamilton, Ontario

Earth, Environment, and Society

TITLE: Assessment of the sources and biodegradation potential of hydrocarbons and naphthenic acids in an oil sand end pit lake

AUTHOR: Mohamed El-Waraky, B.Sc., M.Sc. (Alexandria University, University of Tulsa)

SUPERVISOR: Prof. Gregory F. Slater

NUMBER OF PAGES: xi, 127

## Abstract

Reclamation efforts have been ongoing to manage and reclaim the mined-out pits and the tailings produced from oil sands production. Syncrude has implemented the first end pit lake, known as Base Mine Lake (BML), by using water cap tailing technology (WCTT). The lake was constructed by capping 186 million $m^3$ of fluid fine tailings (FFT) with a 65 million $m^3$ water column from OSPW (oil sand process water) and Beaver Creek Reservoir (BCK) forming a total depth of 48m. The organic compounds present within the FFT, such as hydrocarbons and naphthenic acids (NAs), are residual organic matter from the bitumen after extraction or the diluent naphtha. Consumption of residual organic compounds through syntrophic fermentation coupled to methanogenesis in the FFT generates methane that can be transported upward to the water column through advection, diffusion or ebullition. The oxidation of the methane by methanotrophs depletes the oxygen concentration in the water column. An integral part of the success of the WCTT is the demonstration of stable oxygen conditions in the water column that would facilitate the biodegradation of residual organic matter which can be transported into the water column from the FFT. This dissertation utilized multidimensional chromatography to assess the residual organic compounds in BML and evaluate their biodegradation potential. Assessment of the hydrocarbons in the FFT indicated that the low molecular weight compounds are being biodegraded at shallower intervals and potentially driving methane production. The analysis of NAs distribution in BML revealed that additional input of NAs into the water column, through biodegradation of hydrocarbons or advection from the FFT, is being balanced by ongoing microbial degradation in the water column. Evaluation of the biodegraded metabolites revealed that hydrocarbons are anaerobically degraded in the FFT while NAs are aerobically degraded in the water column of BML. This study demonstrates that studying the molecular fingerprint distribution of residual organic compounds using multidimensional chromatography indicated that biodegradation is managing the release of compounds of concern, and could help assess the success of reclamation and obtaining certification.

**Acknowledgment**

First and foremost, I offer my gratitude to Allah (God) for giving me the guidance and strength to complete this work. I would like to thank my supervisor Dr. Greg slater for the opportunity to conduct this research in his lab. Dr. Slater, thanks for your teachings, guidance, patience, and support throughout the years. You always gave me all the time I needed for guidance, provided me with all the necessary training and resources to conduct my research, and always encouraged me to implement my own ideas. My academic research and laboratory skills have significantly developed since I started my Ph.D. under your supervision.

I would like to thank my collaborators at WHOI, Dr. Chris Reddy and Robert Nelson for inviting me to their institute to get trained on working on the GC×GC, and use the instrument to run my samples. I would also like to thank Dr. Lesley Warren's research group for collecting and providing us with the majority of the samples that were used for this study. My appreciation also goes to my committee members Dr. Jim Smith, Dr. Sang-Tae Kim, and Dr. Karl Jobst for your advice and guidance throughout the years of my study.

A special thanks go to Jennie Kirby, our lab technician, for training me on all the lab techniques that I needed to accomplish my study. I would also like to thank all my lab colleagues who I had the chance to share great memories and learn from. Thanks to Dr. David Bowman, Dr. Allyson Brady, Dr. Kelly Martin, Sian Ford, Corey Goad, Resia San Pedro, Robbyn Darling, Rebecca Hale, Jacob Bothen, Mike Dereviankin, Chris Chang, Hayden Bao, Johnny Pereira, and Wang Chenlu.

Last but not least, I would like to thank my family for their inspiration, support, and guidance. Thank you, mom, Dr. Fadia Hossin, thanks dad, Dr. E-Saeed El-Waraky, and thanks to all my siblings, Dr. Ahmed El-Waraky, Dr. Allaa El-Waraky, and LT. Mahmoud El-Waraky.

## Preface

This thesis consists of three manuscripts (chapters two, three, and four). Chapters two were in collaboration with Dr. Chris Reddy and Robert Nelson (WHOI), and Dr. Lesley Warren (University of Toronto). Chapters three and four were in collaboration with Dr. David Bowman (Brock University), Dr. Chris Reddy and Robert Nelson (WHOI) and Dr. Lesley Warren (University of Toronto). Mohamed El-Waraky completed all analyses, designed the study, and interpreted the data with assistance from Dr. Greg Slater. Mohamed El-Waraky wrote the manuscripts with editing from Dr. Greg Slater, Dr. David Bowman, Dr. Chris Reddy, Robert Nelson, and Dr. Lesley Warren. Jennie Kirby Dr. David Bowman helped with training on performing the extraction methods for these studies. Dr. David Bowman also helped with the GC×GC analysis and provided his intellectual input regarding data processing and interpretation. Dr. Chris Reddy and Robert Nelson helped with training on using the GC×GC in addition to analyzing the samples on their instrument at WHOI. Dr. Lesley Warren helped with collecting and providing us with the majority of the samples used in all three studies.

## Table of contents

## List of Figures

### Chapter one



### Chapter two

**Chapter three**

**Chapter four**

## List of Tables

### Chapter two



### Chapter three



### Chapter four

## Chapter one: Introduction

While society is working towards alternative energy sources, oil remains the main source used for the foreseeable future. Canada is considered one of the largest oil-producing countries in the world with estimated recoverable oil reserves of 178 billion barrels (National Petroleum Council, 2011). Most of this oil is recovered from bitumen, a heavily degraded black crude oil with high viscosity, present as oil sands which is a mixture of sand, clay, and bitumen (Redelius, 2009). Canada's bitumen reserves are located in the Athabasca, Cold Lake, and Peace River deposits of northwestern Alberta (National Petroleum Council, 2011). The oil production from these reserves has resulted in the production of an estimated 1.18 trillion liters of tailings (Natural resources defense council, 2016), with the expectation of an increase in production to meet the market demands. Regulations require that oil sands producers develop methods to manage tailings and to reclaim mined landscapes to conditions similar to before mining (Natural resources defense council, 2016).

The bitumen of the oil sands requires special treatments for recovery due to its high viscosity. It is either extracted from the subsurface through in-situ drilling or surface mining (Government of Alberta, 2015). The greatest landscape impacts are associated with surface mining that accounts for about 20% of oil sands extraction and issued for shallower deposits where huge trucks excavate oil sand deposits that are composed of bitumen mixed with clay and sand (Government of Alberta, 2015). Oil sands are carried to processing facilities where the bitumen is separated from the sand using the hot water Clark method generating a large volume of waste tailings as a product of this process (Government of Alberta, 2015).

As a result of the no-discharge policy applied by the Canadian government, the tailings are disposed to huge settling basins, near on-site facilities, that are known as oil sand tailing ponds, covering an area of about 220 $km^2$ in Alberta (Slingerland et al., 2019). Due to the presence of hazardous chemicals in the tailing ponds reclamation efforts to manage landscape sites and associated tailings have been implemented.

## 1- BaseMine lake overview

In 2012, Syncrude commissioned the first end pit lake, BaseMine lake (BML), to demonstrate the effectiveness of water cap tailings technology (WCTT) for sequestering fluid fine tailings (FFT) present in tailing ponds and achieving reclamation certification for mining sites. The lake (Figure 1) was constructed by discharging 186 million $m^3$ ($Mm^3$) of fluid fine tailings (FFT) derived from Syncrude tailings ponds into WIP (west in pit). The FFT is composed of silt, clay, residual bitumen, and diluent naphtha from the extraction of the oil sands.

After tailings deposition was completed in 2012, the FFT was capped with 65 $Mm^3$ of water column derived from oil sands process water (OSPW) and freshwater from Beaver Creek Reservoir. The total depth of the lake after commissioning was 48 m that constitutes 40 m of FFT in addition to 8 m of water column. Due to the consolidation of FFT and release of pore water, the water column depth has continued to increase over time (Carrier et al. 2007). However, the rate of FFT consolidation hasn't been consistent throughout the lake. Thus, the change in the depth of the FFT water interface (FWI) from 2012 to 2018 was reported to average between 1-6 m throughout the lake (Syncrude Canada Ltd., 2019). The lake is subjected to thermal stratification in the summer and winter following spring and fall turn over events (Kathryn A. Dompierre and Barbour, 2016).

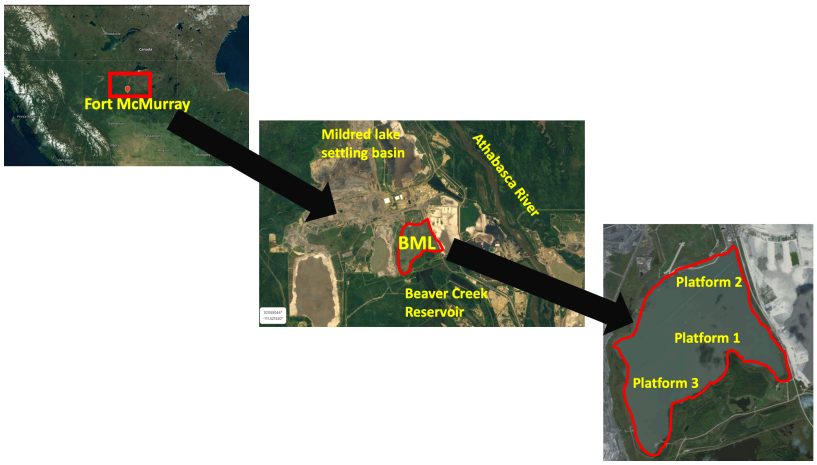


Figure 1: A satellite image that shows the study site ( BML) enclosed by a red outline in every panel.

The residual organic compounds within the FFT, diluent naphtha and residual bitumen, were recognized as potential substrates for methane generation through syntrophic fermentation coupled to methanogenesis (Siddique et al., 2011, 2007, 2006). The diluent naphtha hydrocarbons are composed of light molecular weight alkanes ( $C_6$-$C_{10}$) and mono aromatics that are readily degraded (Siddique et al., 2006), while the bitumen is a heavily degraded oil that is composed of recalcitrant compounds such as the branched and cyclic hydrocarbons and organic biomarker compounds (Yang et al., 2011). Oil sand tailings methanogenic microcosm studies amended with naphtha components were shown to generate methane after a short lag phase of two to five weeks (Siddique et al., 2007, 2006). Other studies that amended the tailings microcosm with the more bio-resistant bitumen components also showed methane generation, but after a more lengthy lag phase between 180 to 630 days (Siddique et al., 2020, 2011). Methane production was reported from oil sand tailings microcosms, which included BML inoculates amended with naphthenic acids (NAs), after a lengthy lag phase of 175 days (Holowenko et al., 2001a). Oil sand tailing microcosm studies imply that residual naphtha components are consumed first by microbiota followed by NAs and bitumen components. Thus, continuous methane production can be expected to occur from the residual organic compounds in BML even after the depletion of naphtha components.

Oxygen in the water column of BML was found to be strongly impacted by methane release early in the lake development (Arriaga et al., 2019; Risacher et al., 2018a). Understanding the potential for current and future methane release, as a result of hydrocarbons biodegradation, is important in evaluating oxygen levels in the water column. Additionally, the aerobic water column allows for aerobic degradation of toxic compounds that might be released from the FFT and provides a further barrier to the release of these compounds to the environment. The oxygen levels in the water column, in addition to the toxicity of residual organic compounds released from the FFT, are the key parameters that control the water quality of BML. An understanding of the identity of residual organic compounds in BML, their biological cycling, and their potential release into the water column will help evaluate the oxygen and toxicity parameters. Assessment

of the water quality through these parameters can validate WCTT in BML demonstration, and help inform future managerial decisions towards the reclamation of BML.

Thus, this dissertation will focus on studying the characteristics and biodegradation potential of hydrocarbons that can lead to methane and impacting oxygen levels in BML. As NAs are the most hazardous compounds within the residual organic compounds in BML, this dissertation also focused on studying their sources and biodegradation potential in the water column of BML.

## 2- Background

### 2.1 residual organic compounds

The residual organic compounds present in the FFT include naphtha used during extraction and residual bitumen that contains a range of petroleum hydrocarbons (Siddique et al., 2006; Yang et al., 2011) and naphthenic acids (NAs) (Bowman et al., 2020). Hydrocarbons are composed entirely of hydrogen and carbon atoms and are originally formed from the diagenetic alteration of organic matter that was subjected to heat and pressure through burial (Meinschein, 1969; Peters et al., 2005; Simoneit, 2002). Hydrocarbons can be divided according to polarity (Figure 2), where the non-polar fraction includes the saturates, aromatics, and biomarkers, while the polar fraction contains the asphaltenes and oxygenated compounds (Peters et al., 2005).

For the non-polar fraction, the saturated hydrocarbons ( Figure 2) are compounds that have a linear or a cyclic carbon chain with no double bonds such as alkanes, branched alkanes, and cyclic alkanes (Meinschein, 1969; Peters et al., 2005). The aromatic hydrocarbons are compounds that possess a benzene ring that has alternating single and double bonds (Meinschein, 1969; Peters et al., 2005). Finally, biomarkers are multicyclic and branched compounds such as steranes, terpanes and hopanes (Peters et al., 2005). These compounds are widely used in fingerprinting studies as they retain the hydrocarbon skeleton of their original precursor (Meinschein, 1969; Peters et al., 2005; Simoneit, 2002).

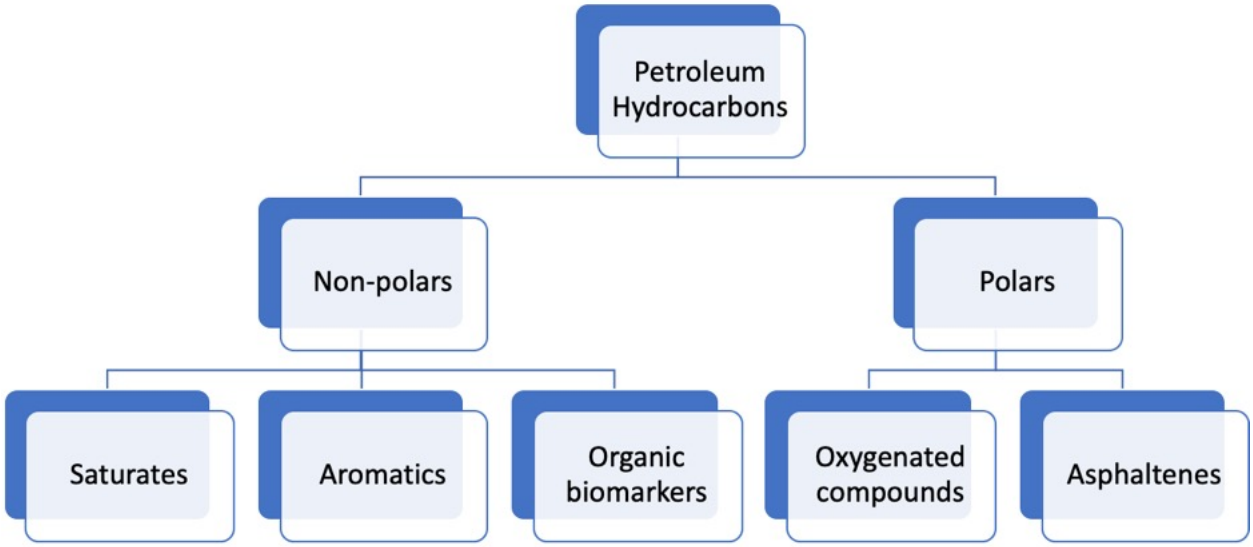


Figure 2: Fractions of petroleum hydrocarbons (Peters et al., 2005).

For the polar fraction, the asphaltenes are compounds with complex structures that contain aliphatic side chains, multiple aromatic and cyclic rings along with heteroatoms such as oxygen, nitrogen, and sulfur (Peters et al., 2005; Koshlaf and Ball, 2017). The asphaltenes are found in a higher percentage in highly biodegraded oils such as the bitumen of the oil sands (Peters et al., 2005). Other polar compounds are the oxygenated metabolic intermediates, from hydrocarbons biodegradation, that are composed of alcohols, aldehydes, ketones and carboxylic acids (Aeppli et al., 2012; Hall et al., 2013; Head et al., 2003).

Carboxylic acids, which can also be known as naphthenic acids (NAs), are composed of a non-polar hydrocarbon chain bonded directly to an array of branched, acyclic, mono or polycyclic polar carboxylic acids that coexist with other heteroatomic ( O, N, S) chemical species (Figure 3) (Eickhoff and Laroulandie, 2010; Kindzierski et al., 2012). The general formula for NAs is $C_nH_{2n+z}O_2$ , where n represents the carbon number and Z relates to the number of cyclic rings (Eickhoff and Laroulandie, 2010; Kindzierski et al., 2012). These compounds are generally found as a constituent of petroleum or they can be produced as metabolites from hydrocarbons biodegradation (W Meredith et al., 2000; Tissot and Welte, 1985).

Due to their high solubility they become concentrated in OSPW as the water is recycled in the extraction of oil sands (Eickhoff and Laroulandie, 2010). As a result of their associated toxicity, their release into the environment is a matter of concern (Eickhoff and Laroulandie, 2010). The toxicity of NAs is a result of their narcosis mode of action where the non-polar hydrocarbon chain can enter cell and cause disruption (Brown and Ulrich, 2015). An increase in the carboxylic acid content of NAs compounds was found to result in a reduction in toxicity (Frank et al., 2009). Also high molecular weight NAs were reported to be less toxic than low molecular weight NAs (Clemente and Mackinnon, 2004; Holowenko et al., 2002). Thus, understanding the structural configuration of NAs and other residual organic compounds is key towards assessing their toxicity.

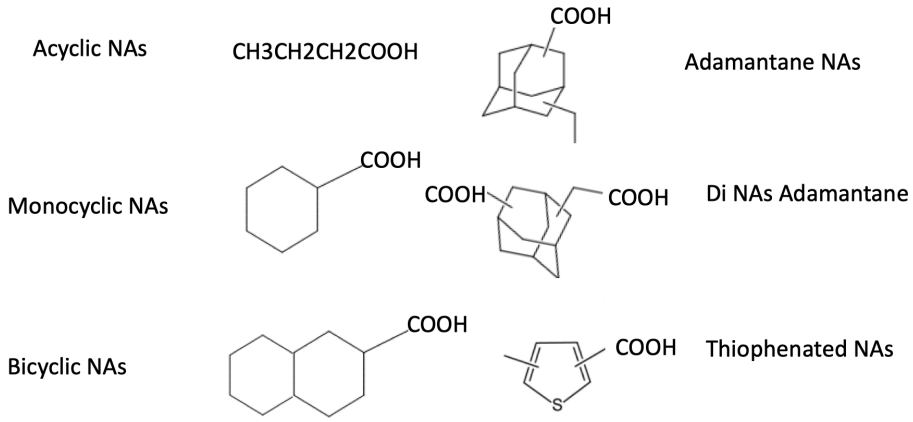


Figure 3: chemical structure of NAs (Eickhoff and Laroulandie, 2010).

## 2.2 Biodegradation

Biodegradation is a process by which microorganisms degrade organic compounds in the environment through various microbial process in order to obtain the energy necessary for their growth, and subsequently detoxify their environment (Head et al., 2010, 2003). These microorganisms can either use respiration or fermentation process to breakdown a wide range of organic compounds. Fermentation breaks down complex organic compounds into simpler byproducts without using an external terminal acceptor (Schulz, 2006). However, fermentation releases much less energy than respiration (Jones, 1985; Konhauser et al., 2002).

In respiration, the electrons from an electron donor (organic substrate) are transferred to a NAD molecule that is reduced to NADH (Reece and Campbell, 2002). Then, the NADH is processed through the electron transport chain where it finally releases the electrons to be captured by an external terminal electron acceptor (TEA) (Reece and Campbell, 2002).

Microbial respiration process encompass aerobes (that uses $O_2$ as a TEA) and anaerobes which use ( $N_2$, Mn, Fe, $SO_4$, $CO_2$ as a TEA)(Kendall et al., 2003; Lovley and Chapelle, 1995; Röling et al., 2003). Aerobes that uses $O_2$ as their TEA yield the highest energy, and they have the ability to oxidize a wide range of organic compounds (sugars, amino acids, aromatics, long-chain fatty acids) (Damien et al., 2011; Konhauser et al., 2002; Lovley and Chapelle, 1995). After the $O_2$ is consumed by microorganisms, nitrate reducers convert $NO_3$ to $N_2$ releasing less energy than aerobes from the oxidation of organic compounds (Konhauser et al., 2002). This is followed by a further lowering of the redox potential in the subsurface where Fe and Mn reducers convert their TEA Mn(IV) and Fe(III) to Mn (II) and Fe (II) respectively (Konhauser et al., 2002). These organisms yield less energy from the oxidation of long-chain fatty acids and aromatics (Lovley and Chapelle, 1995). Subsequently, when Mn and Fe are exhausted sulfate reducers prevails reducing their TEA $SO_4$ to $S^-$. Finally, when all the TEAs in the subsurface are depleted methanogens can prevail (Kendall et al., 2003; Konhauser et al., 2002; Lovley and Chapelle, 1995). Fermentation play an important role in methanogenic conditions by which the initial hydrocarbon substrates are metabolized by syntrophic fermentative organisms into metabolic intermediates as acetate and hydrogen (Figure 4) (Gieg et al., 2014). The acetate can be subsequently metabolized by acetate fermentation while hydrogen can be used as the electron donor in CO2 reduction pathway (Gieg et al., 2014).

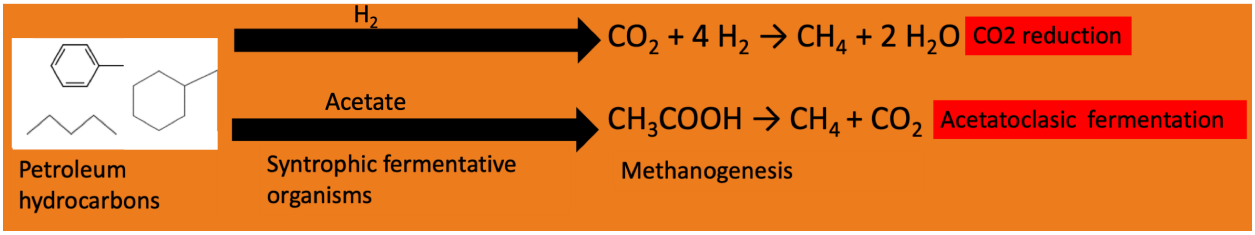


Figure 4: Pathway for methane production from the biodegradation of petroleum hydrocarbons through syntrophic fermentation followed by methanogenesis (Gieg et al., 2014).

### 2.2.1 Biodegradation effect on compositional structure of Hydrocarbons

Previous studies on the biodegradation process in petroleum reservoirs and oil spills have revealed that the biodegradation of hydrocarbon compounds proceeds in a semi-quasi stepwise order according to the number of carbon atoms, cyclic rings, alkyl substituents, and steric hindrances (Conan, 1984; Palmer, 1993; Peters, 1993; Wenger and Isaksen, 2002; Head et al., 2003; Peters et al., 2005). This removal sequence initiates with the degradation of n-alkanes, and then as the extent of biodegradation increases the acyclic isoprenoids, cycloalkanes, aromatics, and biomarkers compounds are degraded respectively (Bailey et al., 1973; Conan, 1984; Palmer, 1993; Peters, 1993; Wenger et al., 2002; Wenger and Isaksen, 2002).

The n-alkanes are the most susceptible compounds to biodegradation within the saturate fraction due to their lower molecular weight and absence of branching that hinders microbial attack (Bailey et al., 1973; Connan, 1984; Volkman et al., 1984; Williams et al., 1986; Palmer, 1993; Wenger et al., 2002; Wenger and Isaksen, 2002). With the removal of n-alkanes, cycloalkanes and acyclic isoprenoids become preferentially enriched before they are depleted with increasing the extent of biodegradation (Connan, 1984; Palmer, 1993; Wenger et al., 2002). The resistance of these compounds increases with increasing the number of alkyl substituents (Solano-Serena et al., 1999). The most bio-resistant saturates are the highly branched alkanes such as the trimethyl alkanes (Solano-Serena et al., 1999).

The extent of biodegradation of aromatic compounds decreases with increasing the number of aromatic rings or alkyl substituents (Palmer, 1993; Solano-Serena et al., 1999; Volkman et al., 1984; Wang et al., 2001, 1998). The most susceptible aromatics to biodegradation are compounds with single aromatic rings such as BTEX and alkylbenzenes (Palmer, 1993; Wang et al., 2001, 1998; Williams et al., 1986). As the biodegradation levels increase compounds that have more than one aromatic ring such as naphthalene and dibenzothiophene are degraded (Palmer, 1993; Wang et al., 2001, 1998). Alkylated aromatics with more than two rings, such as

methyl phenanthrene, are the most bio-resistant aromatics that only degrade in highly degraded oils (Rowland et al., 1986; Volkman et al., 1984; Wang et al., 2001, 1998).

The hydrocarbon biomarker compounds start to degrade in moderate to severally degraded oils after the removal of acyclic isoprenoids and aromatics (Bost et al., 2001; Palmer, 1993; Seifert and Moldowan, 1979; Williams et al., 1986). The general order for removal of these compounds starts with the degradation of steranes followed by hopanes, and diasteranes (Connan, 1984; Palmer, 1993; Seifert and Moldowan, 1979). Hopanes are degraded through demethylation process that forms new compounds known as 25-norhopanes (Seifert and Moldowan, 1979;Volkman et al., 1983; Brooks et al., 1988; Trendel et al., 1990; Peters and Moldowan, 1991). The most resistant compounds are tricyclic terpanes and tri-aromatic steroids which could still be found in severely degraded oils (Connan, 1984; Palmer, 1993; Seifert and Moldowan, 1979). The biodegradation extent of hydrocarbons can be determined from studying the ratios between the more preferential degraded compounds as n-alkanes to the less preferentially degraded as the organic biomarkers. Additionally, the biodegradation extent can be determined from studying the biodegradation metabolites generated as a result of hydrocarbons biodegradation.

### 2.2.2 Biodegradation production of oxygenated intermediate metabolites

The biodegradation of hydrocarbons results in the production of a succession of intermediate oxygenated compounds that are composed of alcohols, aldehydes, ketones and fatty acids via aerobic or anaerobic process (Aeppli et al., 2012; Hall et al., 2013; Head et al., 2003). Each hydrocarbon can show different types of oxygenated intermediates due to the different mechanisms and chemical reactions that each microbial process uses in order to degrade these hydrocarbons. Oxygenated compounds are identified in studies that track the production of new metabolic intermediates through incubating hydrocarbons under lab conditions (Aitken et al., 2017; Watkinson and Morgan, 1990; West et al., 2014). Intermediate metabolites produced can then be related to their hydrocarbon precursor through chemical structure comparisons.

The most known hydrocarbon metabolites are those identified in surface systems via aerobic biodegradation of petroleum hydrocarbons. The petroleum hydrocarbons are transformed in these aerobic systems through hydroxylation, dehydrogenation, hydrolysis or oxygenolytic ring cleavage to form alcohols, ketones, aldehydes, and fatty acids (Fritsche and Hofrichter, 2008; Rojo, 2009; Varjani, 2017; Watkinson and Morgan, 1990). Then the fatty acids produced (that can also be called NAs) are further metabolized by β-oxidation to form acetyl-CoA that can enter the intermediatory metabolism of the cell through the tricarboxylic acid cycle (TCA) (Fritsche and Hofrichter, 2008; Rojo, 2009; Varjani, 2017; Watkinson and Morgan, 1990).

Previous studies were able to successfully identify the oxygenated metabolites products in the aerobic biodegradation of alkanes, cycloalkanes, and aromatics (Das and Chandran, 2011; Olajire and Essien, 2014; Rojo, 2009; Sierra-Garcia and de Oliveira, 2013; van der Heul, 2009). The oxygenated metabolites from the biodegradation of alkanes follow the pathway outlined in figure 5. The primary n-alkane alcohols are recognized as a product of the oxidation of alkanes by mono or dioxygenase enzymes at the terminal position in the chain through hydroxylation reactions. The corresponding aldehyde is identified as a product of dehydrogenation of the previously formed alcohols. Finally, fatty acids or naphthenic acids can form as a product of hydrogenation reaction to the previously formed aldehydes. Another type of secondary alcohol can be produced through the oxidation of the parent alkane sub-terminally. Other oxygenated compounds related to this secondary alcohol such as secondary ketones implied that this was another microbial pathway for the aerobic degradation of alkanes. The secondary ketone formed in this subterminal pathway is transformed to acetyl ester which is found to form primary alcohol that can then be oxidized to fatty acids. The methyl groups of alkylated cycloalkanes are activated through a terminal or subterminal carbon as noted for the alkanes above. Non-alkylated cycloalkanes show resistance to biodegradation due to the absence of an exposed methyl group. Nonetheless, cyclohexanol has been identified as an initial oxidative product of cyclohexane, that can be further transformed to cyclohexanone as a result of dehydrogenation, followed by adipic acid formation through hydrolysis and ring opening (van der Heul, 2009; Rojo, 2009). The oxygenated aromatics produced via aerobic pathways are aromatic acids that are transformed into acetyl coA via opening of the aromatic ring through ortho position (o-cleavage) (van der Heul, 2009; Rojo, 2009; Das and Chandran, 2011; Olajire and Essien, 2014). Another

transformation pathway recognized is the cleavage of the aromatic ring at the meta position which yield final intermediates acetaldehyde and pyruvate to be incorporated into the TCA (Sierra-Garcia and de Oliveira, 2013; Varjani, 2017).

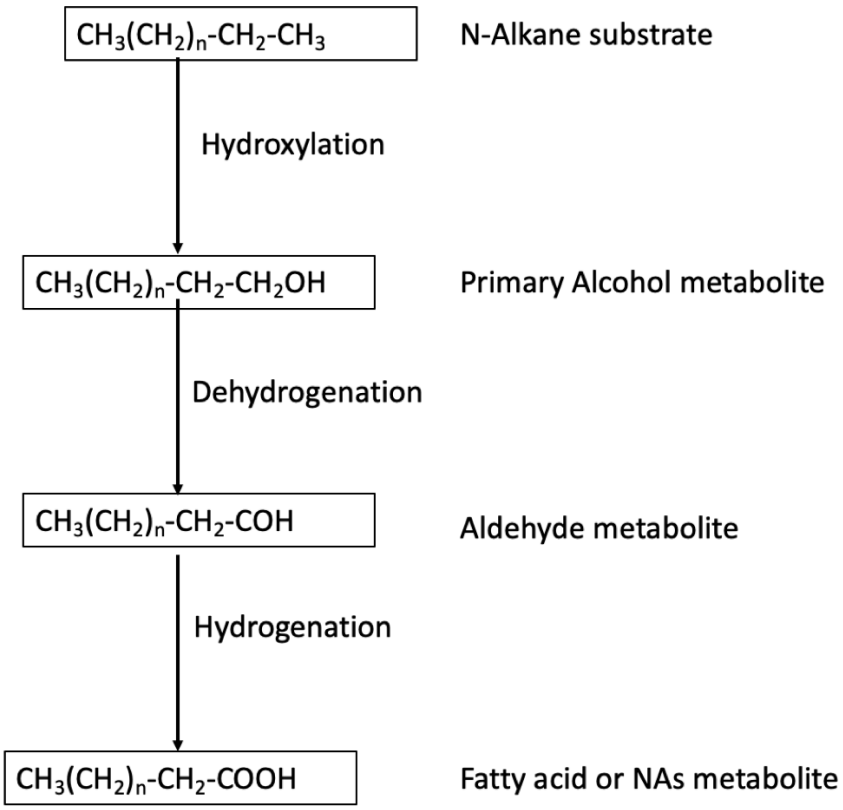


Figure 5: Metabolites produced from the aerobic biodegradation of NAs. Modified from (Fritsche and Hofrichter, 2008).

The aerobic metabolic pathways of the alkanes and aromatics generate fatty acids (also known as NAs) after a succession of oxidative steps as noted in Figure 5. It has been shown that biodegradation level correlates with high acidity levels and formation of NAs compounds as products of hydrocarbon degradation (Behar and Albrecht, 1984; Jaffé and Gallardo, 1993a; W. Meredith et al., 2000). Previous studies have attempted to resolve specific groups of NAs compounds that were found to be generated in biodegraded oils (Behar and Albrecht, 1984;

Bennett and Abbott, 1998; Jaffé and Gallardo, 1993a; Jaffe and Gardinali, 1990; Mackenzie et al., 1981; Meredith et al., 2000; Watson et al., 2002). For instance (Jaffé and Gallardo, 1993b) have found that biodegraded oils were characterized by a high abundance of tricyclic acids, while acyclic acids were not significantly different between degraded and non-degraded oils. Another study by (Meredith et al., 2000) has found that $C_{30}$-$C_{32}$ hopanoid is directly related to increasing biodegradation levels, however, their concentration decreased in very high degraded oils which, might imply their further transformation.

The NAs metabolites produced from the biodegradation of hydrocarbons can be further degraded by microorganisms through the ß and/or α pathways producing hydroxylated NAs as intermediate metabolites as outlined by (Quagraine et al., 2005). The biodegradation pathways for NAs were studied only via aerobic routes, nonetheless, a study by (Beam and Perry, 1974) have noted that long-chain carboxylic acids can be biodegraded via the β-oxidation pathway under anaerobic settings. Hydroxylated NAs are formed via the (β-oxidation) pathways through a sequence of oxidations at the β-Carbon. The terminal product of this pathway is another carboxylic acid with two fewer carbons than its parent. Another pathway through ω oxidation was also noted by (Johnson et al., 2012) where the aerobic transformation of alkylated aromatic acids generated Di NAs through the carboxylation of the exposed methyl group. Few studies have attempted to identify hydroxylated NAs (Han et al., 2008; Rowland and Jones, et al., 2011; Wang et al., 2013). For instance, a study by (Han et al., 2008a) identified hydroxylated NAs as metabolites produced from incubating OSPW and commercial NAs. Additionally, $C_{19}$ and $C_{20}$ monoaromatic hydroxyl acids have been identified by (Rowland et al., 2011). Furthermore, (Wang et al., 2013) detected oxygenated NAs from oil field waters that represent the $O_3$ NAs and $O_4$ NAs species, the latter was also identified in OSPW (Lengger et al., 2013).

In contrast to the aerobic biodegradation pathways, the metabolic process for the biodegradation via anaerobic pathways is not fully understood yet. Nonetheless, there have been several metabolites identified that could be traced back to their original precursor. Several studies have detected alkyl succinates metabolites (Figure 6) during the biodegradation of alkanes and aromatics (Widdel and Rabus 2001, Boll 2002, Dan and chandran 2011). These studies hypothesized that the succinates were formed as a result of an activation at the sub-terminal

carbon of n-alkanes by the addition of fumarate(Matthias Boll et al., 2002; Das and Chandran, 2011; Widdel and Rabus, 2001). Also, benzyl succinates were reported to be produced as a result of activation of toluene through the addition to fumarate (Widdel and Rabbus, 2001). Another pathway for the biodegradation of alkanes and aromatics was found to occur through carboxylation (Widdel and Rabbus, 2001). For instance, a study by (So et al., 2003) found that fatty acids with even numbers of carbon were produced from the biodegradation of alkanes with an odd number of carbons through a carboxylation reaction followed by the removal of two sub-terminal C2 units from the alkane chain to yield a fatty acid one-carbon unit shorter than the parent alkane. Naphthalene was also reported to biodegrade through carboxylation reactions forming naphthoate and the tetrahydro naphthoic acids metabolites (Atiken, 2004).

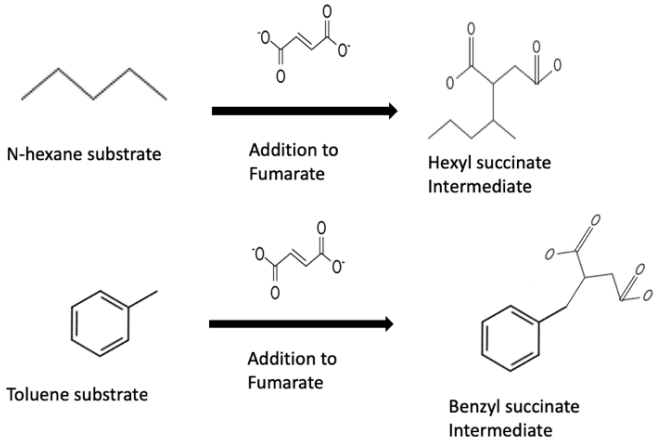


Figure 6: Alkyl succinates metabolites identified from the activation to fumarate reactions for saturates and aromatics. Modified from (Widdel and Rabus, 2001).

Since aerobic conditions prevail in the water column of BML, it would be expected to detect NAs metabolites, generated from the NAs that were transported from the FFT, if biological processing is active in the water column of BML (Figure 6). While, as a result of the anaerobic conditions in the FFT, biodegradation occurrence would be confirmed through the detection of the succinates or carboxylated signature anaerobic metabolites for hydrocarbons and NAs degradation (Figure 7). The presence of complex mixtures of petroleum hydrocarbons and NAs within the heavily degraded bitumen and residual naphtha in BML in addition to the potential

presence of aerobic and/or anaerobic biodegradation metabolites indicate that there are highly complex mixtures of residual organic compounds in BML.

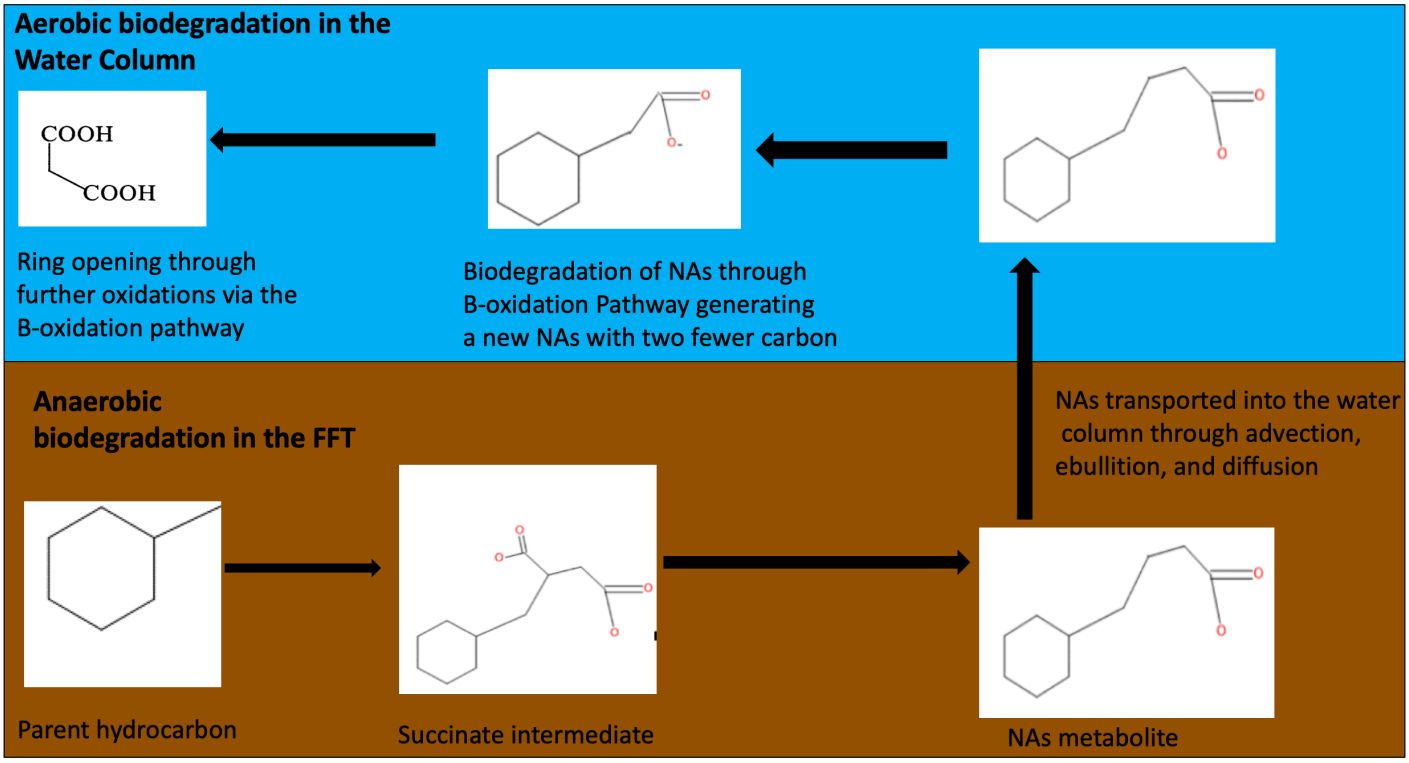


Figure 7: A diagram that shows the metabolites generated from the biodegradation of hydrocarbons in the FFT and NAs water column of BML.

### 2.3- Resolving complex mixtures using multi-dimensional chromatography

Heavily biodegraded environmental samples are not easily resolved using common analytical techniques due to the pronounced (unresolved complex mixture) UCM that dominates these samples. This UCM was first observed in 1970 (Blumer et al.,1970 ), and it appeared as a raised baseline hump of unresolved peaks in the chromatograph produced by conventional GC-MS. Since then, the UCM has been reported widely in petroleum contaminant studies, for example, (Cortes et al., 2012; Sutton et al., 2005; Volkman et al., 1984).

The analysis of hydrocarbons and NAs in the heavily biodegraded oil sand tailings was hampered due to the presence of the UCM in these samples. Previous studies from oil sand tailings focused on the analysis of NAs due to their associated toxicity. Preliminary work for the analysis of NAs used Fourier transform infrared spectroscopy (FTIR) to elucidate the carbonyl and carboxylic acids functional groups through measuring their monomer and dimer absorbances (Holowenko et al., 2001b). However, FTIR doesn't have the ability to distinguish NAs from any other compounds with a carboxylic acid moiety. Thus, this technique would be more suitable to estimate total acid extractable organic matter (Grewer et al., 2010). Subsequent analysis using gas chromatography- low-resolution mass spectrometry (GC-MS) was able to better elucidate structural features of NAs species as carbon number and Z families (Holowenko et al., 2002). However, due to the absence of reference standards for most NAs, misidentifications of the mass spectrum obtained by the low-resolution mass spectrometry were a disadvantage. The use of high-resolution mass spectrometry recently has enabled the unequivocal identification of NAs (Barrow et al., 2004; Headley et al., 2011). The advantage of high-resolution techniques is due to their ability to measure the m/z ratio in several decimal places, and thus provide the exact mass for the unknown compounds. The recent development of the GC×GC has enhanced structural elucidation of NAs compounds through the separation and identification of each individual isomer (Rowland et al., 2011; Wilde et al., 2015; Bowman et al., 2020). This feature was not achieved by the other analytical techniques. The identification of individual NAs isomers is crucial as the levels of toxicity differ among the isomers (Eickhoff and Laroulandie, 2010; Kindzierski et al., 2012).

The identification of unknown compounds resolved by the GC is performed through mass spectrum analysis. The confirmation of the compound identity is achieved through matching with a mass spectrum and a retention time of the standard of that compound. In the case of absence for an available standard tentative identification can be achieved through the comparison of the unknown compound mass spectrum with that of a mass spectra library or published mass spectrum of that compound. Tentative identifications can also be achieved through the interpretation of the mass spectrum through first hand principles.

The emergence of the GC×GC has increased our ability to identify complex compounds within the UCM in addition to enhanced isomer separation compared with the more conventional GC-MS technique. A conventional GC-MS and a GC×GC are able to separate and identify compounds through coupling a gas chromatograph to a mass spectrometer. A conventional GC-MS consists of an oven, a gas mobile phase, and a column with specific dimensions as a stationary phase. As the sample is injected in the injection port inside a GC it is volatilized and carried with the mobile gas phase through the column. Compounds are separated from the sample based on their difference in volatility (as they are heated inside the GC oven) and in polarity (as the compounds interact with the stationary phase). GC×GC system is better suited to resolve compounds within the UCM due to the introduction of another dimension in separation inside the gas chromatograph. The gas chromatograph of the GC×GC system as outlined by (Frysinger, 2002; Ong and Marriott, 2002; Stauffer et al., 2008; Vazquez-Roig and Pico, 2012) consists of two-serially connected columns, an oven, mobile phase, and a modulator. These two columns produce a two-dimension separation of the compounds with 2 retention times. As the sample is introduced into the GC×GC system, it's volatilized and carried with the mobile phase to be separated mainly according to the volatility of the compounds in the primary column. Then as the effluent passes through the column it's collected by a modulator that focuses the effluent and re-inject it to the secondary column after a fixed interval. The modulator consists of cold jets and hot jets, the cold jets trap and immobilize the effluent while the hot jets re-mobilize the effluent to be injected into the secondary column. This secondary column is short and the separation of the compounds is very rapid (5-15s) according to the polarity of compounds. The two-dimension separation provided by the GC×GC system allows for enhanced separation of complex mixtures compared to a conventional GC-MS system.

Since method establishment the GC×GC has been successfully used for resolving hydrocarbons from complex mixtures in heavily biodegraded oil. For instance, a study by (Frysinger et al., 2002) used the GC×GC system in order to resolve individual branched alkanes, cycloalkanes and alkylated aromatics of the UCM of petroleum-contaminated sediments that was not resolved by a conventional GC-MS. Furthermore, (Hall et al., 2013) studied the deep horizon spill using GC×GC TOFMS in order to resolve the specific hydrocarbons that were disappearing from the oil within the reservoir along the spill pathway. The study successfully resolved a suite of

hydrocarbons that were degrading in this order: alkylcyclopentanes, alkylcyclohexane, alkylated bicyclic saturated compounds, tricyclic terpanoids, alkylbenzenes, and $C_{19}$-$C_{26}$ steranes and diasteranes. The GC×GC system has also been successfully applied to resolve the chemical composition and isomer fingerprint of NAs from oil sand tailings that have been previously ambiguous (Rowland et al., 2011a; Rowland et al., 2011b; Bowman et al., 2014; Wilde et al., 2015). These studies were successfully able to identify the following NA compounds: acyclic n-acids, methyl branched acids, acyclic isoprenoids acids, cyclohexyl acids, perhydroindan acids, and decalin acids, tricyclic diamondoid, thiophene, indane, tetralin, cyclohexane, and adamantane type acids. Thus, all these studies imply that the GC×GC system has a clear advantage in resolving compounds from complex mixtures.

## 3- Research summary and objectives

The overall objective of this thesis was to evaluate the sources, distribution, and biodegradation potential of hydrocarbons and NAs in BML. The assessment of the biodegradation potential of hydrocarbons in BML was critical due to their potential role in methane generation. Evaluation of NAs stability and sources of input to the water column of BML was significant due to their associated toxicity. Since the biodegradation of hydrocarbons and NAs is associated with the production of oxygenated metabolic intermediates, the identification of such intermediates provides direct evidence for biodegradation occurrence in BML. A summary of all the projects of this study is provided below:

**Project (1) Initial Characterization of the identity and biodegradation potential of the hydrocarbons in fluid fine tailings underlying an oil sand end pit lake:** The objective of this study was to characterize the hydrocarbons that can be contributing to methanogenesis and consequential methanotrophy within BML. The hypothesis was that biological processing of low molecular weight hydrocarbons could be driving methane production relatively close to the FFT-water interface. Hydrocarbons were initially analyzed in bulk, then a GC×GC system was used to resolve branched alkanes and alkylated aromatics. The biodegradation potential of all

hydrocarbon constituents was analyzed to elucidate their contribution towards methane generation in the lake.

**Project (2) Evaluation of NAs sources and biodegradation potential in an oil sand end pit lake:** The objective of the study was to determine sources of NAs into the water column of BML and their potential for biodegradation. The hypothesis was that the distinct NA fingerprints of FFT porewater, OSPW, bitumen can elucidate sources of NAs and their biodegradation potential in the water column of BML. The identification and tracking of a suite of NAs species and their isomers using the high resolving power of the GC×GC enabled the evaluation of NAs stability in the water column of BML. Additionally, monitoring the NAs identified in the water column across FFT samples elucidated the contribution of advective diffusive input into the water column, while the comparison to OSPW samples assessed the contribution from remnant OSPW during initial lake filling, and comparison to bitumen samples evaluated the potential input of recently produced NAs from in-situ hydrocarbons biodegradation.

**Project (3): Evaluation of biodegradation in an oil sand end pit lake using oxygenated metabolic intermediates:** The GC×GC system was used to identify signature metabolic intermediates indicative of biodegradation occurrence either via aerobic routes in the water column or anaerobic routes in the FFT of BML. The hypothesis was that these metabolites were generated and altered as a result of the intrinsic biodegradation of hydrocarbons and NAs in BML.

**References:**


Aitken C. M., Head I. M., Jones D. M., Rowland S. J., Scarlett A. G. and West C. E. (2017) Comprehensive two-dimensional gas chromatography-mass spectrometry of complex mixtures of anaerobic bacterial metabolites of petroleum hydrocarbons. *J. Chromatogr. A*. Available at: http://dx.doi.org/10.1016/j.chroma.2017.06.027.

Arriaga D., Nelson T. C., Risacher F. F., Morris P. K., Goad C., Slater G. F. and Warren L. A. (2019) The co-importance of physical mixing and biogeochemical consumption in controlling water cap oxygen levels in Base Mine Lake. *Appl. Geochemistry* **111**, 104442. Available at: https://doi.org/10.1016/j.apgeochem.2019.104442.

Bailey N. J. ., Jobson A. . and Rogers M. (1973) Bacterial degradation of crude oil: comparaison of field and experimental data. *Chem. Geol.* **11**, 203–221.

Barrow M. P., Headley J. V., Peru K. M. and Derrick P. J. (2004) Fourier transform ion cyclotron resonance mass spectrometry of principal components in oilsands naphthenic acids. *J. Chromatogr. A* **1058**, 51–59.

Beam H. W. and Perry J. J. (1974) Microbial degradation and assimilation of n alkyl substituted cycloparaffins. *J. Bacteriol.* **118**, 394–399.

Behar F. H. and Albrecht P. (1984) Correlations between carboxylic acids and hydrocarbons in several crude oils. Alteration by biodegradation. *Org. Geochem.* **6**, 597–604.

Bennett B. and Abbott G. (1998) A natural pyrolysis experiment—hopanes from hopanoic acids? *Org. Geochem.* **30**, 1509–1516. Available at: http://linkinghub.elsevier.com/retrieve/pii/S0146638099001229%0Apapers3://publication/uuid/F0045356-1727-45D2-B0AD-E95BB9B3FEE1.

Boll M., Fuchs G. and Heider J. (2002) Anaerobic oxidation of aromatic compounds and hydrocarbons. *Curr. Opin. Chem. Biol.* **6**, 604–611.

Bost F. D., Frontera-Suau R., McDonald T. J., Peters K. E. and Morris P. J. (2001) Aerobic biodegradation of hopanes and norhopanes in Venezuelan crude oils. *Org. Geochem.* **32**, 105–114.

Bowman D. T., Slater G. F., Warren L. A. and McCarry B. E. (2014) Identification of individual thiophene-, indane-, tetralin-, cyclohexane-, and adamantane-type carboxylic acids in composite tailings pore water from Alberta oil sands. *Rapid Commun. Mass Spectrom.* **28**, 2075–2083. Available at: http://doi.wiley.com/10.1002/rcm.6996 [Accessed March 13, 2018].

Bowman D. T., Warren L. A. and Slater G. F. (2020) Isomer-specific monitoring of naphthenic acids at an oil sands pit lake by comprehensive two-dimensional gas chromatography–mass spectrometry. *Sci. Total Environ.* **746**, 140985. Available at: https://doi.org/10.1016/j.scitotenv.2020.140985.

Brooks P. W., Fowler M. G. and Macqueen R. W. (1988) Biological marker and conventional organic geochemistry of oil sands / heavy oils , Western Canada Basin *. **12**, 519–538.

Brown L. D. and Ulrich A. C. (2015) Oil sands naphthenic acids: A review of properties, measurement, and treatment. *Chemosphere* **127**, 276–290. Available at: http://dx.doi.org/10.1016/j.chemosphere.2015.02.003.

Clemente J. S. and Mackinnon M. D. (2004) Aerobic Biodegradation of Two Commercial Naphthenic Acids Preparations. **38**, 1009–1016.

Connan J. (1984) Biodegradation of crude oils in reservoirs. *Adv. Pet. Geochemistry* **1**, 299–335.

Cortes J. E., Suspes A., Roa S., Gonzlez C. and Castro H. E. (2012) Total petroleum hydrocarbons by gas chromatography in Colombian waters and soils. *Am. J. Environ. Sci.* **8**, 396–402.

Damien D., Sébastien D. and Hervé M. (2011) How early diagenesis reveals in situ biodegradation of herbicides in sediment. *Intechopen*.

Das N. and Chandran P. (2011) Microbial degradation of petroleum hydrocarbon contaminants: an overview. *Biotechnol. Res. Int.* **2011**, 941810.

Dompierre K. A. and Barbour S. L. (2016) Characterization of physical mass transport through oil sands fluid fine tailings in an end pit lake: A multi-tracer study. *J. Contam. Hydrol.* **189**, 12–26. Available at: http://dx.doi.org/10.1016/j.jconhyd.2016.03.006.

Eickhoff C. and Laroulandie J. (2010) A review of the Nature of Naphthenic Acid Occurrence, Toxicity, and Fate in Refinery and Oil Sands Extraction Wastewaters. *Presentation*.

Frank R. A., Fischer K., Kavanagh R., Kent Burnison B., Arsenault G., Headley J. V., Peru K. M., Van Glen Kraak D. E. R. and Solomon K. R. (2009) Effect of carboxylic acid content on the acute toxicity of oil sands naphthenic acids. *Environ. Sci. Technol.* **43**, 266–271.

Fritsche W. and Hofrichter M. (2008) Aerobic Degradation by Microorganisms. *Biotechnol. Second. Complet. Revis. Ed.* **11**–**12**, 144–167.

Frysinger G. (2002) GC×GC—A New Analytical Tool For Environmental Forensics. *Environ. Forensics* **3**, 27–34. Available at: http://linkinghub.elsevier.com/retrieve/pii/S1527592202900777.

Frysinger G. S., Gaines R. B. and Reddy C. M. (2002) Resolving the unresolved complex mixture in petroleum contaminated sediments. *ACS Div. Environ. Chem. Prepr.* **42**, 1653–1662.

Gieg, L.M., Fowler, S.J., Berdugo-Clavijo, C., 2014. Syntrophic biodegradation of hydrocarbon contaminants. Curr. Opin. Biotechnol. 27, 21–29. https://doi.org/10.1016/j.copbio.2013.09.002

Government of Alberta (2015) *Tailings Management Framework for Mineable Athabasca Oil Sands (TMF)*., Available at: http://esrd.alberta.ca/focus/cumulative-effects/cumulative-effects-management/management-frameworks/documents/LARP-TailingsMgtAthabascaOilsands-Mar2015.pdf.

Grewer D. M., Young R. F., Whittal R. M. and Fedorak P. M. (2010) Naphthenic acids and other acid-extractables in water samples from Alberta: What is being measured? *Sci. Total Environ.* **408**, 5997–6010. Available at: http://dx.doi.org/10.1016/j.scitotenv.2010.08.013.

Hall G. J., Frysinger G. S., Aeppli C., Carmichael C. A., Gros J., Lemkau K. L., Nelson R. K. and Reddy C. M. (2013) Oxygenated weathering products of Deepwater Horizon oil come from surprising precursors. *Mar. Pollut. Bull.* **75**, 140–149.

Han X., Scott A. C., Fedorak P. M., Bataineh M. and Martin J. W. (2008) Influence of molecular structure on the biodegradability of naphthenic acids. *Environ. Sci. Technol.* **42**, 1290–1295.

Head I. M., Jones D. M. and Larter S. R. (2003) Biological activity in the deep subsurface and the origin of heavy oil. *Nature* **426**, 344–352.

Head I. M., Larter S. R., Gray N. D., Sherry A., Adams J. J. and Aitken C. M. (2010) "Hydrocarbon degradation in petroleum reservoirs,." In *Handbook of Hydrocarbon and Lipid Microbiology* (eds. J. R. van derMeer, V. De Lorenzo, K. N. Timmis, and T. J. McGenity). (Heidelberg: Springer). pp. 3097–3109.

Headley J. V., Barrow M. P., Peru K. M., Fahlman B., Frank R. A., Bickerton G., McMaster M. E., Parrott J. and Hewitt L. M. (2011) Preliminary fingerprinting of Athabasca oil sands

polar organics in environmental samples using electrospray ionization Fourier transform ion cyclotron resonance mass spectrometry. *Rapid Commun. Mass Spectrom.* **25**, 1899–1909.
van der Heul R. (2009) Environmental Degradation of petroleum hydrocarbons. *Presentation*.
Holowenko F. M., MacKinnon M. D. and Fedorak P. M. (2002) Characterization of naphthenic acids in oil sands wastewaters by gas chromatography-mass spectrometry. *Water Res.* **36**, 2843–2855.
Holowenko F. M., MacKinnon M. D. and Fedorak P. M. (2001a) Naphthenic acids and surrogate naphthenic acids in methanogenic microcosms. *Water Res.* **35**, 2595–2606.
Holowenko F. M., MacKinnon M. D. and Fedorak P. M. (2001b) Naphthenic acids and surrogate naphthenic acids in methanogenic microcosms. *Water Res.* **35**, 2595–2606.
Jaffé R. and Gallardo M. T. (1993a) Application of carboxylic acid biomarkers as indicators of biodegradation and migration of crude oils from the Maracaibo Basin, Western Venezuela. *Org. Geochem.* **20**, 973–984.
Jaffé R. and Gallardo M. T. (1993b) Application of carboxylic acid biomarkers as indicators of biodegradation and migration of crude oils from the Maracaibo Basin, Western Venezuela. *Org. Geochem.* **20**, 973–984. Available at: http://www.sciencedirect.com/science/article/pii/014663809390107M [Accessed November 7, 2017].
Jaffe R. and Gardinali P. R. (1990) Generation and Maturation of Carboxylic-Acids in Ancient Sediments from the Maracaibo Basin, Venezuela. *Org. Geochem.* **16**, 211–218.
Johnson R. J., West C. E., Swaih A. M., Folwell B. D., Smith B. E., Rowland S. J. and Whitby C. (2012) Aerobic biotransformation of alkyl branched aromatic alkanoic naphthenic acids via two different pathways by a new isolate of Mycobacterium. *Environ. Microbiol.* **14**, 872–882.
Jones J. (1985) Microbes and microbial processes in sediments. *R. Soc. Publ.* **17**, 3–17.
Kendall M. M., Jeanthon C., Corre E. and Reysenbach A. L. (2003) Microbial diversity of petroleum reservoirs. *Encycl. Environ. Microbiol.*
Kindzierski W., Jin J. and Gamal El-Din M. (2012) Review of Health Effects of Naphthenic Acids: Data Gaps and Implications for Understanding Human Health Risk. Available at: https://era.library.ualberta.ca/public/view/item/uuid:1a3f664e-9cd9-4a7b-8b88-9f4a78a0efad/.
Konhauser K. O., Mortimer R. J. G., Morris K., Dunn V., Keith-Roach M. J. and Livens F. R. C. N.-B.-0000046 (2002) The role of microorganisms during sediment diagensis: Implications for radionuclide mobility. *Interact. Microorganims ith Radionuclides*, 61-100 ST-The role of microorganisms during sed. Available at: t:%5CScholar E-library%5CBook Chapters%5CBKCH-0000046.pdf LB - Radionuclide mobility: role of microorganisms.
Koshlaf E. and Ball A. (2017) Soil bioremediation approaches for petroleum hydrocarbon polluted environments. *AIMS Microbiol.* **3**, 25–49. Available at: http://www.aimspress.com/article/10.3934/microbiol.2017.1.25.
Lengger S. K., Scarlett A. G., West C. E. and Rowland S. J. (2013) Diamondoid diacids ("O4" species) in oil sands process-affected water. *Rapid Commun. Mass Spectrom.* **27**, 2648–2654.
Lovley D. R. and Chapelle F. H. (1995) Deep subsurface microbial processes. *Rev. Geophys.* **33**, 365–381.
Mackenzie A. S., Wolff G. A. and Maxwell J. R. (1981) Fatty acids in some biodegraded petroleums. Possible origins and significance. 637–649.

Mccaffrey A., Petroleum C., Company T. and Habra L. (1995) LETTER A novel microbial hydrocarbon demethylation degradation pathway revealed by hopane in a petroleum reservoir. **59**, 1891–1894.

Meinschein W. G. (1969) Hydrocarbons — Saturated, Unsaturated and Aromatic. In *Organic Geochemistry* Springer Berlin Heidelberg, Berlin, Heidelberg. pp. 330–356. Available at: http://link.springer.com/10.1007/978-3-642-87734-6_15 [Accessed April 26, 2017].

Meredith W., Kelland S. J. and Jones D. M. (2000) Influence of biodegradation on crude oil acidity and carboxylic acid composition. *Org. Geochem.* **31**, 1059–1073.

Meredith W., Kelland S. and Jones D. M. (2000) Influence of biodegradation on crude oil acidity and carboxylic acid composition. **31**.

National Petroleum Council (2011) Crude Oil and Natural Gas Resources and Supply. *Prudent Dev. Realiz. Potential North Am. Abund. Nat. Gas Oil Resour.* **2009**, 43–165. Available at: http://www.npc.org/reports/NARD-ExecSummVol.pdf.

Natural resources defense council (2016) Alberta ' s tailings ponds. , 1–8.

Olajire A. A. and Essien J. P. (2014) Aerobic Degradation of Petroleum Components by Microbial Consortia. *J. Pet. Environ. Biotechnol.* **5**, 1–22. Available at: http://search.proquest.com/docview/1640763600?accountid=171201.

Ong R. C. Y. and Marriott P. J. (2002) A review of basic concepts in comprehensive two-dimensional gas chromatography. *J. Chromatogr. Sci.* **40**, 276–291. Available at: https://academic.oup.com/chromsci/article-lookup/doi/10.1093/chromsci/40.5.276.

Palmer S. E. (1993) Effect of biodegradation and water washing on crude oil composition. *Org. Geochemistry Princ. Appl.*, 511–533.

Peters K. E. (1993) Geochemistry of selected oils and rocks from the central portion of the West Siberian Basin, Russia. *Am. Assoc. Pet. Geol. Bull.* **77**, 863–887.

Peters K. E. (1996) Selective biodegradation of extended hopanes to 25 norhop[retrieved-2016-11-16].pdf.

Peters K. E. and Moldowan J. M. (J. M. (2005) *The biomarker guide.*, Cambridge University Press.

Peters K. E. and Moldowan J. M. (1991) Effects of source, thermal maturity, and biodegradation on the distribution and isomerization of homohopanes in petroleum. *Org. Geochem.* **17**, 47–61.

Quagraine E. K., Headley J. V. and Peterson H. G. (2005) Is biodegradation of bitumen a source of recalcitrant naphthenic acid mixtures in oil sands tailing pond waters? *J. Environ. Sci. Heal. - Part A Toxic/Hazardous Subst. Environ. Eng.* **40**, 671–684.

Redelius P. (2009) Asphaltenes in bitumen, what they are and what they are not. *Road Mater. Pavement Des.* **10**, 25–43.

Reece J. B. and Campbell N. A. (2002) *Campbell biology*., Benjamin Cummings / Pearson. Available at: https://books.google.ca/books?id=39vMSgAACAAJ&dq=campbell+biology&hl=en&sa=X&ved=0ahUKEwiEqsfZn8faAhUE7IMKHYWhDQkQ6AEIKjAA [Accessed April 19, 2018].

Risacher F. F., Morris P. K., Arriaga D., Goad C., Nelson T. C., Slater G. F. and Warren L. A. (2018) The interplay of methane and ammonia as key oxygen consuming constituents in early stage development of Base Mine Lake, the first demonstration oil sands pit lake. *Appl. Geochemistry* **93**, 49–59. Available at: https://doi.org/10.1016/j.apgeochem.2018.03.013.

Rojo F. (2009) Degradation of alkanes by bacteria: Minireview. *Environ. Microbiol.* **11**, 2477–

2490.
Röling W. F. M., Head I. M. and Larter S. R. (2003) The microbiology of hydrocarbon degradation in subsurface petroleum reservoirs: Perspectives and prospects. *Res. Microbiol.* **154**, 321–328.
Rowland S. J., Alexander R., Kagi R. I. and Jones D. M. (1986) Microbial degradation of aromatic components of crude oils: A comparison of laboratory and field observations. *Org. Geochem.* **9**, 153–161. Available at: http://www.sciencedirect.com/science/article/pii/0146638086900653.
Rowland Steven J, Scarlett A. G., Jones D., West C. E. and Frank R. A. (2011) Diamonds in the rough: Identification of individual naphthenic acids in oil sands process water. *Environ. Sci. Technol.* **45**, 3154–3159.
Rowland Steven J., West C. E., Jones D., Scarlett A. G., Frank R. A. and Hewitt L. M. (2011) Steroidal aromatic Naphthenic Acids in oil sands process-affected water: Structural comparisons with environmental estrogens. *Environ. Sci. Technol.* **45**, 9806–9815.
Rowland Steven J., West C. E., Scarlett A. G. and Jones D. (2011) Identification of individual acids in a commercial sample of naphthenic acids from petroleum by two-dimensional comprehensive gas chromatography/mass spectrometry. *Rapid Commun. Mass Spectrom.* **25**, 1741–1751.
Schulz H. D. (2006) *Marine Geochemistry*.,
Seifert W. K. and Moldowan J. M. (1979) The effect of biodegradation on steranes and terpanes in crude oils. *Geochim. Cosmochim. Acta* **43**, 111–126.
Seifert W. K., Moldowan J. M. and Demaison G. J. (1984) Source correlation of biodegraded oils. *Org. Geochem.* **6**, 633–643.
Siddique T., Fedorak P. M. and Foght J. M. (2006) Biodegradation of Short-Chain n -Alkanes in Oil Sands Tailings under Methanogenic Conditions. **40**, 5459–5464.
Siddique T., Penner T., Semple K. and Foght J. M. (2011) Anaerobic Biodegradation of Longer-Chain n -Alkanes Coupled to Methane Production in Oil Sands Tailings. , 5892–5899.
Siddique T., Phillip M. and Mackinnon M. D. (2007) Metabolism of BTEX and Naphtha Compounds to Methane in Oil Sands Tailings. **41**, 2350–2356.
Siddique T., Semple K., Li C. and Foght J. M. (2020) Methanogenic biodegradation of iso-alkanes and cycloalkanes during long-term incubation with oil sands tailings. *Environ. Pollut.* **258**, 113768. Available at: https://doi.org/10.1016/j.envpol.2019.113768.
Sierra-Garcia I. N. and de Oliveira V. M. (2013) Microbial Hydrocarbon Degradation: Efforts to Understand Biodegradation in Petroleum Reservoirs. *Biodegrad. Eng. Technol.*, 47–82. Available at: http://cdn.intechopen.com/pdfs/45087/InTech-Microbial_hydrocarbon_degradation_efforts_to_understand_biodegradation_in_petroleum_reservoirs.pdf%5Cnhttp://www.intechopen.com/books/biodegradation-engineering-and-technology/microbial-hydrocarbon-degradation-eff.
Simoneit B. R. T. (2002) Molecular indicators (biomarkers) of past life. *Anat. Rec.* **268**, 186–195.
Slingerland N., Beier N. A. and Wilson G. W. (2019) Oil sands tailings storage facilities: Design considerations for ease of closure. *CIM J.* **10**.
So C. M., Phelps C. D. and Young L. Y. (2003) Anaerobic transformation of alkanes to fatty acids by a sulfate-reducing bacterium, strain Hxd3. *Appl. Environ. Microbiol.* **69**, 3892–3900.
Solano-Serena F., Marchal R., Ropars M., Lebeault J. M. and Vandecasteele J. P. (1999)

Biodegradation of gasoline: Kinetics, mass balance and fate of individual hydrocarbons. *J. Appl. Microbiol.* **86**, 1008–1016.
Stauffer E., Dolan J. A., Newman R., Stauffer E., Dolan J. A. and Newman R. (2008) Gas Chromatography and Gas Chromatography—Mass Spectrometry. In *Fire Debris Analysis* Elsevier. pp. 235–293.
Sutton P. A., Lewis C. A. and Rowland S. J. (2005) Isolation of individual hydrocarbons from the unresolved complex hydrocarbon mixture of a biodegraded crude oil using preparative capillary gas chromatography. *Org. Geochem.* **36**, 963–970.
Syncrude Canada Ltd. (2019) Base Mine Lake Monitoring and Research Summary Report: Results from 2013-2018. , 1–69.
Tissot B. P. and Welte D. H. (1985) *Petroleum Formation and Occurrence*., Available at: http://doi.wiley.com/10.1029/EO066i037p00643.
Trendel J.-M., Guilhem J., Crisp P., Repeta D., Connan J. and Albrecht P. (1990) Identification of two C-10 demethylated C28 hopanes in biodegraded petroleum. *J. Chem. Soc. Chem. Commun.*, 424–425. Available at: http://dx.doi.org/10.1039/C39900000424%5Cnhttp://pubs.rsc.org/en/content/articlepdf/1990/c3/c39900000424.
Varjani S. J. (2017) Microbial degradation of petroleum hydrocarbons. *Bioresour. Technol.* **223**, 277–286. Available at: http://dx.doi.org/10.1016/j.biortech.2016.10.037.
Vazquez-Roig P. and Pico Y. (2012) Gas chromatography and mass spectroscopy techniques for the detection of chemical contaminants and residues in foods. In *Chemical Contaminants and Residues in Food* Elsevier. pp. 17–61. Available at: http://linkinghub.elsevier.com/retrieve/pii/B9780857090584500025 [Accessed March 27, 2018].
Volkman J. K., Alexander R., Kagi R. I., Rowland S. J. and Sheppard P. N. (1984) Biodegradation of aromatic hydrocarbons in crude oils from the Barrow Sub-basin of Western Australia. *Org. Geochem.* **6**, 619–632.
Volkman J. K., Alexander R., Kagi R. I. and Woodhouse G. W. (1983) Demethylated hopanes in crude oils and their applications in petroleum geochemistry. *Geochim. Cosmochim. Acta* **47**, 785–794.
Wang B., Wan Y., Gao Y., Yang M. and Hu J. (2013) Determination and characterization of oxy-naphthenic acids in oilfield wastewater. *Environ. Sci. Technol.* **47**, 9545–9554.
Wang Z., Fingas M., Blenkinsopp S., Sergy G., Landriault M., Sigouin L., Foght J., Semple K. and Westlake D. W. S. (1998) Comparison of oil composition changes due to biodegradation and physical weathering in different oils. *J. Chromatogr. A* **809**, 89–107.
Wang Z., Fingas M., Owens E. H., Sigouin L. and Brown C. E. (2001) Long-term fate and persistence of the spilled Metula oil in a marine salt marsh environment: Degradation of petroleum biomarkers. *J. Chromatogr. A* **926**, 275–290.
Watkinson R. J. and Morgan P. (1990) Physiology of aliphatic hydrocarbon-degrading microorganisms. *Biodegradation* **1**, 79–92.
Watson J. S., Jones D. M., Swannell R. P. J. and Van Duin A. C. T. (2002) Formation of carboxylic acids during aerobic biodegradation of crude oil and evidence of microbial oxidation of hopanes. *Org. Geochem.* **33**, 1153–1169.
Wenger L. M., Davis C. L. and Isaksen G. H. (2002) Multiple Controls on Petroleum Biodegradation and Impact on Oil Quality. *SPE Reserv. Eval. Eng.* **5**, 375–383. Available at: http://www.onepetro.org/doi/10.2118/80168-PA.

Wenger L. M. and Isaksen G. H. (2002) Control of hydrocarbon seepage intensity on level of biodegradation in sea bottom sediments. *Org. Geochem.* **33**, 1277–1292.

West C. E., Pureveen J., Scarlett A. G., Lengger S. K., Wilde M. J., Korndorffer F., Tegelaar E. W. and Rowland S. J. (2014) Can two-dimensional gas chromatography/mass spectrometric identification of bicyclic aromatic acids in petroleum fractions help to reveal further details of aromatic hydrocarbon biotransformation pathways? *Rapid Commun. Mass Spectrom.* **28**, 1023–1032.

Widdel F. and Rabus R. (2001) Anaerobic biodegradation of saturated and aromatic hydrocarbons. *Curr. Opin. Biotechnol.* **12**, 259–276.

Wilde M. J., West C. E., Scarlett A. G., Jones D., Frank R. A., Hewitt L. M. and Rowland S. J. (2015) Bicyclic naphthenic acids in oil sands process water: Identification by comprehensive multidimensional gas chromatography-mass spectrometry. *J. Chromatogr. A* **1378**, 74–87.

Williams J. A., Bjorøy M., Dolcater D. L. and Winters J. C. (1986) Biodegradation in South Texas Eocene oils - Effects on aromatics and biomarkers. *Org. Geochem.* **10**, 451–461.

Yang C., Wang Z., Yang Z., Hollebone B., Brown C. E., Landriault M. and Fieldhouse B. (2011) Chemical Fingerprints of Alberta Oil Sands and Related Petroleum Products. *Environ. Forensics* **12**, 173–188. Available at: http://www.tandfonline.com/doi/abs/10.1080/15275922.2011.574312.

## Chapter two: Initial characterization of the identity and biodegradation potential of the hydrocarbons in fluid fine tailings underlying an end pit lake

*Mohamed El-Waraky, Robert Nelson, Christopher Reddy, Lesley Warren, Greg Slater*

**Abstract**

Efforts are underway to develop effective methods to manage tailings and reclaim land impacted by the extraction of the Alberta oil sands. Syncrude Canada Ltd. has undertaken the first full-scale demonstration of Water-Capped Tailings Technology (WCTT) via the development of Base Mine Lake (BML); a pit lake commissioned in 2012. A key factor that will impact the success of BML is in the production and the release of methane from the fluid fine tailings (FFT) underlying the water column. Methane release is important as it is a greenhouse gas, and also because its oxidation in the water column can impact oxygen levels within the lake, a central requirement of this reclamation technology. In addition, methane ebullition may result in the transport of organic compounds from the FFT into the water column resulting in further impacts on oxygen concentrations and/or introducing hazardous compounds from the FFT into the water column. Methane is produced primarily via fermentation of the residual organic compounds within the tailings. Understanding the characteristics, abundances, and variabilities of the organic compounds present within the FFT will enable the assessment of the current and future methane generation potential from the tailings and inform future management decisions. This study characterized the hydrocarbon present in the FFT between shallow depth intervals (~1m below FFT water interface) and deeper intervals (~6m below FFT water interface) across 3 locations from BML. The total organic content (TOC) of the FFT varied with depth and location comprising a range from 4.9 to 9 %. Gravimetric analysis of total lipid extracts (TLEs) represented 37 to 63 % of the TOC. The TLE was slightly enriched in the polar fraction which comprised a range of 31- 52 % while the saturates comprised a range of 21-41%, and the aromatics comprised a range of 21-45 %. Subsequent analysis using multidimensional gas chromatography (GC×GC) showed that the resolved compounds from the FFT UCM included groups of alkylated aromatics, branched and cyclic alkanes in addition to biomarker compounds such as steranes and hopanes. The distribution of these compound groups was similar between all samples; however, their concentrations were variable spatially and with depth. This variability pattern across platforms implied that, as expected, the hydrocarbons makeup is heterogeneous in the FFT. Consequently, methane production is expected to be spatially variable across the lake. Notwithstanding this heterogeneity, shallow samples at P2 and P3 had systematically lower concentrations of highly biodegradable compounds despite higher concentrations of TOC and higher molecular weight and less biodegradable compounds implying loss of these hydrocarbons driven by biodegradation at shallower depths. Gaining insight into the organic compounds driving methanogenesis and other biogeochemical processes in the FFT underlying BML, and that may potentially be mobilized during ebullition, will inform predictions of future lake behavior and thus inform adaptive management of this reclamation site.

# 1-Introduction

Petroleum extraction in the Alberta oil sands region has resulted in the generation of more than 1.18 trillion liters of tailings currently stored in settling tailings ponds in Alberta and is expected to increase with continuing increases in the oil sand production (Natural resources defense council, 2016). The tailings stored in these ponds are composed of sand, that rapidly settles out in these basins, in addition to clay, fine solids and residual bitumen that form a suspended layer known as fluid fine tailings (FFT) that can take decades to settle (Hyndman et al., 2018). Approaches are currently being developed and applied to manage the FFT and reclaim mined areas after the cessation of extraction activities. In 2012, Syncrude Ltd commissioned Base Mine Lake (BML), the first full-scale application of water capped tailing technology (WCTT) in the Alberta Oil Sands Region. The goal of WCTT is to eventually establish a stable, oxygenated water column overlying the tailings that will prevent the mobilization of residual bitumen and related compounds to the environment and allow for the development of a functioning lake ecosystem. Compounds of concern in this context include petroleum hydrocarbons and naphthenic acids (NAs), the latter has been associated with toxicity to aquatic life (Brown and Ulrich, 2015).

The main sources of hydrocarbons in the FFT underlying BML include residual bitumen that was not extracted during processing and any residual naphtha diluent that was added during the extraction process (Siddique et al., 2006; Small et al., 2015). The diluent naphtha that is used by Syncrude is composed of low molecular weight alkanes, iso-alkanes ($C_6$-$C_{14}$), and monoaromatics (Siddique et al., 2007). On the other hand, the bitumen is a heavily degraded oil consisting of resins, asphaltenes, oxygenated compounds, degradation resistant compounds such as cycloalkanes, PAHs, terpanes, steranes and hopanes while depleted in less resistant compounds such as alkanes and isoprenoids (Yang et al., 2011).

Methane is generated as an end product of the anaerobic degradation of hydrocarbons through syntrophic fermentation followed by methanogenesis within the oil sand tailing ponds (Faidz et al., 2017; Holowenko et al., 2000; Siddique et al., 2011). Syntrophic fermentative bacteria ferment the complex hydrocarbons first to acetate or hydrogen which can then be metabolized by

methanogens or any other microorganisms(Jones et al., 2008; Kendall et al., 2003; Lovley and Chapelle, 1995; Röling et al., 2003). Methanogens can then produce methane through oxidizing hydrogen coupled to CO2 reduction (hydrogenotrophic methanogenesis) or fermenting acetate ( acetolactic methanogenesis) (Slater et al., in prep; Head et al., 2014; Kendall et al., 2003; Lovley and Chapelle, 1995).

Previous laboratory studies have demonstrated that the low molecular weight organic matter that are components of naphtha can drive methane generation in laboratory incubation experiments of oil pond samples (Faidz et al., 2017, 2016; Siddique et al., 2020, 2015, 2012, 2007, 2006). The amended hydrocarbons used in these studies comprised whole Syncrude naphtha, several components of naphtha such as low molecular weight n-alkanes ($C_{10}$, $C_8$, $C_7$, $C_6$), and low molecular weight aromatics (BTEX; benzene, toluene, ethylbenzene, xylene) along with some components that constitute the bitumen including branched and cyclic alkanes. The studies that used the naphtha components detected an increase in methane generation after a short lag phase of 2-5 weeks until it halted with the depletion of these components (Siddique et al., 2006; Siddique et al., 2007 ). On the other hand, the study that used the bitumen components started to detect methane production after a lengthy lag phase of 180 days (Siddique et al., 2011). Accordingly, the results of these studies imply that methanogenesis will initiate first with the naphtha components then progress to the residual bitumen

The methane produced within the FFT is transferred to the water column through mainly advective-diffusive mass transport (Dompierre and Barbour, 2016; Slater et al., In prep). The expected microbial oxidation of dissolved methane released from the FFT into the water column ( Figure 1), was indicated to be a major control on oxygen concentrations in BML water column early in the lake development (Arriaga et al., 2019; Risacher et al., 2018a). The maintenance of oxygen levels within the water column is important to support a functioning ecosystem and enable aerobic microbial biodegradation of residual organic compounds released into the surface water contributing to preventing their release to the broader environment (Saidi-Mehrabad et al., 2013; Small et al., 2015). Aerobic biodegradation pathways are the most preferable for microorganisms as they release higher energy and can oxidize a wide range of organic contaminant (Kendall et al., 2003; Lovley and Chapelle, 1995). In addition to methane

being seen as a key oxygen-consuming constituent, it poses an issue related to greenhouse gas emissions. Therefore, understanding the potential for ongoing hydrocarbon biodegradation and methane production is key to evaluating and managing the long-term behavior of the BML system.

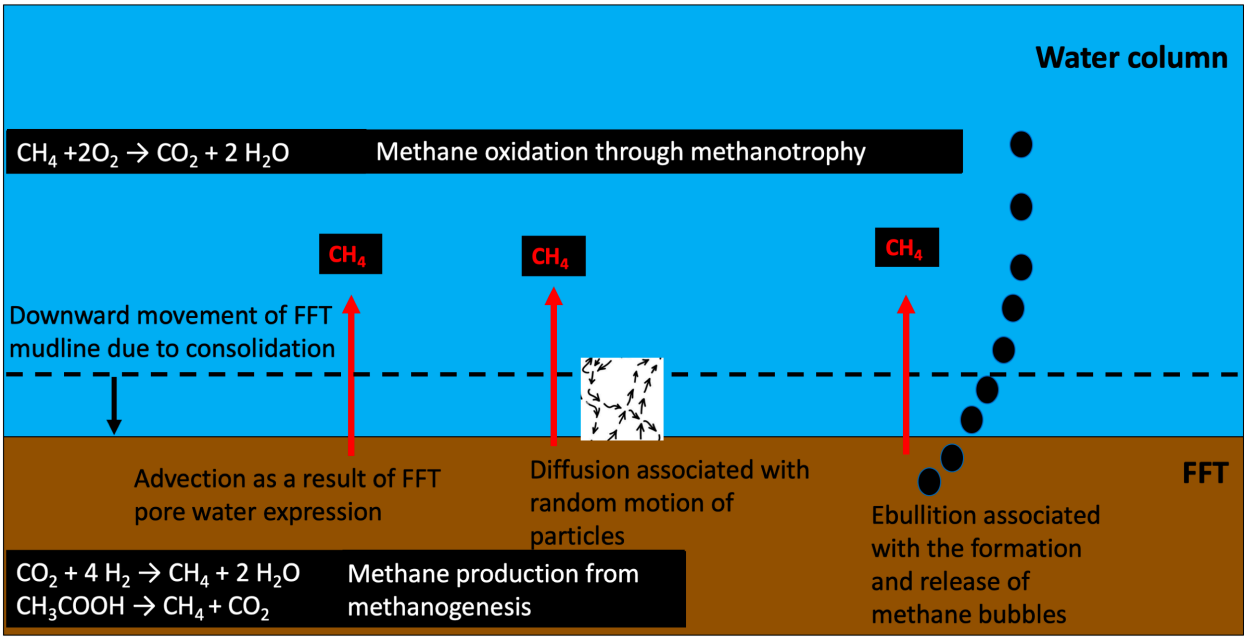


Figure 1: A cross section of BML that shows how methane, that is generated from the FFT, is oxidized by methanotrophs in the water column.

Accordingly, the objective of this study is to evaluate the presence of petroleum hydrocarbons that comprises the naphtha or the bitumen directly within the FFT in BML then evaluate the biodegradation and methane generation potential of the identified compounds. This was accomplished through the analysis of the organic carbon pools present in the FFT through using gravimetrical techniques and resolving the identity of the hydrocarbons present using multi-dimensional chromatography. The concentrations of the resolved hydrocarbons were compared spatially and via depth to assess their variability. This variability assessment provided insights related to the distribution of hydrocarbons and the occurrence of in-situ biodegradation within the FFT.

## 2- Methods

### 2.1 Study area and sampling

A total of 6 samples were collected from two depths at three locations (Platforms 1, 2, and 3) in BML site, north of Fort McMurray, Alberta, Canada during summer 2015 sampling campaign (Figure 2). The samples were collected in glass jars and stored in the freezer upon arrival. The shallow samples at each site were collected at 10m below the water surface, within 1 m from the FFT water interface (FWI), while the deeper samples were collected from at least 16m below the water surface ( ~6m from FWI). These samples were analyzed through bulk analysis, solvent extraction, and fractionation (Figure 3) to characterize the total organic matter present and its constituents (TLE, Saturates, aromatics, polars). Subsequently, target compounds were analyzed, identified, and quantified using multidimensional chromatography as explained in detail below.

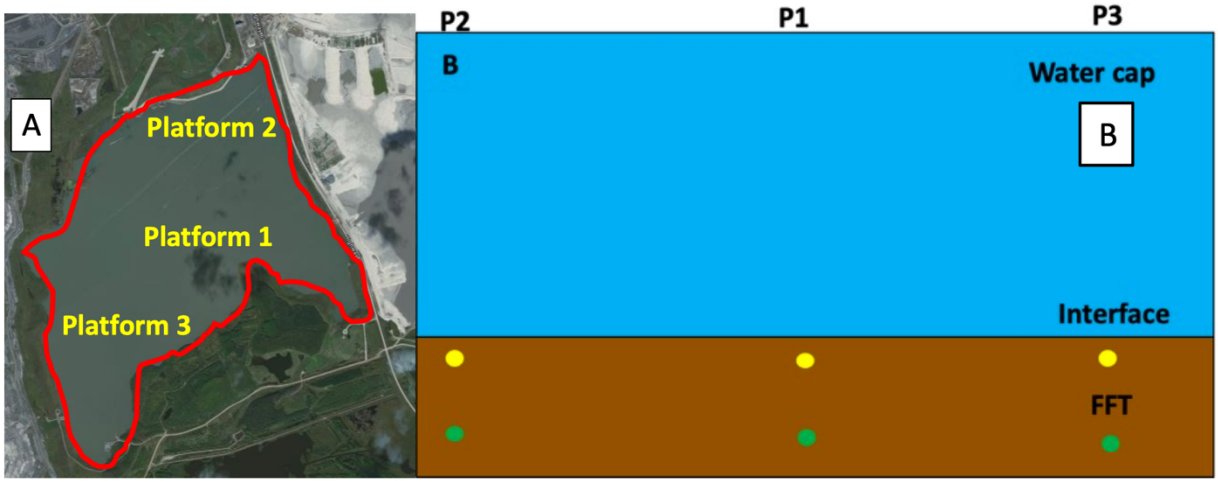


Figure 2: (A) A satellite image of BML that shows P1, P2, P3 (B) A cross section of BML that shows where the samples were collected. The yellow circles represent the shallow samples while the green circles represent the deep samples.

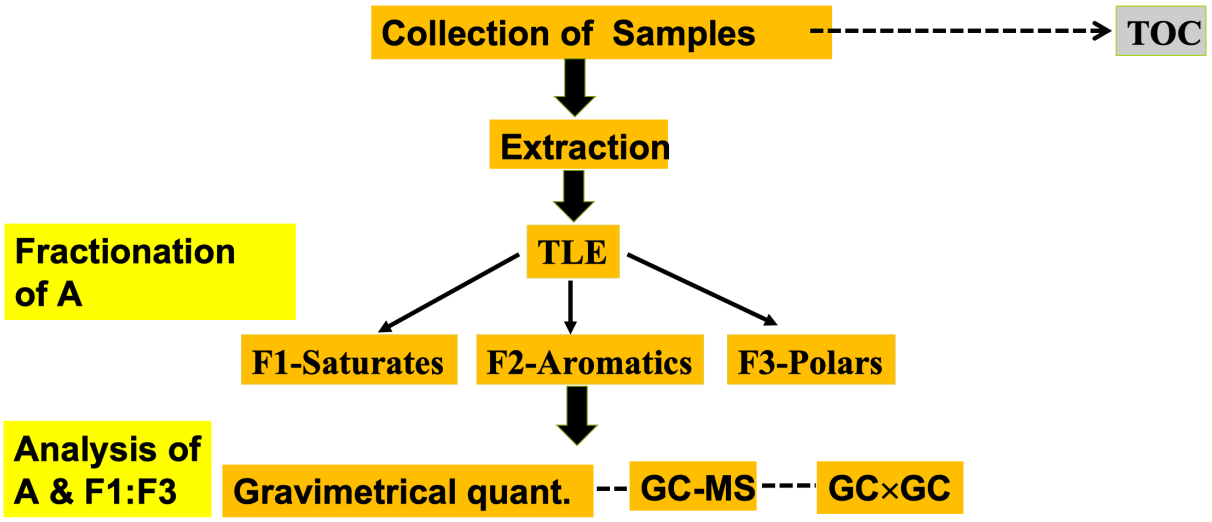


Figure 3: A summary of the extraction, fractionation, and analysis of FFT samples.

## 2.2 Sample extraction

Total organic carbon content (TOC) was analyzed by combustion at CC HATCH labs using the elementar isotope cube. In brief, approximately 10 mg of samples is measured into tin capsules, then the samples are loaded into the instrument, and are flash combusted at 1800°C with the addition of oxygen. Finally, using a trap and purge method a thermoconductivity detector (TCD) measures the gases as they are released. Solvent extractable organic matter were characterized by duplicate extractions of 10 grams of freeze dried FFT in a MARS X microwave extraction system using 30 ml 1:1 hexane acetone. The microwave program was as follows: the temperature was ramped up to 115 °C in 10 minutes, then was held at 115 °C for 15 minutes. Following extraction samples were filtered to separate residual solid materials and to obtain the (total lipid extracts) TLE containing the solvent extractable organic matter. The TLE was split into two aliquots: 1) The first aliquot was evaporated to dryness to determine the TLE gravimetrically (expressed in mg/g of sample) , and 2) the second aliquot was fractionated using the method adopted from (Ventura et al., 2008). In brief, alumina oxide chromatography (activated >2h at 150°C) was used to fractionate the extract into polar and nonpolar fractions. The non-polar fraction was eluted using hexane: DCM (9:1) while the polar fraction was eluted using DCM: MeoH (1:1). Then, the non-polar fractions are separated into saturates and aromatics by silica chromatography where the saturates are eluted using hexane and aromatics

are eluted using DCM:MeOH (7.5:1 ). After separation, each fraction is divided into two aliquots. The first aliquot is analyzed using the GC-MS & GC×GC and the other aliquot was weighed gravimetrically.

## 2.3 Instrumental analysis

The instrumental analysis of this study was performed using gas-chromatography mass spectrometry (GC-MS), Comprehensive two-dimensional gas chromatography time of flight mass spectrometry (GC×GC TOFMS), and two-dimensional gas chromatography flame ionization detection (GC×GC FID). Two-dimensional chromatography is used due to its high resolving power in comparison with a conventional gas chromatograph. This high resolving power, as outlined by (Frysinger, 2002; Ong and Marriott, 2002; Stauffer et al., 2008; Vazquez-Roig and Pico, 2012), is due to its multiple dimension separation via two columns connected serially compared to regular GC-MS that only separate compounds via one column. The first-dimension of separation in both GC-MS and GC×GC occurs the within the primary column mainly depending on the volatility of the compounds. Then, a modulator, connected between the two columns, collects the effluent from the primary column and trap it using cold jets then re-inject it into the secondary column using hot pulse that re-mobilize the trapped effluent after a fixed interval. The effluent then passes very rapidly through the secondary column to produce a second-dimension separation depending on the polarity of the compounds.

### 2.3.1 Gas-chromatography mass spectrometry

The samples were analyzed on an Agilent Technologies 6890N gas chromatograph with an Agilent DB5-MS capillary column (30 m × 0.32 mm, 0.25 μm film thickness) coupled to a 5973-quadrupole mass spectrometer. The oven was programmed as follows: the temperature was initiated at 50 °C, then ramped to 320 °C at a rate of 4 °C /min.

### 2.3.2 Comprehensive two-dimensional gas chromatography flame ionization detection

The samples were analyzed on a LECO GC×GC FID system using a dual cryogenic modulator, and a 7890 A Agilent gas chromatograph. The system used a splitless injection mode, hydrogen as the carrier gas with a flow rate of 1 ml/min, and a front inlet that was held at 310 °C. The primary column used was a Restek Rtx-1 column (60 m, 0.25mm ID, 0.25 µm film thickness). While, the secondary column used was an SGE BPX-50 column (1.25 m, 0.10mm ID, 0.10 µm film thickness). The primary oven temperature was started at 70 °C ( held for 10 minutes), then the temperature was ramped up to 340 °C ( held for 1 minute) at a rate of 1.25°C /min. On the other hand, the secondary column was initiated at 75 °C ( held for 10 minutes), then the temperature was ramped up to 345 °C ( held for 1 minute) at a rate of 1.25 °C /min. The modulation period used was 7s.

### 2.3.3 Comprehensive two-dimensional gas chromatography time of flight mass spectrometry

The samples were analyzed on a LECO Pegasus 4D GC × GC–TOFMS system using a dual cyrogenic modulator, a 6890 agilent gas chromatograph, and a 7683 HP injector. The system used the splitless injection mode, hydrogen as the carrier gas with a flow rate of 1 ml/min, and a front inlet that was held at 310 °C. The primary column used was a Restek Rtx-1 column (60 m, 0.25mm ID, 0.25 µm film thickness), and the secondary column was an SGE BPX-50 column (1.25 m, 0.10mm ID, 0.10 µm film thickness). The primary oven temperature was initiated at 80 °C (held for 15 minutes), then the temperature was ramped up to 335 °C with a rate of 1.66 °C /min. Whereas, the secondary oven temperature was initiated at 85 °C ( held for 15 minutes), then the temperature was ramped up to 340 °C with a rate of 1.66 °C /min. The modulation period used was 7.5s. The TOFMS data acquisition rate was 100 HZ, the detector voltage was 1425 V, and the mass spectrometer used a voltage energy of -70 eV.

## 2.3.4 Processing methods

### *2.3.4.1 Compounds identification:*

The processing of all the samples was performed using LECO software Chroma TOF version 4.5.1. The search for the target compound within all the FFT samples was completed using their diagnostic target ions with the TLE, saturates, and aromatics fractions. These compounds were then identified using an in house library, in addition to the library of the processing software along with published peak positions (Swarthout et al., 2016). The list of all compounds identified is provided in the appendix (A2).

### *2.3.4.2 Quantification:*

The identified compounds from the GC×GC TOF analysis were located on the GC×GC FID chromatograph, then each peak was manually integrated through the chroma TOF software. The compounds were semi-quantified using an internal calibration curve of the following compounds from SRM 1582: ( 1,6,7-Trimethylnaphthalene: $R^2$=0.98, 1,7-Dimethylphenanthrene: $R^2$= 0.98; Dibenzothiophene: $R^2$=0.97; Fluorene: $R^2$=0.98; 17α(H), 21β(H)-22S-Homohopane: $R^2$=0.94). Additionally the low molecular weight compounds in the samples in the range of $C_{12}$-$C_{16}$ were quantified using an alkane standard mix (N-$C_{14}$ : $R^2$=0.96) . The internal standard that was used is 5∝-cholestane.

### *2.3.4.3 Difference chromatographs:*

The GC×GC FID chromatographs of the TLEs were extracted as a raw data that represent pixel points, then the baseline was first corrected through Matlab software using the Gros-Eilers-Arey code (Eilers, 2004; Gros et al., 2014). This was followed by aligning the retention times of the two chromatographs required for subtraction through applying the Gros-Arey code (Gros et al., 2012). The difference chromatographs generated are provided in Appendix: Figure A2, and a summary of the data generated from the chromatographs are presented in Table A3. Compounds that are present in higher abundances in one chromatogram than the other are indicated in blue and those that are present in lower abundances are indicated in red.

#### *2.3.4.4 Principal component analysis:*

The PCA scores plot for all the quantified compounds across all samples was performed using MetaboAnalyst 4.0 online platform. The quantified concentrations were preprocessed first in order to remove any bias terms from the data through centering and scaling the data (centering means subtracting the mean from each column in the data matrix then it is scaled through dividing by the standard deviation). All the samples are represented with 2 points which represent duplicate analysis except samples P1-16.9 and P2-10.9 have one point that represents just one analysis.

#### 2.3.4.5 Statistical testing:

The significance of the variance of the quantified compounds across the 3 platforms was tested using one-way ANOVA while between shallow vs deep intervals was tested using T-test. One-way ANOVA tests for the variation between 3 or more means whereas these variations are considered significant if they have a P-value <0.05. The one-way ANOVA test was followed by a Tukey test in order to determine what specific pairs had the significant variance. On the other hand, T-test is used for the variation between two conditions. The variation was considered significant if the P-value is < 0.05 for the one-way ANOVA and the T-test performed. The analysis was performed using Minitab 19 and MetaboAnalyst 4.0.

## 3-Results and discussion

### 3.1 Assessment of hydrocarbons identity and biodegradation potential in the FFT of BML:

The result of the bulk analysis of the hydrocarbon pools in the FFT of BML (Figure 4) revealed that the total amount of organic carbon ranged from 49 to 94 mg/g (uncertainty for duplicate analysis ± 0.2 to 13 % RSD). This range of TOC corresponds to 4.9 to 9.4% which is within the published range of TOC for the bitumen from the oil sands of 4.5 to 11.4 % (Majid et al., 1982). Statistical analysis using a one-way ANOVA test followed by a Tukey test revealed that the

TOC concentrations showed a significant elevation at P2 compared to P1 and P3 at the shallow intervals. While statistical analysis didn't show a significant variation for the TOC concentrations between shallow and deep intervals, the elevated concentrations of the TOC at the shallow intervals for P2 and P3 implied a greater initial loading of organic matter at shallow interval for these sites.

Gravimetrical quantifications showed that TLE ranged from 25 to 43 mg/g (uncertainty for duplicate analysis: ± 4 to 23% RSD ). The quantified TLE represented 37 to 63% of the TOC present in the FFT implying that the remainder amount are the larger compounds that could be bound to the clay particles of the tailings and/or too large for extraction, and thus would be less bioavailable. Of the extractable components, the polar fraction was slightly dominant with a range of 8 to 21 mg/g that constituted 31 to 52% of the TLE (uncertainty for duplicate analysis: ± 1 to 34% RSD ), followed by the saturate fraction with a range of 8 to 13 mg/g which represent 21 to 41% of the TLE (uncertainty for duplicate analysis: ± 1 to 27%RSD), then the aromatic fraction with a range of 9 to 11 mg/g which represent 21 to 45 % of the TLE. The composition of petroleum usually shows a more dominant abundances of saturates and aromatics relative to polars (Welte, 1978). However, previous studies found that biodegradation consume the compounds within the saturates and aromatics fraction and produce oxygenated metabolic intermediates that are constituents of the polar fraction (Aeppli et al., 2012; Oudot, 1984). The slight enrichment of the polar fraction reported here would point to the production of oxygenated metabolites as a result of the preferential biodegradation of parent hydrocarbons within the saturate and aromatic fractions.

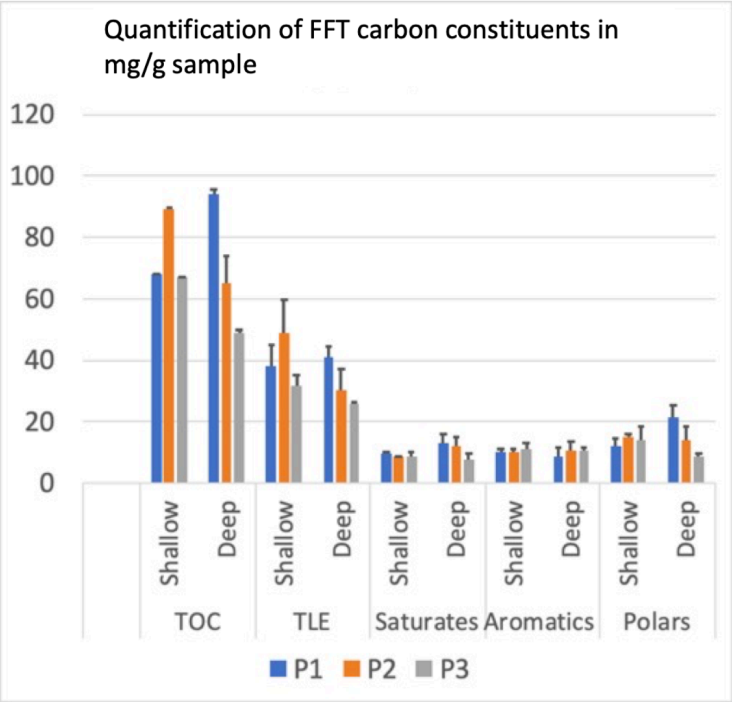


Figure 4: The mass of FFT carbon consituents: TOC, TLE, saturates, aromatics, and polars.

Gas chromatography analysis using GC-MS and GC×GC was used to further characterize the hydrocarbons present within the solvent extractable organic matter. The GC-MS analysis failed to resolve any hydrocarbons as all the compounds appeared as one large UCM (Unresolved complex mixture) hump containing thousands of unresolved compounds (Appendix: Figure A1). This UCM is commonly found in oil sands bitumen , and all other biodegraded hydrocarbons (Gouch et al., 1992; Killops and Al-Juboori, 1990; Yang et al., 2011). Thus, the GC×GC system was used to increase the resolution of the hydrocarbons within the FFT UCM.

From the GC×GC chromatogram of the TLE fraction a total of 126 well resolved compounds (listed in Appendix: Table A2) that could be confidently identified based on known retention times and/or mass spectral library comparisons were selected. These compounds (Figure 5) included several alkylated groups of two-ring PAHs: naphthalene ( $C_3$-Nap, $C_4$-Nap), fluorenes ($C_1$-Fl, $C_2$-Fl), three-ring PAHs: phenanthrenes ($C_1$-PH,$C_2$-PH, $C_3$-PH), four-ring PAHs:

pyrenes, chrysene, thiophene-fused PAHS: dibenzothiophenes ($C_1$-DBT, $C_2$-DBT, $C_3$-DBT), Benzonaphthothiophene, Phenanthrothiophene. Additionally, biomarker compounds such as steranes, hopanes, and benzohopanoids were also present in the samples with the highest peak in the chromatogram of all the samples being a tricyclic terpanoid. Other compounds that could not be confidently identified due to low similarity using library hits and uncertainty in their identification were not selected for this analysis. The processing diluent naphtha components in the FFT, that have been shown to be the primary driver for methane generation (Siddique et al., 2006; Siddique et al., 2007), were not detected within the resolution of this analysis. While the analytical methods employed here were not optimized for detection of low molecular weight hydrocarbons, they would be detected if present in sufficient concentrations.

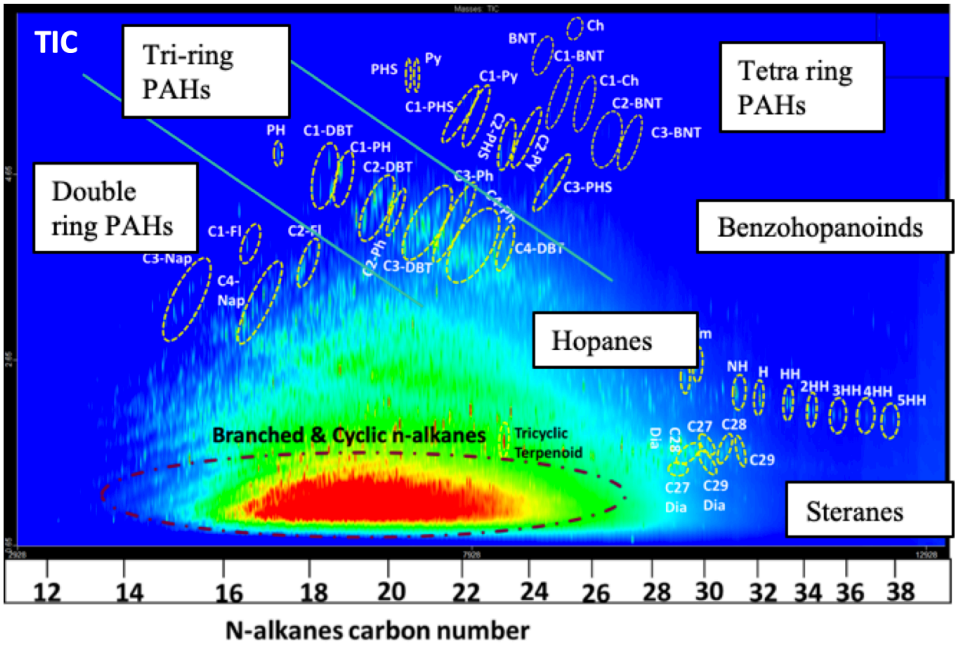


Figure 5: Target compounds identified within the GC×GC chromatograph. Nap: naphthalene, F1: Fluorene, PH: Phenanthrene, Py: Pyrene, Ch: Chrysene, DBT: Dibenzothiophene, BNT: Benzonaphthothiophene, PHS: Phenanthrothiophene, NH: $C_{29}$ Norhopane, H: $C_{30}$ Hopane, HH: Homohopanes 22S+22R($C_{31}$-$C_{35}$), C27-C29 Dia: $C_{27}$- $C_{29}$ Diasteranes βα 20S+20R, αβ 20S+20R, C27-C29 Steranes: $C_{27}$ - $C_{29}$ ααα 20S+20R, αββ 20S+20R.

The resolved alkylated PAHs and hopanes from the GC×GC FID chromatographs were semi-quantified using internally calibrated curves of the compounds with the most similar retention time and chemical configuration in SRM 1582 standard (details in the method section above). The total mass of alkylated PAH groups quantified ranged from 1 to 31 µg/g sample (Figure 6A), while the hopanes abundance ranged from 5 to 20 µg/g sample (Figure 6B).

Branched and cyclic alkanes were not identified in the samples as they were present within the UCM. Nonetheless, the chromatograph of the samples was compared to a chromatogram of SRM 1582 that include well resolved alkanes from $C_{12}$ to $C_{38}$, in order to assess the carbon number range of the compounds within the UCM. The alkane carbon number equivalent to each retention time determined from SRM 1582 is overlaid on the x-axis of the GC×GC chromatograph of the samples (figure 5). This overlay shows that the UCM is comprised of compounds with a range of carbon number that corresponds to n-alkanes from $C_{12}$ to $C_{30}$. Total peak area of the UCM that eluted over the intervals corresponding to carbon chain lengths in the range of $C_{12}$-$C_{14}$ and in the range of $C_{14}$-$C_{16}$ were semi-quantified using an n-alkane standard mix. These ranges will be abbreviated as UCM interval (UI)-$C_{12}$-$_{14}$ and UI-$C_{14}$-$C_{16}$ for future reference in the paper. The UI-$C_{12}$-$C_{14}$ compounds ranged from 50 to 450 µg/g sample while UI- $C_{14}$- $C_{16}$ compounds ranged from 460 to 2600 µg/g (Figure 6C).

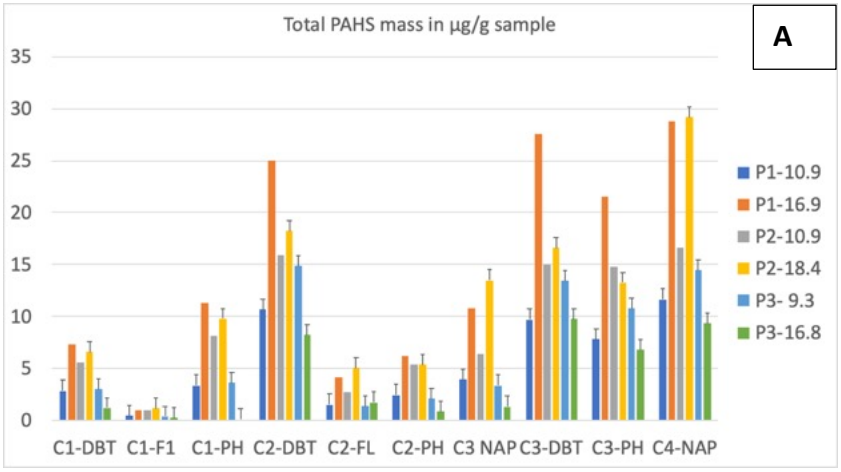

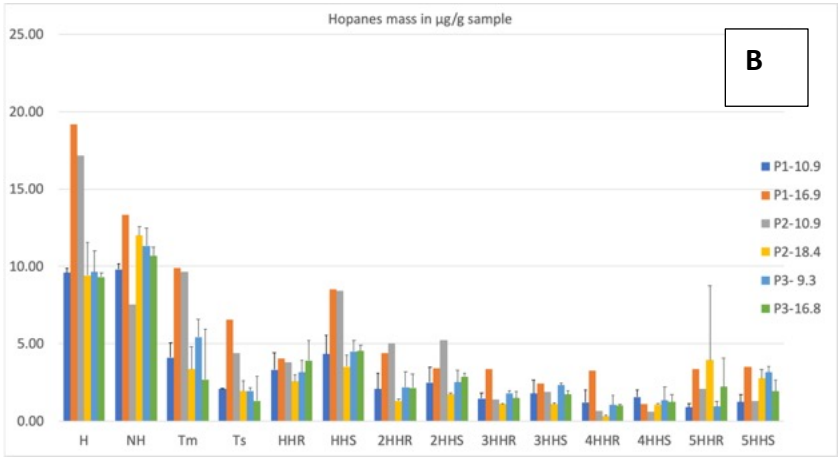


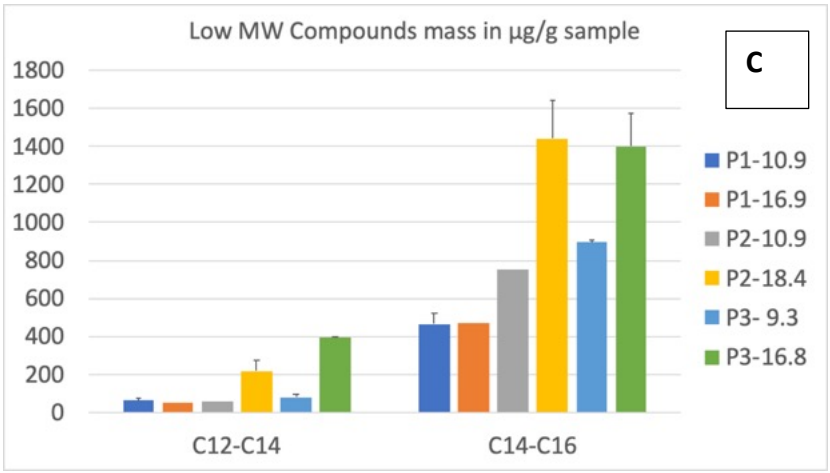


Figure 6: (A) The quantified mass of total PAHs compounds for each alkylation group (B) the quantified mass of Hopanes (C) The quantified mass of Low MW Compounds. Error bars for the replicates between samples is represented in A, B, C.

The biodegradation scale developed by Peters and Moldowan (1993) and Wenger et al. (2008) was used to determine the biodegradation potential for the resolved compounds. This scale ranks the biodegradability of hydrocarbons according to their molecular weight, structural configuration, and degree of branching (Table 1). Whereas, lowest alkyl molecular weight, lowest alkyl branching and hopane compounds with a 22R steric configuration are preferentially degraded (Connan, 1984; Wang et al., 1998; Wenger et al., 2002; Wenger and Isaksen, 2002;Head et al., 2003; Head et al., 2010).

| Compounds/ biodegradation extent | High biodegradability | Low biodegradability | Reason |
|---|---|---|---|
| Low MW Alkanes | $C_{12}$-$C_{14}$ | UI-$C_{14}$-$C_{16}$ | Molecular weight |
| Alkylated Aromatics | $C_1$-DBT, $C_1$-Fl, $C_1$-Ph, $C_3$-Nap | $C_3$-DBT, $C_2$-Fl, $C_3$-Ph, $C_3$-Nap, $C_4$-Nap | Alkyl branching |
| Homohopanes | C31-C35 (22R) configuration | $C_{31}$-$C_{35}$ (22 S) configuration | Steric configuration |

Table 1: Scheme of ranking the biodegradation level of the resolved hydrocarbons in the FFT of BML.

The analysis of the quantified mass of the high biodegradability vs low biodegradability compounds show that the high biodegradability compounds were relatively depleted in all of the FFT samples. The comparison of the mass for the low molecular weight alkanes revealed that the UI-$C_{12}$-$C_{14}$ compounds (higher biodegradability) were relatively depleted compared to the UI-$C_{14}$-$C_{16}$ compounds (lower biodegradability) (Figure 6C). Additionally, the ratio of the higher biodegradability PAHs (less alkylated) were compared to the lower biodegradability PAHs (more alkylated) (Ratio of quantified mass between: $C_1$-DBT vs $C_3$-DBT, $C_1$-Fl vs $C_2$-Fl, $C_1$-Ph vs $C_3$-Ph, $C_3$-Nap vs $C_4$-Nap). This comparison revealed that the lower alkylated PAHs were relatively depleted in all of the samples for the naphthalene and fluorene, while phenanthrene were relatively enriched for P1-16.9, P2-10.9, P2-18.4, and the DBT were relatively enriched in all of the samples (Figure 7). Furthermore, most of the homohopanes ( $C_{31}$-$C_{35}$) with the 22R epimer configuration ( Higher biodegradability) had a lower abundances compared to 22S epimer configuration ( Lower biodegradability) in most samples (Figure 8).

Similar to the enrichment of polar fraction, the overall depletion of the high biodegradability compounds would also support that the FFT samples shows a biodegradation signature. The observation of a biodegradation signature within the BML FFT organic matter may however be a result of the fact that the oil sands bitumen is known to be heavily biodegraded ( Yang et al.,

2011). Demonstrating the occurrence and/or extent of in-situ biodegradation within the BML FFT thus requires a higher level of assessment.

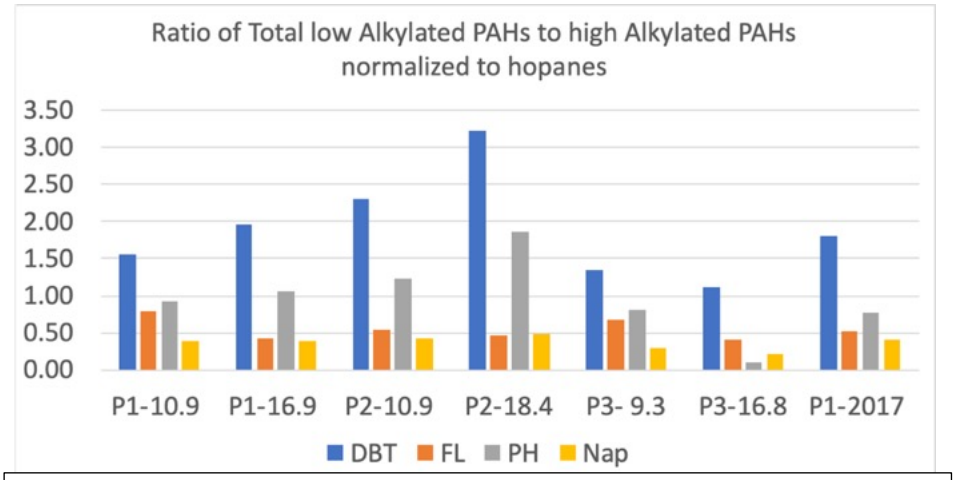


Figure 7: A plot for the ratio between low Alkylated PAHS to high alkylated PAHs normalized to hopanes.

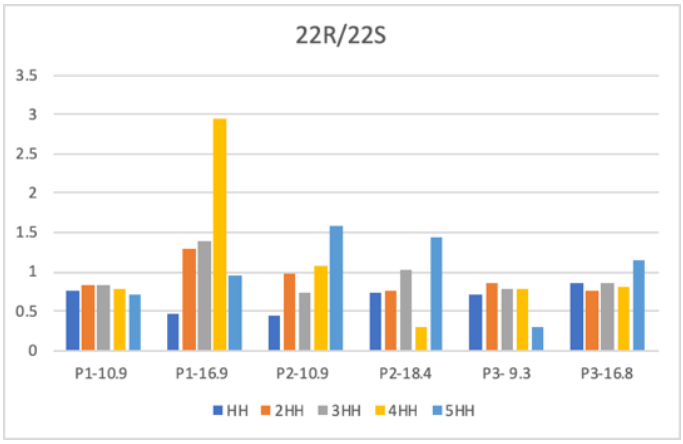


Figure 8: A plot for the ratio between 22R/22S homohopanes.

### 3.2 Assessment of the spatial variability for the identified hydrocarbons in the FFT of BML

The spatial variability of hydrocarbons was evaluated in order to look for evidence of systematic changes that might indicate in-situ biodegradation within the FFT of BML. The assessment was

accomplished through comparing the concentrations of GC×GC resolved compounds in BML across the three platforms (P1, P2, P3) at the shallow interval (10 m, ~1m below FWI), and at the deep interval (16m, ~6m below FWI). Spatial variation of hydrocarbons at depth was also assessed using difference chromatograms produced by overlaying two GC×GC chromatograms and subtracting one from the other. This approach was used previously by (Nelson et al., 2006) in order to track the weathering of the oil spill at Buzzards bay, and (Wardlaw et al., 2008) to highlight the occurrence of biodegradation at oil seeps from offshore Santa Barbara.

### *3.2.1 Characterization of the variability between shallow FFT samples*

Variability between the shallow samples from the three platforms was evaluated using the selected set of GC×GC resolvable compounds (The summed concentrations of all the isomers of the following compounds: $C_3$-Nap, $C_4$-Nap, $C_1$-Fl, $C_2$-Fl, $C_1$-PH, $C_2$-PH, $C_3$-PH, $C_1$-DBT, $C_2$-DBT, $C_3$-DBT, UI-$C_{12}$-$C_{14}$, UI-$C_{14}$-$C_{16}$). A PCA plot implemented using the concentrations of these compounds indicated that P2 was separated from P1 and P3 on PC1 that explained most of the variability (71%) (Figure 9). This difference was primarily driven by higher concentrations of alkylated PAHs at P2 as shown in the loadings plot (Figure 9). A one-way ANOVA test found that $C_1$-DBT, $C_1$-PH, $C_2$-PH are the only groups to have significant variance. The Tukey test indicated that these groups only had a significant variance between P2-P1 and P2-P3.

Overall, the assessment of the suite of GC×GC targeted compounds revealed that P2 is consistently showing higher concentrations of hydrocarbons compared to the other platforms at the shallow interval. The elevated concentrations of hydrocarbons at P2 relative to P1 and P3, would imply a greater potential for methane generation from the biodegradation of hydrocarbons. Indeed, a study by (Rudderham, 2019) reported that P2 had the highest concentration of dissolved methane concentration in FFT pore water.

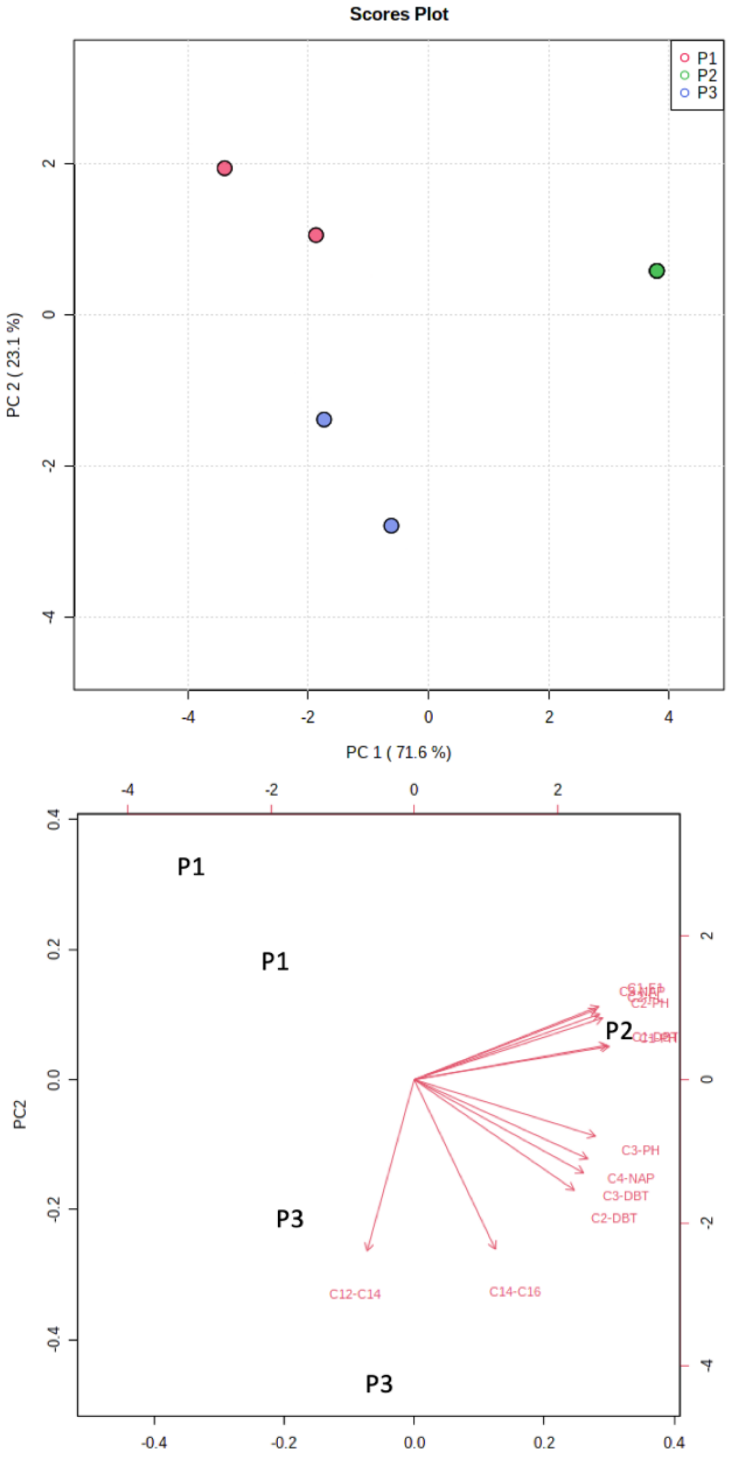


Figure 9: PCA scores and loadings plot for the GC×GC selected set of compounds concentrations at shallow interval. Replicates are represented by the same color on the PCA plot and the same letter on the loadings plot.

### *3.2.2 Characterization of the variability between deep FFT samples*

The comparisons of GC×GC resolvable compounds in the deep samples showed a different pattern compared to the shallow sample in that P3 was distinct from P1 and P2 on PC1 that explained most of the variability (84.9%) as shown in the PCA plot (Figure 10). The loadings plot shows that the lower abundances for the alkylated aromatics and higher abundances for UI-$C_{12}$-$C_{16}$ compounds at P3 were driving this separation. A one-way ANOVA test coupled to a Tukey test indicated that the following PAHs are the only significant groups that explain that variance between P3-P2 and P3-P1 ($C_1$-DBT, $C_1$-PH, $C_2$-DBT, $C_2$-Fl, $C_2$-PH, $C_3$-Nap, $C_4$-Nap). These tests have also indicated that the variance of UI-$C_{12}$-$C_{14}$ & $C_3$-DBT is only significant between P3-P1.

Thus, the analysis of GC×GC amenable compounds in deep FFT samples enabled the recognition of a distinct variation pattern in comparison to the shallow FFT samples. The variation in the pattern of resolved compounds across sites between shallow and deep FFT samples would indicate a heterogeneous distribution of hydrocarbons in the FFT. Heterogeneity in the FFT of BML has been reported previously for NAs spatial distribution analysis (Bowman et al., 2020). This heterogeneity is likely due to the various input sources that go through the oil extraction process, and the mixing of the residual bitumen through the FFT settling and deposition.

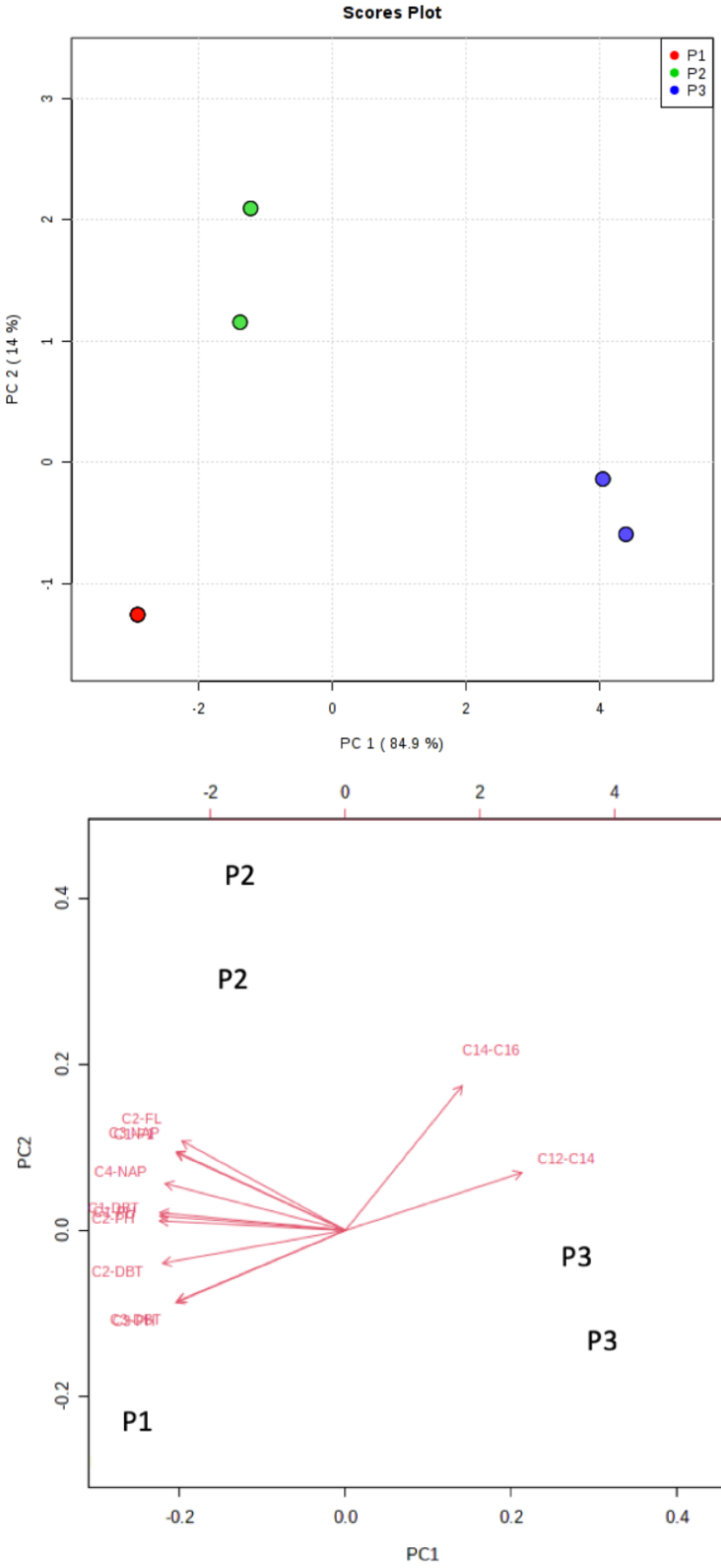


Figure 10: PCA scores and loadings plot for the GC×GC selected set of compounds concentrations at the deep interval. Replicates are represented by the same color on the PCA plot and the same letter on the loadings plot.

### 3.2.3 characterization of shallow vs deep variability

Despite the heterogeneity observed between sites at each depth interval, difference chromatographs generated between depths at all three sites showed changes in hydrocarbon distributions between shallow (10 m, ~1m below FWI) and deep (16m, ~6m below FWI) intervals. The difference chromatographs (Figure 11) between shallow vs deep at P2 and P3 is dominated by the blue color which indicates higher values at the shallow interval for the higher molecular weight and less biodegradable compounds (UI-C16-C34) in addition to compounds plotting with the highest second dimension retention times (4-6 seconds) that includes the alkylated aromatics as phenanthrenes and dibenzothiophenes. In contrast, the front end of the chromatographs, primarily for compounds with a short second dimension retention time (2-3 seconds), is dominated by the red color that indicates lower values at the shallow intervals at P2 and P3 for the low molecular weight and high biodegradable compounds (UI-C12-C16) that includes the branched and cyclic alkanes. Statistical analysis using t-test has revealed that there was a significant difference for the high biodegradability compounds with UI-C12-C14 having a P-value of 0.02 while UI-C14-16 having a less significant variation with a P-value of 0.07. This pattern is consistent with biodegradation depleting the more biodegradable compounds (UI-C12-C16) at the shallow depths at these sites, despite the indication of higher initial loadings implied by the higher molecular weight compounds and TOC data.

Unlike P2 and P3 , the difference chromatographs at P1 showed an opposite trend where the red color (depletion at shallow) dominated most of the high molecular weight end (UI-C26- C34) and aromatic region (higher second dimension retention time) of the chromatograph while the blue color (enrichment at shallow) dominated the front end that included the low molecular weight and high biodegradable compounds (UI-C12-C16). Consistent with the variation in the pattern of GC resolved compounds spatially between sites at the shallow and deep interval, the variation in the difference chromatogram patterns between shallow and deep interval at P1 compared to P2 and P3 is likely a result of the heterogeneity of the FFT within BML. This may relate to some differences in the specific compounds deposited, but also variations in the occurrence and extent of biodegradation such that there is evidence of biodegradation in the surface samples at P2 and P3 and little indication of such biodegradation at P1.

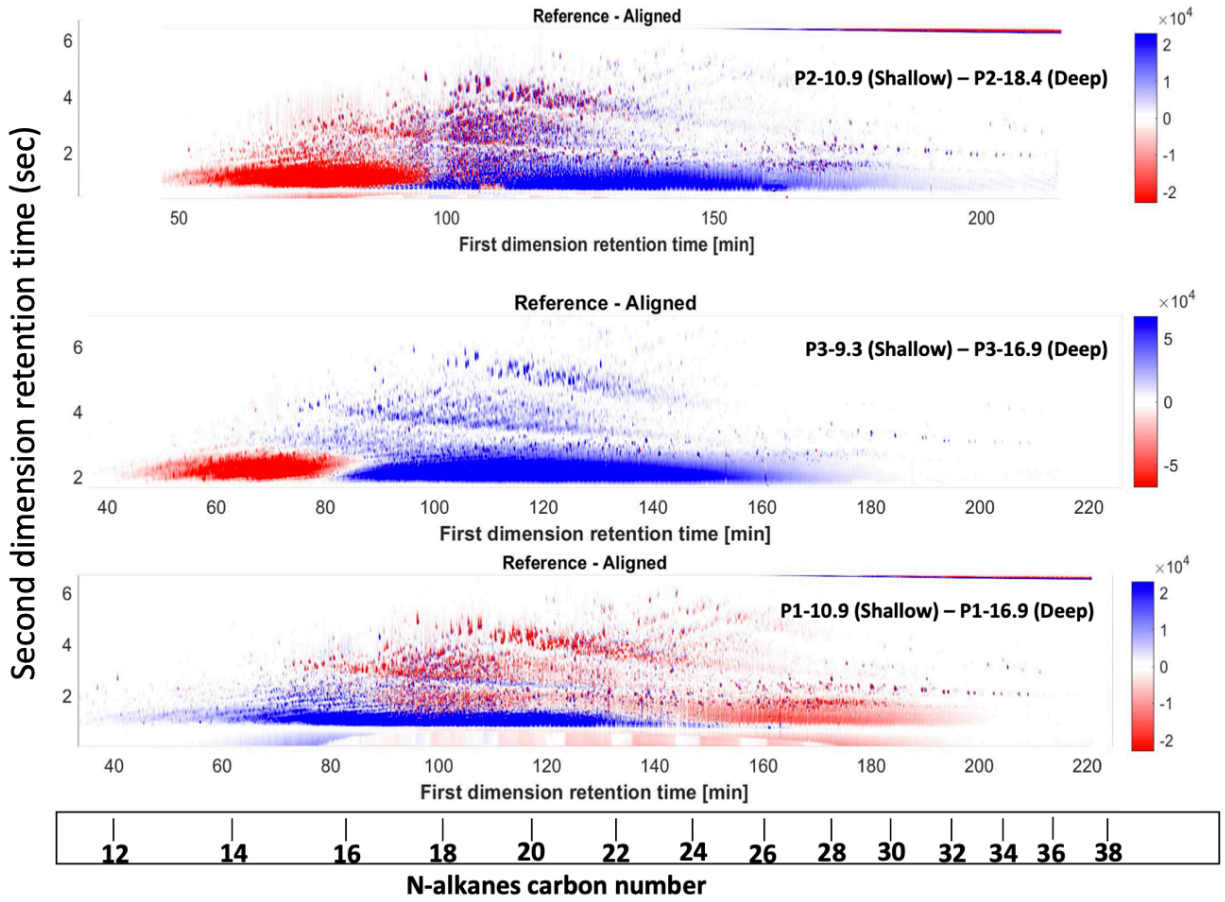


Figure 11: Difference chromatographs that shows the variability between shallow vs deep samples across P1, P2, P3.

## 3.3-Evaluation of the distribution of the hydrocarbons in BML in relation to biological cycling and methane production

Despite the heterogeneity in the system, the consistent depletion of the low molecular weight compounds UI-C12-C16 (higher biodegradability) in the difference chromatograms at shallow intervals of P2 and P3 are indicative that biodegradation is occurring. These compounds did not show a significant spatial variance when compared between the deep or the shallow intervals across the two platforms, implying that their variation at depth is not a result of the heterogeneity observed between platforms. The indication of biodegradation is further supported by the observation of higher concentrations of TOC at shallow depths of P2 and P3 (Figure 12) in addition to the remainder of the GC amenable compounds (higher molecular weight/ less

biodegradable). The presence of higher concentrations of these compounds indicates that there was likely a greater initial loading of organic matter to these sediments that would be expected to include the lower molecular weight components. The observation of biodegradation signature in the shallow sediments is consistent with the higher microbial activity that is expected to occur close to the water interface as a result of mixing of electron acceptors in the upper 1.1 m of the FFT with the water column (Dompierre et al., 2016).

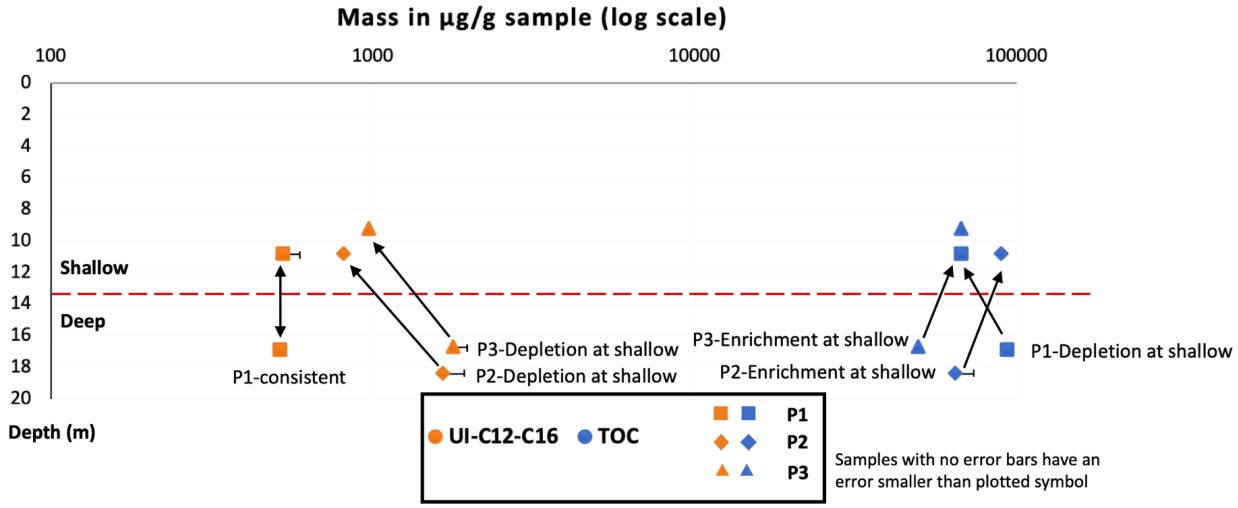


Figure 12: A plot of the concentration of the UI-C12-C16 and TOC between shallow and deep intervals.

While biodegradation is the most likely explanation for the depletion of these biodegradable compounds at P2 and P3, methane ebullition could have also contributed to their depletion. Upon oversaturation of methane, generated from hydrocarbons biodegradation in the FFT, ebullition starts to happen where methane bubbles can fracture the sediments moving upward through the water column and stripping other low molecular weight compounds through partitioning on the bubble surface or particle suspension (Yuan et al., 2007). However, since gas ebullition is a consequence to methane production, this potential explanation is also in the end evidence of a greater extent of biological degradation of hydrocarbons. Future analysis of the compounds on the bubble surface, and suspended particles could help distinguish between the contribution of

biodegradation vs ebullition towards the depletion of low molecular weight hydrocarbons in the FFT.

## 4- Conclusions

The analysis of the identity and distribution of hydrocarbons in the FFT of BML provided insights into their potential role towards methane generation within the lake. Bulk analysis of hydrocarbons in FFT showed a variable amount of TOC (49 to 93 mg/g) across platforms that are capable of generating methane. Further inspecting specific compounds using multidimensional chromatography indicates that the compounds present within the FFT included branched and cyclic alkanes, alkylated aromatics, biomarker compounds such as terpanes and hopanes. These compounds were present across all FFT samples from all platforms and depth intervals. However, the concentrations of these compounds were variable in the shallow and deep intervals across all three platforms. The low molecular weight naphtha components, that were indicated to contribute to methanogenesis in the lab, were not detected in this study, implying their absence or their presence at concentrations below the detection limit. However, there is still the possibility of their presence at sufficient concentrations to support methane production, and this possibility will be the focus of ongoing work.

The spatial variability of the TOC and the GC×GC resolved compounds indicated statistically significant higher inputs for P2 at the shallow interval ( 1m below FWI) compared to the other sites. In contrast, in the deep samples (6m below FWI) the variability did not follow the same pattern. In this case, the TOC didn't show a significant difference while the GC×GC resolved compounds showed variation in concentrations at P3 compared to the other sites. Also, the pattern of differences of GC amenable compounds between shallow and deep intervals was distinct at P1 compared to P2 and P3. This variability implies that the hydrocarbon components within the FFT are subjected to heterogeneity due to variations in source input, and thus methane production will also be expected to also vary across sites. Evidence for the occurrence of biodegradation was detected despite the heterogeneity observed for these resolved hydrocarbons across platforms. The preferential depletion of the high biodegradability compounds in concordance with the enrichment of the TOC and low biodegradability compounds at shallow

depths in P2 and P3 indicated the occurrence of in-situ biodegradation. The continuous tracking of these high biodegradability compounds spatially and temporally would provide a better understanding of the biogeochemical cycling in BML and the potential for future methane generation.

## 5- References


Aeppli, C., Carmichael, C.A., Nelson, R.K., Lemkau, K.L., Graham, W.M., Redmond, M.C., Valentine, D.L., Reddy, C.M., 2012. Oil weathering after the Deepwater Horizon disaster led to the formation of oxygenated residues. Environ. Sci. Technol. 46, 8799–8807. https://doi.org/10.1021/es3015138

Arey, J.S., Nelson, R.K., Reddy, C.M., 2007. Disentangling oil weathering using GC x GC. 1. Chromatogram analysis. Environ. Sci. Technol. 41, 5738–5746. https://doi.org/10.1021/es070005x

Arriaga, D., Nelson, T.C., Risacher, F.F., Morris, P.K., Goad, C., Slater, G.F., Warren, L.A., 2019. The co-importance of physical mixing and biogeochemical consumption in controlling water cap oxygen levels in Base Mine Lake. Appl. Geochemistry 111, 104442. https://doi.org/10.1016/j.apgeochem.2019.104442

Bowman, D.T., Warren, L.A., Slater, G.F., 2020. Isomer-specific monitoring of naphthenic acids at an oil sands pit lake by comprehensive two-dimensional gas chromatography–mass spectrometry. Sci. Total Environ. 746, 140985. https://doi.org/10.1016/j.scitotenv.2020.140985

Brown, L.D., Ulrich, A.C., 2015. Oil sands naphthenic acids: A review of properties, measurement, and treatment. Chemosphere 127, 276–290. https://doi.org/10.1016/j.chemosphere.2015.02.003

Connan, J., 1984. Biodegradation of crude oils in reservoirs. Adv. Pet. Geochemistry 1, 299–335.

Dompierre, K.A., Barbour, S.L., 2016. Characterization of physical mass transport through oil sands fl uid fi ne tailings in an end pit lake : a multi-tracer study. J. Contam. Hydrol. 189, 12–26. https://doi.org/10.1016/j.jconhyd.2016.03.006

Dompierre, K.A., Lindsay, M.B.J., Cruz-Hernández, P., Halferdahl, G.M., 2016. Initial geochemical characteristics of fluid fine tailings in an oil sands end pit lake. Sci. Total Environ. 556, 196–206. https://doi.org/10.1016/j.scitotenv.2016.03.002

Eilers, P.H.C., 2004. Parametric Time Warping 76, 404–411. https://doi.org/10.1021/ac034800e

Faidz, M., Shahimin, M., Foght, J.M., Siddique, T., 2016. Science of the Total Environment Preferential methanogenic biodegradation of short-chain n -alkanes by microbial communities from two different oil sands tailings ponds 553, 250–257.

Faidz, M., Shahimin, M., Siddique, T., 2017. Sequential biodegradation of complex naphtha hydrocarbons under methanogenic conditions in two different oil sands tailings * 221.

Frysinger, G., 2002. GC×GC—A New Analytical Tool For Environmental Forensics. Environ. Forensics 3, 27–34. https://doi.org/10.1006/enfo.2002.0077

Goad, C., 2017. METHANE BIOGEOCHEMICAL CYCLING OVER SEASONAL AND ANNUAL SCALES. Thesis.
Gouch, M.A., Rhead, M.M., Rowland, S.J., 1992. Biodegradation studies of unresolved complex mixtures of hydrocarbons: model UCM hydrocarbons and the aliphatic UCM. Org. Geochem. 18, 17–22. https://doi.org/10.1016/0146-6380(92)90139-O
Gros, J., Nabi, D., Dimitriou-christidis, P., Rutler, R., Arey, J.S., 2012. Robust Algorithm for Aligning Two-Dimensional Chromatograms. https://doi.org/10.1021/ac301367s
Gros, J., Reddy, C.M., Aeppli, C., Nelson, R.K., Carmichael, C.A., Arey, J.S., 2014. Resolving biodegradation patterns of persistent saturated hydrocarbons in weathered oil samples from the Deepwater Horizon disaster. Environ. Sci. Technol. 48, 1628–1637. https://doi.org/10.1021/es4042836
Head, I.M., Gray, N.D., Larter, S.R., 2014. Life in the slow lane; biogeochemistry of biodegraded petroleum containing reservoirs and implications for energy recovery and carbon management. Front. Microbiol. 5, 1–23. https://doi.org/10.3389/fmicb.2014.00566
Head, I.M., Jones, D.M., Larter, S.R., 2003. Biological activity in the deep subsurface and the origin of heavy oil. Nature 426, 344–352. https://doi.org/10.1038/nature02134
Head, I.M., Larter, S.R., Gray, N.D., Sherry, A., Adams, J.J., Aitken, C.M., 2010. "Hydrocarbon degradation in petroleum reservoirs," in: van derMeer, J.R., Lorenzo, V. De, Timmis, K.N., McGenity, T.J. (Eds.), Handbook of Hydrocarbon and Lipid Microbiology. (Heidelberg: Springer), pp. 3097–3109. https://doi.org/10.1007/978-3-540-77587-4
Holowenko, F.M., MacKinnon, M.D., Fedorak, P.M., 2000. Methanogens and sulfate-reducing bacteria in oil sands fine tailings waste. Can. J. Microbiol. 46, 927–937. https://doi.org/10.1139/w00-081
Hyndman, A., Sawatsky, L., McKenna, G., Vandenberg, J., 2018. Fluid Fine Tailings Processes: Disposal, Capping, and Closure Alternatives. Iostc 2018.
Jones, D.M., Head, I.M., Gray, N.D., Adams, J.J., Rowan, A.K., Aitken, C.M., Bennett, B., Huang, H., Brown, A., Bowler, B.F.J., Oldenburg, T., Erdmann, M., Larter, S.R., 2008. Crude-oil biodegradation via methanogenesis in subsurface petroleum reservoirs. Nature 451, 176–180. https://doi.org/10.1038/nature06484
Kendall, M.M., Jeanthon, C., Corre, E., Reysenbach, A.L., 2003. Microbial diversity of petroleum reservoirs. Encycl. Environ. Microbiol. https://doi.org/10.1002/0471263397.env080
Killops, S.D., Al-Juboori, M.A.H.A., 1990. Characterisation of the unresolved complex mixture (UCM) in the gas chromatograms of biodegraded petroleums. Org. Geochem. 15, 147–160. https://doi.org/10.1016/0146-6380(90)90079-F
Lovley, D.R., Chapelle, F.H., 1995. Deep subsurface microbial processes. Rev. Geophys. 33, 365–381. https://doi.org/10.1029/95RG01305
Majid, A., Sirianni, A.F., Ripmeester, J.A., 1982. Comparative study of three laboratory methods for the extraction of bitumen from oil sands. Fuel 61, 477–479. https://doi.org/10.1016/0016-2361(82)90077-1
Natural resources defense council, 2016. Alberta ' s tailings ponds 1–8.
Nelson, R.K., Kile, B.M., Plata, D.L., Sylva, S.P., Xu, L., Reddy, C.M., Gaines, R.B., Frysinger, G.S., Reichenbach, S.E., 2006. Tracking the weathering of an oil spill with comprehensive two-dimensional gas chromatography. Environ. Forensics 7, 33–44. https://doi.org/10.1080/15275920500506758
Ong, R.C.Y., Marriott, P.J., 2002. A Review of Basic Concepts in Comprehensive Two-

Dimensional Gas Chromatography. J. Chromatogr. Sci. 40, 276–291. https://doi.org/10.1093/chromsci/40.5.276
Oudot, J., 1984. Rates of microbial degradation of petroleum components as determined by computerized capillary gas chromatography and computerized mass spectrometry. Mar. Environ. Res. 13, 277–302. https://doi.org/10.1016/0141-1136(84)90034-5
Palmer, S.E., 1993. Effect of biodegradation and water washing on crude oil composition. Org. Geochemistry Princ. Appl. 511–533.
Risacher, F.F., Morris, P.K., Arriaga, D., Goad, C., Nelson, T.C., Slater, G.F., Warren, L.A., 2018. The interplay of methane and ammonia as key oxygen consuming constituents in early stage development of Base Mine Lake, the first demonstration oil sands pit lake. Appl. Geochemistry 93, 49–59. https://doi.org/10.1016/j.apgeochem.2018.03.013
Röling, W.F.M., Head, I.M., Larter, S.R., 2003. The microbiology of hydrocarbon degradation in subsurface petroleum reservoirs: Perspectives and prospects. Res. Microbiol. 154, 321–328. https://doi.org/10.1016/S0923-2508(03)00086-X
Rudderham, S., 2019. GEOMICROBIOLOGY AND GEOCHEMISTRY OF FLUID FINE TAILINGS IN AN OIL SANDS END PIT LAKE A. M. Sc Thesis.
Saidi-Mehrabad, A., He, Z., Tamas, I., Sharp, C.E., Brady, A.L., Rochman, F.F., Bodrossy, L., Abell, G.C., Penner, T., Dong, X., Sensen, C.W., Dunfield, P.F., 2013. Methanotrophic bacteria in oilsands tailings ponds of northern Alberta. ISME J. 7, 908–921. https://doi.org/10.1038/ismej.2012.163
Siddique, T., Faidz, M., Shahimin, M., Zamir, S., Semple, K., Li, C., Foght, J.M., 2015. Long-Term Incubation Reveals Methanogenic Biodegradation of C 5 and C 6 iso -Alkanes in Oil Sands Tailings. https://doi.org/10.1021/acs.est.5b04370
Siddique, T., Fedorak, P.M., Foght, J.M., 2006. Biodegradation of Short-Chain n -Alkanes in Oil Sands Tailings under Methanogenic Conditions 40, 5459–5464.
Siddique, T., Penner, T., Klassen, J., Nesbø, C., Foght, J.M., 2012. Microbial communities involved in methane production from hydrocarbons in oil sands tailings. Environ. Sci. Technol. 46, 9802–9810. https://doi.org/10.1021/es302202c
Siddique, T., Penner, T., Semple, K., Foght, J.M., 2011. Anaerobic Biodegradation of Longer-Chain n -Alkanes Coupled to Methane Production in Oil Sands Tailings 5892–5899.
Siddique, T., Phillip, M., Mackinnon, M.D., 2007. Metabolism of BTEX and Naphtha Compounds to Methane in Oil Sands Tailings 41, 2350–2356.
Siddique, T., Semple, K., Li, C., Foght, J.M., 2020. Methanogenic biodegradation of iso-alkanes and cycloalkanes during long-term incubation with oil sands tailings. Environ. Pollut. 258, 113768. https://doi.org/10.1016/j.envpol.2019.113768
Slater, G.F., Goad, C.A., Lindsay, M., Mumford, K.G., Colenbrander Nelson, T.E., Risacher, F., Jessen, G., Mori, Morris, P., Arriage, D., Warren, L., n.d. Dynamics of methane sources and microbial cycling during early development of the first oil sand pit lake.
Small, C.C., Cho, S., Hashisho, Z., Ulrich, A.C., 2015. Emissions from oil sands tailings ponds: Review of tailings pond parameters and emission estimates. J. Pet. Sci. Eng. 127, 490–501. https://doi.org/10.1016/j.petrol.2014.11.020
Stauffer, E., Dolan, J.A., Newman, R., Stauffer, E., Dolan, J.A., Newman, R., 2008. Gas Chromatography and Gas Chromatography—Mass Spectrometry, in: Fire Debris Analysis. Elsevier, pp. 235–293. https://doi.org/10.1016/B978-012663971-1.50012-9
Swarthout, R.F., Gros, J., Arey, J.S., Nelson, R.K., Valentine, D.L., Reddy, C.M., 2016. Comprehensive Two-Dimensional Gas Chromatography to Assess Petroleum Product

Weathering 129–149. https://doi.org/10.1007/8623
Vazquez-Roig, P., Pico, Y., 2012. Gas chromatography and mass spectroscopy techniques for the detection of chemical contaminants and residues in foods, in: Chemical Contaminants and Residues in Food. Elsevier, pp. 17–61. https://doi.org/10.1533/9780857095794.1.17
Ventura, G.T., Kenig, F., Reddy, C.M., Frysinger, G.S., Nelson, R.K., Mooy, B. Van, Gaines, R.B., 2008. Analysis of unresolved complex mixtures of hydrocarbons extracted from Late Archean sediments by comprehensive two-dimensional gas chromatography (GC×GC). Org. Geochem. 39, 846–867. https://doi.org/10.1016/j.orggeochem.2008.03.006
Wang, Z., Fingas, M., Blenkinsopp, S., Sergy, G., Landriault, M., Sigouin, L., Foght, J., Semple, K., Westlake, D.W.S., 1998. Comparison of oil composition changes due to biodegradation and physical weathering in different oils. J. Chromatogr. A 809, 89–107. https://doi.org/10.1016/S0021-9673(98)00166-6
Wardlaw, G.D., Arey, J.S., Reddy, C.M., Nelson, R.K., Ventura, G.T., Valentine, D.L., 2008. Disentangling oil weathering at a marine seep using GCxGC: Broad metabolic specificity accompanies subsurface petroleum biodegradation. Environ. Sci. Technol. 42, 7166–7173. https://doi.org/10.1021/es8013908
Welte, B.P.T.H., 1978. Chapter 1. Composition of Crude Oils. Pet. Form. Occur. 333–368.
Wenger, L.M., Davis, C.L., Isaksen, G.H., 2002. Multiple Controls on Petroleum Biodegradation and Impact on Oil Quality. SPE Reserv. Eval. Eng. 5, 375–383. https://doi.org/10.2118/80168-PA
Wenger, L.M., Isaksen, G.H., 2002. Control of hydrocarbon seepage intensity on level of biodegradation in sea bottom sediments. Org. Geochem. 33, 1277–1292. https://doi.org/10.1016/S0146-6380(02)00116-X
Yang, C., Wang, Z., Yang, Z., Hollebone, B., Brown, C.E., Landriault, M., Fieldhouse, B., 2011. Chemical Fingerprints of Alberta Oil Sands and Related Petroleum Products. Environ. Forensics 12, 173–188. https://doi.org/10.1080/15275922.2011.574312
Yuan, Q., Valsaraj, K.T., Reible, D.D., Willson, C.S., 2007. A Laboratory study of sediment and contaminant release during gas ebullition. J. Air Waste Manag. Assoc. 57, 1103–1111. https://doi.org/10.3155/1047-3289.57.9.1103

## Appendix

| Sample | Depth | P1 | P2 | P3 |
|---|---|---|---|---|
| **TOC** (mg/g sample) | Shallow | 68 ± 0.1% | 89 ± 0.5% | 67 ± 0.3% |
| | Deep | 94 ± 1.5% | 65 ± 13.4% | 49 ± 1.4% |
| **TLE** (mg/g sample) | Shallow | 38.3 ± 17.5% | 48.8 ± 22.5% | 31.7 ± 10.3% |
| | Deep | 41 ± 8.6% | 30.1 ± 23.3% | 25.6 ± 3.5% |
| **Saturates** (mg/g Sample) | Shallow | 9.4 ± 8.9% | 8.7 ± 0.6% | 8.4 ± 20.3% |
| | Deep | 12.9 ± 24.1% | 12.1 ± 25% | 7.4 ± 27.2% |
| **Aromatics** (mg/g Sample) | Shallow | 10.3 ± 6.6% | 10 ± 12.3% | 11.3 ± 17.6% |
| | Deep | 8.8 ± 31.3% | 10.6 ± 25.7% | 10.4 ± 12.9% |
| **Polars** (mg/g Sample) | Shallow | 11.9 ± 23.5% | 15.2 ± 6.7% | 14 ± 32.1% |
| | Deep | 21.3 ± 19.4% | 13.8 ± 33.6% | 8.4 ± 15.2% |

Table A1:Analysis of TOC, TLE, Saturates, aromatics, polars for shallow and deep intervals across P1,P2,P3 for two replicates.

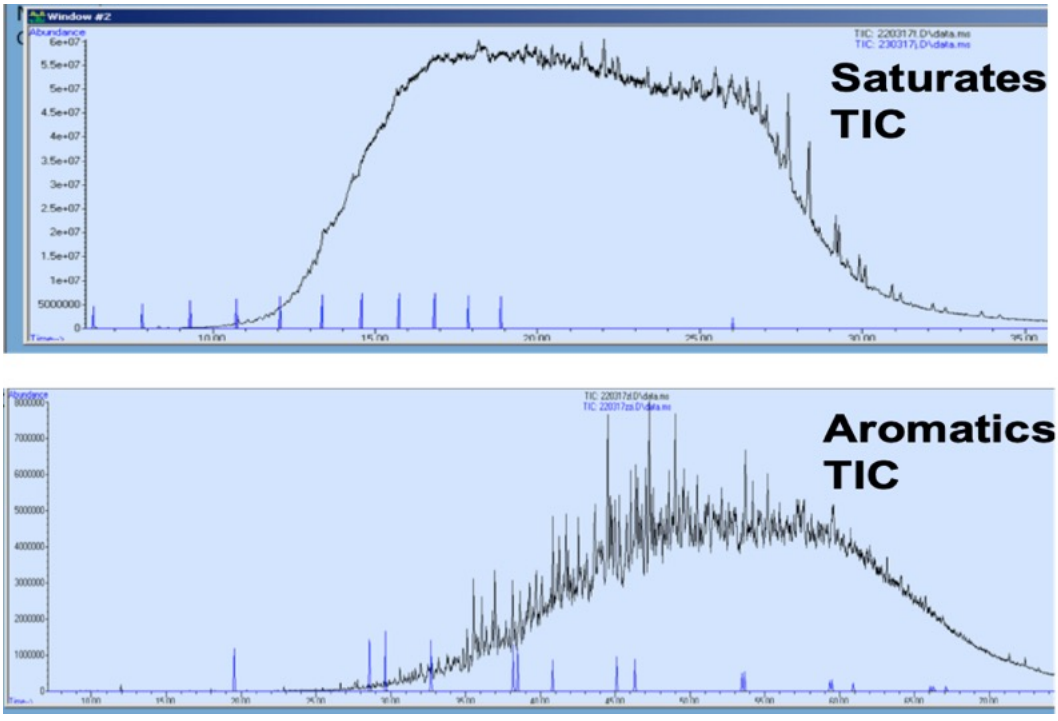


Figure A1: Gas chromatograph of the saturates and aromatics fraction that was obtained from the GC-MS. The blue peaks underneath the UCM hump represents an overlaid alkane and PAH standard.

| Hopanes | |
|---|---|
| | H |
| | NH |
| | Tm |
| | Ts |
| | |
| Homohopanes | |
| | HHR |
| | HHS |
| | 2HHR |
| | 2HHS |
| | 3HHR |
| | 3HHS |
| | 4HHR |
| | 4HHS |
| | 5HHR |
| | 5HHS |
| | |
| C1-DBT | C1-DBT-A |
| | C1-DBT-B |
| | C1-DBT-C |
| | |
| C1-F1 | C1-F1-A |
| | C1-F1-B |
| | |
| C1-PH | |
| | C1-PH-A |
| | C1-PH-B |
| | C1-PH-C |
| | C1-PH-D |

| | |
|---|---|
| C2-DBT | |
| | C2-DBT-A |
| | C2-DBT-B |
| | C2-DBT-C |
| | C2-DBT-D |
| | C2-DBT-E |
| | C2-DBT-F |
| | C2-DBT-G |
| | C2-DBT-H |
| | C2-DBT-I |
| | |
| C2-FL | |
| | C2-Fl-A |
| | C2-Fl-B |
| | C2-Fl-C |
| | C2-Fl-D |
| | C2-Fl-E |
| | C2-Fl-F |
| | |
| C2-PH | |
| | C2-PH-A |
| | C2-PH-B |
| | C2-PH-C |
| | C2-PH-D |
| | C2-PH-E |
| | C2-PH-F |
| | C2-PH-G |
| | C2-PH-H |
| | |

| C3 NAP | |
|---|---|
| | C3 Nap-A |
| | C3 Nap-B |
| | C3 Nap-C |
| | C3 Nap-D |
| | C3 Nap-E |
| | C3 Nap-F |
| | C3 Nap-G |
| | C3 Nap-H |

| C4-NAP | |
|---|---|
| | C4-Nap-A |
| | C4-Nap-B |
| | C4-Nap-C |
| | C4-Nap-D |
| | C4-Nap-E |
| | C4-Nap-F |
| | C4-Nap-G |
| | C4-Nap-H |

| C3-DBT | |
|---|---|
| | C3-DBT-A |
| | C3-DBT-B |
| | C3-DBT-C |
| | C3-DBT-D |
| | C3-DBT-E |
| | C3-DBT-F |
| | C3-DBT-G |
| | C3-DBT-H |
| | C3-DBT-I |
| | C3-DBT-J |
| | C3-DBT-K |
| | |
| C3-PH | |
| | C3-PH-A |
| | C3-PH-B |
| | C3-PH-C |
| | C3-PH-D |
| | C3-PH-E |
| | C3-PH-F |
| | C3-PH-G |
| | C3-PH-H |
| | C3-PH-I |
| | C3-PH-J |
| | C3-PH-K |
| | C3-PH-L |
| | C3-PH-M |

Table A2: List of all compounds resolved by GC×GC.

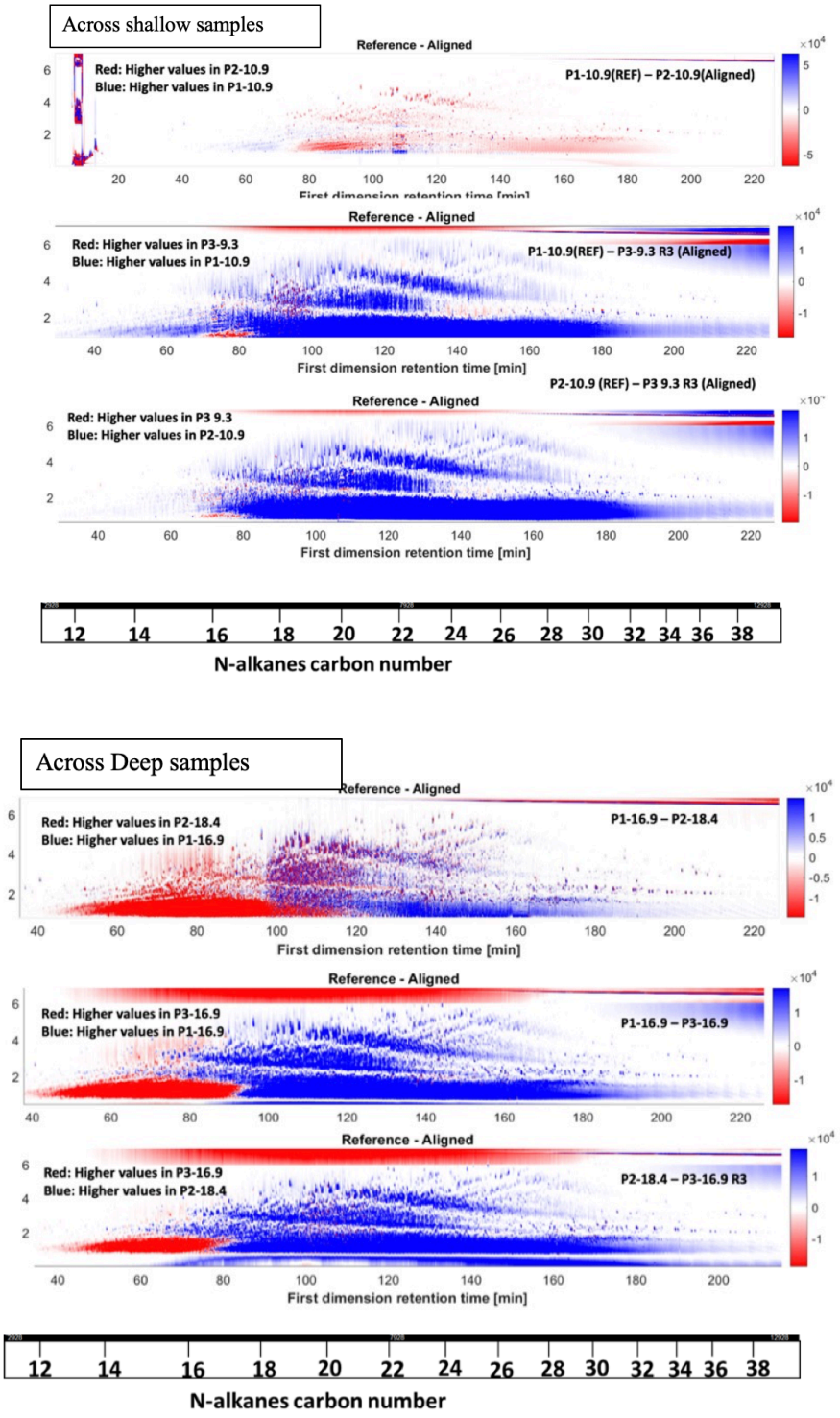





Figure A2 : Difference chromatographs across shallow and deep samples between P1, P2, P3.

A-Shallow

| Compounds | P1 | P2 | P3 |
|---|---|---|---|
| **UI-$C_{12}$-$C_{16}$** |  |  |  |
| **UI-$C_{16}$-$C_{30}$** |  |  |  |
| **Steranes** |  |  |  |
| **Hopanes** |  |  |  |
| **Benzohopanoids** |  |  |  |
| **Two-ring PAHs** |  |  |  |
| **Three-ring PAHs** |  |  |  |
| **Four-ring PAHs** |  |  |  |

B-Deep

| Compounds | P1 | P2 | P3 |
|---|---|---|---|
| **UI-$C_{12}$-$C_{16}$** |  |  |  |
| **UI-$C_{16}$-$C_{30}$** |  |  |  |
| **Steranes** |  |  |  |
| **Hopanes** |  |  |  |
| **Benzohopanoids** |  |  |  |
| **Two-ring PAHs** |  |  |  |
| **Three-ring PAHs** |  |  |  |
| **Four-ring PAHs** |  |  |  |

C-Shallow vs Deep

| Compounds | P1 | P2 | P3 |
|---|---|---|---|
| **UI-$C_{12}$-$C_{16}$** |  |  |  |
| **UI-$C_{16}$-$C_{30}$** |  |  |  |
| **Steranes** |  |  |  |
| **Hopanes** |  |  |  |
| **Benzohopanoids** |  |  |  |
| **Two-ring PAHs** |  |  |  |
| **Three-ring PAHs** |  |  |  |
| **Four-ring PAHs** |  |  |  |

Table A3: Characterization of the variability of GC-GC amenable compounds through difference chromatographs (A) The variation in shallow sample across P1,P2,P3; Red=high values, Yellow=medium values, blue=low values (B) The variation in deep sample across P1,P2,P3; Red=high values, Yellow=medium values, blue=low values (C) The variation in Shallow vs deep sample across P1,P2,P3; Red=higher values at deep interval, Blue=higher values at shallow interval .

# C3- Naphthalene

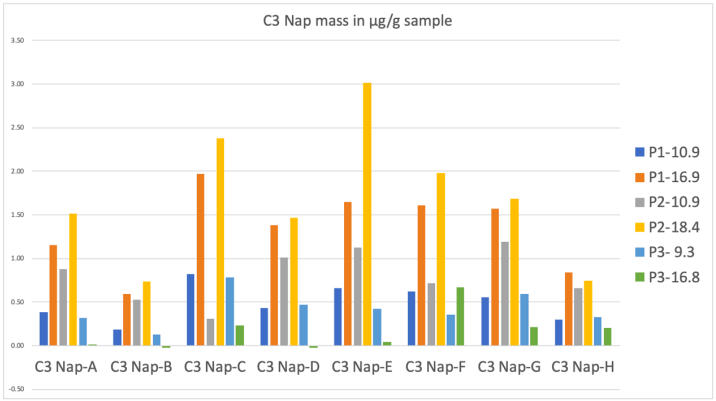


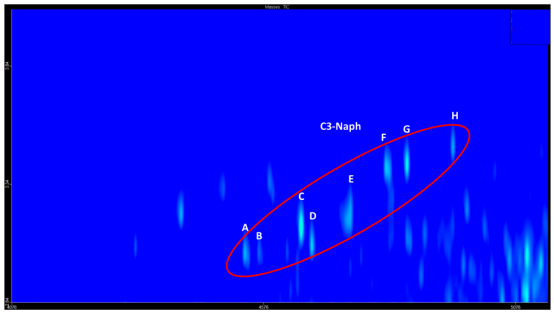


# C4- Naphthalene

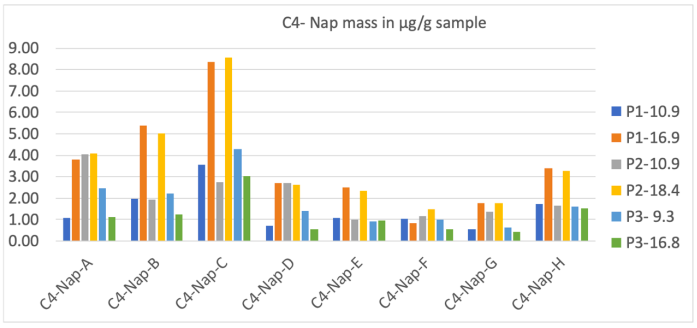


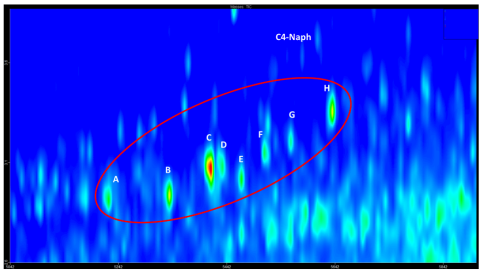


# C1 and C2 Fluorene

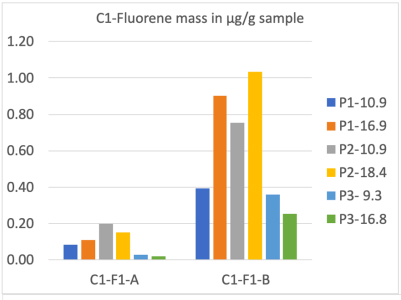


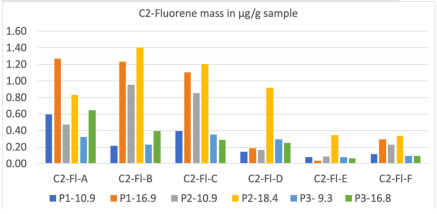


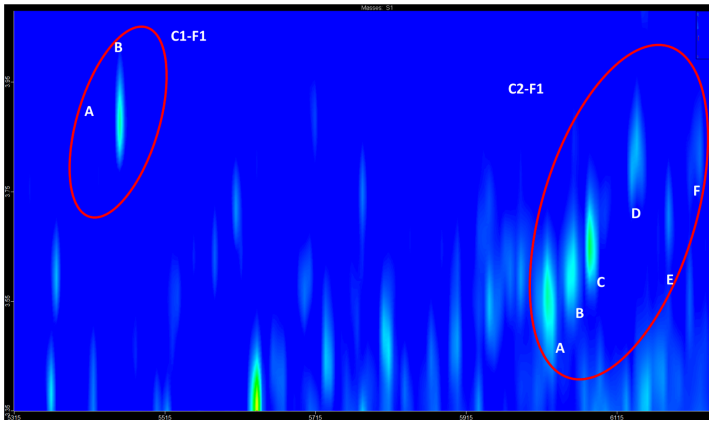

# C1-Dibenzothiophene and C1-Phenanthrene

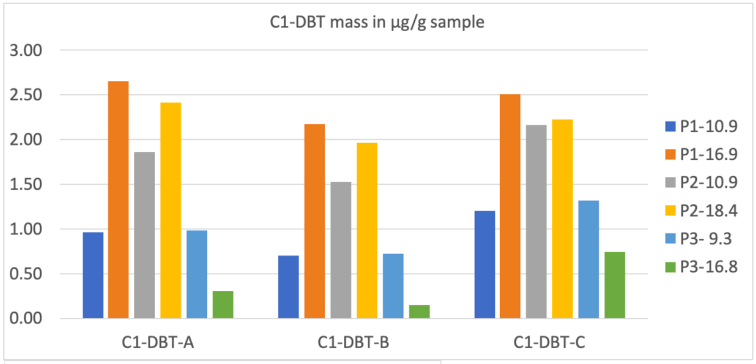


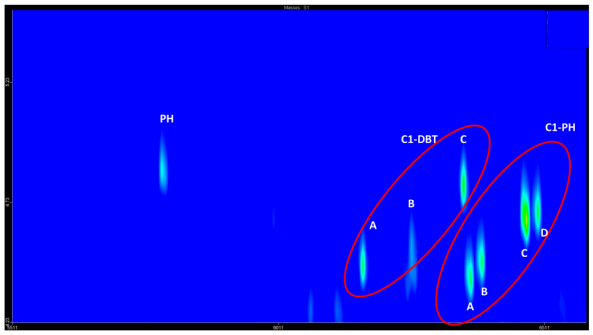


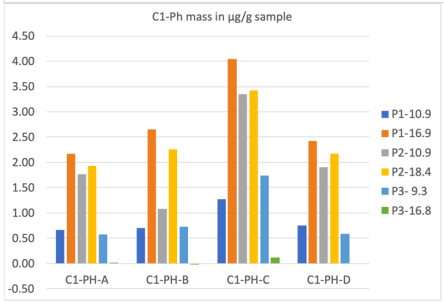


# C2-Dibenzothiophene and C2-Phenanthrene

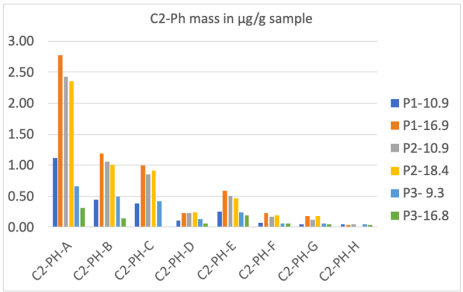


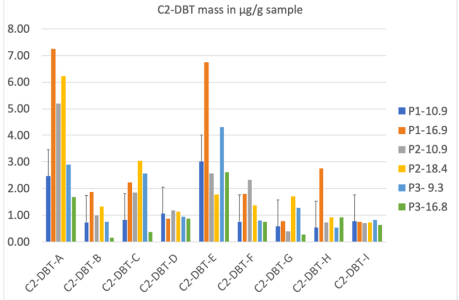


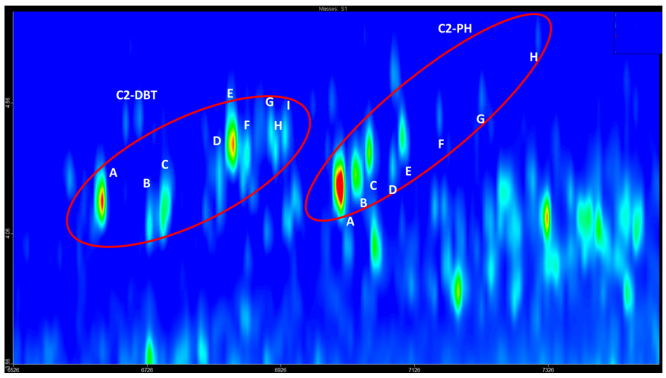

# C3-Dibenzothiophene and C3-Phenanthrene

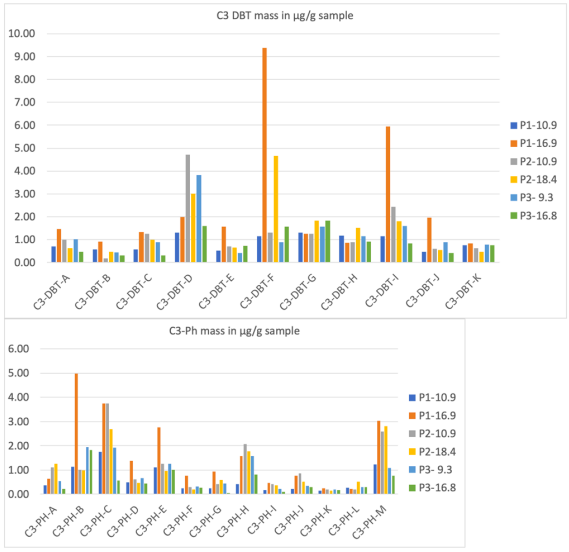





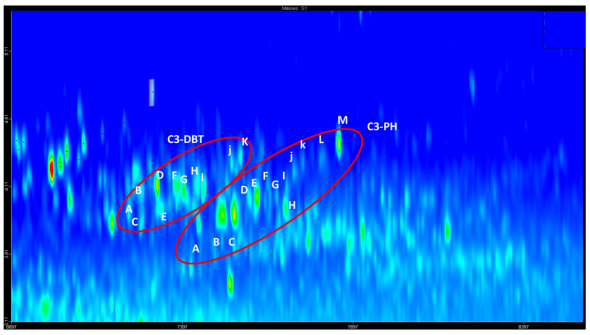


# Hopanes and homohopanes

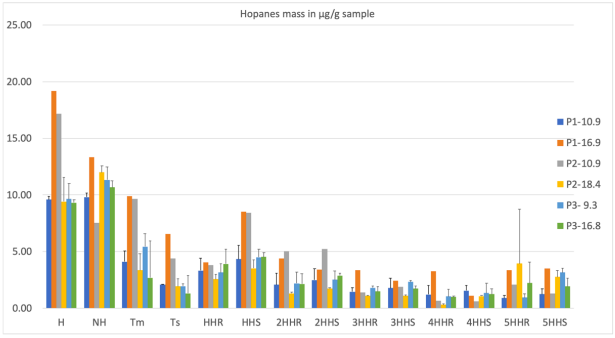


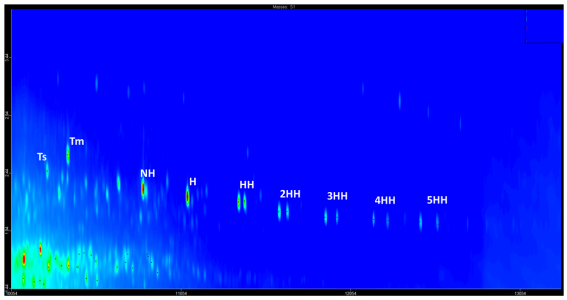


Figure A3: GC×GC chromatograph of resolved hydrocarbons and their quantified concentrations.

## Chapter three: Evaluation of naphthenic acids sources and biodegradation potential in an oil sand end pit lake

*Mohamed El-Waraky, David Bowman Robert Nelson, Christopher Reddy, Lesley Warren, Greg Slater*

### Abstract

Naphthenic (NAs) are considered as the most hazardous components of oil sands process water (OSPW) and tailings and thus understanding their fate is an important component of reclamation of tailings and oil sands sites. Syncrude has undertaken the first full-scale reclamation of oil sands tailings using water capped tailing technology (WCTT) via the commissioning of a pit lake, Base Mine Lake (BML) in 2012. The end goal of BML is the establishment of a self-sustaining ecosystem that naturally releases surface water to the Athabasca River. Understanding the presence and persistence of NAs in the water column of BML is a necessary part of assessing the overall functioning of the lake and the potential for future water release. Demonstrating the effectiveness of BML in controlling the release of hazardous compounds from tailing ponds can validate the use of WCTT.

This study applied comprehensive gas chromatography to investigate the sources and temporal variations of a selected set of analytically well resolved NAs in the BML water column during early lake development in 2015, 2017, and 2019. The analysis revealed a consistent profile of NA species and isomer distributions in all analyzed water column samples across the 4 years of the study. As it is expected that ongoing inputs of NA to the BML water column are occurring from the underlying FFT, the temporal consistency of NAs in the water column indicated that these ongoing inputs were being balanced by active microbial biodegradation. The occurrence of biodegradation was further supported by the preferential depletion of the least alkylated/cyclic species in the water column and minor enrichment of NAs in the hypolimnion relative to the epilimnion. The extent of contribution from potential source(s) of NAs to the water column of BML was assessed by comparing the molecular fingerprints of NA in the water column with those of fluid fine tailings (FFT), OSPW, and bitumen samples. The NA species and most NAs isomers abundances were similar between the water column and shallow FFT sample (at proximity to the interface) indicating the potential of mixing between the two intervals as has

been previously reported. In contrast, the abundances of deep FFT NA species and isomers were elevated relative to the water column implying the possibility of input through advection, diffusion and ebullition from the FFT to the water column. NA species and isomers abundances were comparable in OSPW and the BML water column. Since ongoing freshwater additions to BML would have diluted the NA originally present in OSPW during lake filling, this comparability implied ongoing inputs of NA to the surface water. The production of NAs as metabolites from hydrocarbons biodegradation was indicated by the unique presence of 14 NAs isomers in the water column of BML. Also, the absence of the C-8 bicyclic in bitumen samples implied their production in OSPW tailing sites and BML from biodegradation of bicyclanes. Based on these results it appears that ongoing NAs transported to the water column through advection from the FFT or produced from hydrocarbons biodegradation are being degraded, and thus the water column is providing an effective barrier to their release.

## 1-Introduction

Application of water capped tailing technology for the reclamation of Alberta oil sand mine sites and tailings commenced in 2012 with the establishment of an end-pit lake system known as Base Mine Lake (BML). The lake was developed through overlaying fluid fine tailings (FFT) deposited within the previously mined West-In pit, with a water column. The goal of this reclamation activity is to sequester the FFT below the water column and have the water column develop into a functioning ecosystem that will be a component of the long-term site closure plans for Syncrude. Ideally, this will include providing a barrier against the release of hazardous materials from the FFT via microbial metabolism of any organic compounds released from the FFT to the water column.

A point of concern related to the success of this reclamation solution is the potential release of toxic Naphthenic acids (NAs) from the FFT to the water column of BML. NAs are water-soluble, polar organic compounds with a general formula of $C_nH_{2n+z}O_2$, where n represents the carbon number and Z relates to the number of cyclic rings(Eickhoff and Laroulandie, 2010; Kindzierski et al., 2012). They are composed of a non-polar hydrocarbon chain bonded directly to an array of branched, acyclic, mono or polycyclic polar carboxylic acids that coexist with

other heteroatomic ( O, N, S) chemical species (Eickhoff and Laroulandie, 2010; Kindzierski et al., 2012). NAs are most commonly found in the environment as a constituent of petroleum hydrocarbons in the subsurface. They exist in the form of free fatty acids or bounded to the asphaltene component of hydrocarbons (Seifert, 1975; Tissot and Welte, 1985). They are generated with hydrocarbons during their charge from the kerogen or incorporated from adjacent beds during migration (Seifert, 1975; Tissot and Welte, 1985). NAs may also be generated as an intermediate metabolite during the biological transformation of hydrocarbons (Heider et al., 1998; Widdel and Rabus, 2001). For instance, several studies have found that certain species of NAs, such as $C_{30}$-$C_{32}$ hopanoids and tricyclic acids, were produced as a result of hydrocarbon biodegradation (Bennett and Abbott, 1998; Jaffé and Gallardo, 1993a; W Meredith et al., 2000; Watson et al., 2002).

The results of previous research have shown that structural differences within NAs are more likely to contribute to toxicity rather than mere increases in their concentration (Clemente and Mackinnon, 2004; Frank et al., 2009, 2008; Holowenko et al., 2002). The toxicity of NAs is mainly due to their hydrophobic non-polar chain that can enter the lipid bilayer of aquatic organisms causing disruption and cell death through narcosis (Brown and Ulrich, 2015). Previous studies by (Clemente and Mackinnon, 2004; Frank et al., 2008; Holowenko et al., 2002) have reported lower toxicity for the higher molecular weight range NAs compared to their low molecular weight range counterparts. In addition, a study by (Frank et al., 2009) showed that the increase in the number of carboxylic acid groups led to an overall decrease in hydrophobicity, which resulted in a reduction in toxicity. Accordingly, elucidating NAs molecular fingerprints is crucial towards an accurate evaluation of their toxicity.

Assessing the sources and fates of NAs using molecular fingerprinting approaches has historically been limited due to the analytical difficulties associated with resolving these compounds from the complex mixtures of acid extractable organic matter (AEO) present in most systems of interest. As AEO can contain thousands of acidic compounds, few studies were able to resolve NAs from oil sand tailings and OSPW (Ross et al., 2012; Rowland et al., 2011; Wilde et al., 2015b). Preliminary studies that attempted to identify NAs using analytical techniques, such as gas chromatography-mass spectrometry (GC-MS), were only able to identify carbon

number and Z families of these compounds (Herman et al., 1994; Holowenko et al., 2001a; Hsu et al., 2000; Scott et al., 2005). The use of high-performance liquid chromatography (HPLC) has advanced our analytical abilities through resolving the degree of cyclicity and extent of alkyl branching for NAs compounds (Bataineh et al., 2006; Han et al., 2008a). The application of comprehensive two-dimensional gas chromatography (GC×GC) has further increased the resolving of NAs in complex mixtures and has facilitated the identification of various NAs in oil sand tailings and OSPW (Bowman et al., 2014; Rowland et al., 2011; Rowland et al., 2011d; Wilde and Rowland, 2015). In this system, two columns with different stationary phases are connected sequentially in a GC oven and a modulator is used to fractionate effluent from the primary to the secondary column throughout the run (Frysinger, 2002; Ong and Marriott, 2002; Stauffer et al., 2008; Vazquez-Roig and Pico, 2012). This added dimension of separation greatly enhances the resolution of individual compounds from complex mixtures and specifically enables the resolution of isomers of individual compounds. Resolving structural isomers is particularly important in molecular fingerprinting and source delineation studies as the variation within the isomers could be used as a source parameter as well as an indicator for the various processing process such as biodegradation.

Recent studies have successfully used GC×GC for wide profiling of NAs in tailings and OSPW. For instance, (Rowland et al., 2011a) was the first study to resolve individual NAs in OSPW using the GC×GC. The study identified tricyclic diamondoid acids in OSPW that was suggested to be a byproduct of biodegradation of alkyl adamantane hydrocarbons. This was followed by another study by ( Rowland et al., 2011b) that identified various acyclic, methyl branched, and cyclohexyl acids in a commercial NAs sample refined from petroleum. Subsequently, (Bowman et al., 2014) used the high resolving power of GC×GC to identify NAs group families, in composite tailings pore water from the oil sands of Alberta, that consisted of thiophene, indane, tetralin, cyclohexane & adamantane type acids. Yet another study by (Wilde et al., 2015b) identified bicyclic NAs in OSPW using GC×GC.

In previous work in BML, (Bowman et al., 2020) demonstrated that the NAs fingerprint in the water column of BML was consistent between geochemical zones over 4 months. In contrast, the fingerprint in pore water from two FFT samples was distinct from the water column. Thus, the

study raised the question as to whether NAs were stable within the water column over longer periods, and whether there were ongoing inputs of NA from the FFT into BML. Accordingly, the temporal stability of NAs in the water column was evaluated by using the GC×GC to resolve NAs and compare their profile in the water column over 4 years from 2015-2019. Further characterization of FFT, OSPW, and bitumen samples was implemented to determine their potential contribution from potential sources to the NAs in the water column. As illustrated in figure 1, a comparison of water column NA profiles with the FFT samples assessed the potential transport of NAs upwards from the FFT through advection or ebullition to the water column (Potential source 1). Characterization of OSPW NA profile with the water column profile assessed whether the observed profile may be dominated by inputs that occurred when OSPW originally filled the lake (Potential source 2). Finally, a comparison of these NA profiles to that of raw bitumen confirms the extent to which NAs have been produced in-situ as an intermediate metabolite of hydrocarbon biodegradation (Whitby, 2010) ( potential source 3). A better understanding of stability and sources of input of NAs in a pit lake can confirm the effectiveness of the end pit lake strategy as a barrier to the release of toxic components and thus support the further application of this technology as a component of oil sands tailings reclamation.

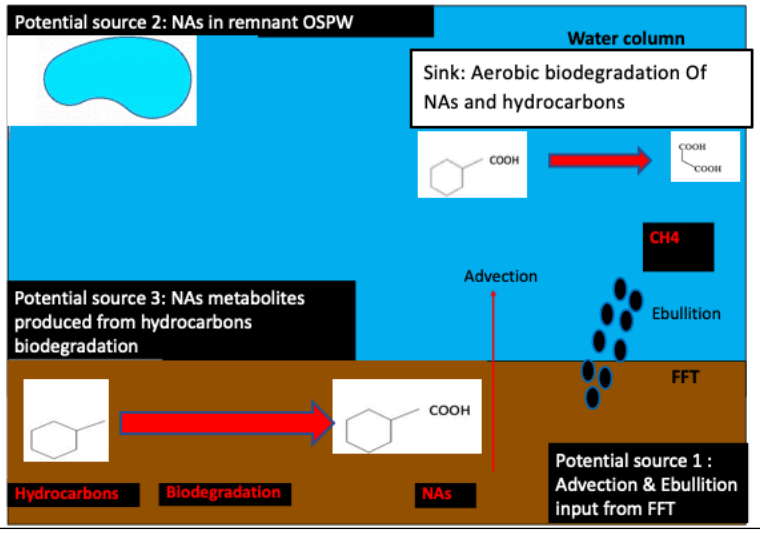


Figure 1: A sketch for the potential sources contributing to the NAs detected in the water column of BML. Methane is the gas bubbling carrying NAs upwards towards the water column on the bubble surface. The three potential sources of transport are highlighted in black text, while the potential sink is highlighted in white text.

## 2-Methods

### 2.1 Study area and sampling:

Samples were collected from Base Mine Lake (BML), mine site, north of Fort McMurray, Alberta, Canada (Figure 2). Water samples were collected by van dorn sampler from the Epilimnion (1.5m) and Hypolimnion (9-10m) at platform 1 of BML during August 2015, June 2017, and May 2019. Additionally, one FFT sample was collected from the FFT-water interface (10-11 m) and two deeper FFT (16m) from 3 locations (BML01, BML06, BML3C) in 2019 (Figure 2). Two OSPW samples were collected from MLSB (Mildred lake settling basin) and SWIP (Southwest end- pit) sites in 2019 (Figure 2). To provide a comparison to the original ore, three raw unrefined bitumen from the production lines were collected in 2019. Water and OSPW samples were collected in Nalgene bottles previously shown to have no NA blank, while FFT was collected into pails and subsamples taken away from the pail sides were then transferred into Nalgene bottles. Bitumen samples were collected in glass jars. All samples were kept frozen before extraction. The analysis of all water column, FFT, OSPW, and bitumen samples was done in triplicates.

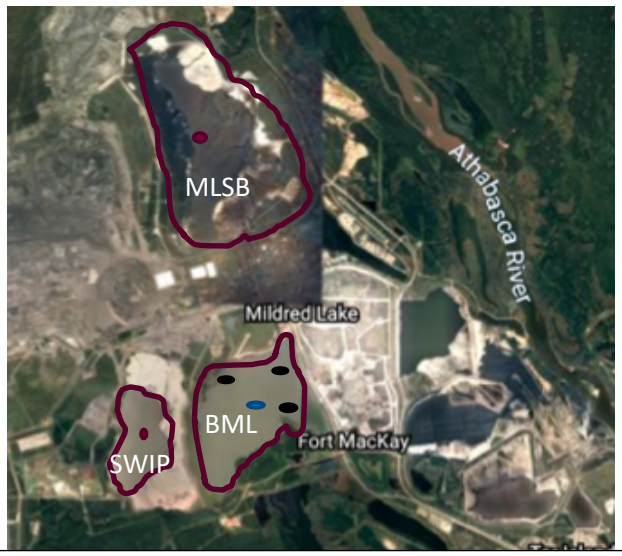


Figure 2: A satellite image of the study area in Mildred Lake, Fort McMurray, Alberta. 6 Water column samples (blue circle) collected from platform 1 in BML over 2015, 2017, 2019 from the Epilimnion and hypolimnion. 3 FFT samples (black circles) were collected from platforms BML-1901, BML-19-06, BML-3C in BML representing two samples at the deep interval ( 15m), and 1 sample at the shallower interval ( 10m). Two OSPW samples (red circle) were collected from MLSB and SWIP tailing ponds.

The water column samples were extracted using the method outlined by(Bowman et al., 2014). Briefly, 20 ml water samples were filtered through a 0.45 μm syringe filter, then acidified to PH< 2, extracted with dichloromethane ( 15 ml× 4) using liquid-liquid chromatography. The extract was blown down with inert $N_2$ gas to 30 μl then derivatized by adding a freshly prepared diazomethane. The diazomethane is prepared by adding Diazold, Dimethylester, Carbitol in an inner tube surrounded by an outer tube that contains DCM. Then the diazomethane generation is initiated by the addition of 1.5 ml of 37% KOH aqueous solution dropwise to the contents of the inner tube via the septum using a plastic syringe with a narrow-gauge (no.22) needle. Then, the diazomethane generated is added to the samples dropwise until the yellow colour persisted to methyl any carboxylic acid groups into methyl esters. Finally, 5∝-cholestane is added as an internal standard, and the extract ran on the GC×GC MS. The fluid fine tailings were centrifuged at 3600 RPM for 90 minutes, and then the supernatant was collected(Bowman et al., 2020), then extracted as the water samples mentioned above. The bitumen samples were first extracted by adding 100 ml water, left to partition for 24 hours, then the aqueous phase was collected, and extracted as mentioned above for the water samples.

**2.3 Instrumental analysis**

Samples were analyzed using a GC×GC Pegasus 4D system that used an Rtx-17sil ms (30 m x 0.25 mm x 0.15 μm) as the primary column and DB-5ms (1 m x 0.1 mm x 0.1 μm) as the secondary column. The analysis method is as follows: the primary oven temperature was initiated at 80 °C (held for 15 minutes), then the temperature was ramped up to 335 °C with a rate of 1.66 °C /min. Whereas the secondary oven temperature was initiated at 85 °C (held for 15 minutes), then the temperature was ramped up to 340 °C with a rate of 1.66 °C /min. The modulation period used was 7.5s. The TOFMS data acquisition rate was 100 HZ, the detector voltage was 1425 V, and the mass spectrometer used voltage energy of -70 eV.

## 2.4 Data processing:

The data processing of all the samples was performed using LECO Chroma TOF 4.5.1. The compounds were identified from the list of NA target compounds in (Bowman et al., 2020), in addition to using an in-house library, and the NIST mass spectral library. The list of all the compounds identified in the sample is presented in Table 1. Following the method by (Bowman et al., 2020), the relative abundance of all identified compounds was calculated by normalizing peak areas to the internal standard 5-α cholestane, then multiplying by 1000.

## 2.5 Statistical testing

The PCA scores plot for all the resolved compounds across all samples was performed using MetaboAnalyst 4.0 online platform. The resolved abundances were preprocessed first to remove any bias terms from the data through centering and scaling the data (centering means subtracting the mean from each column in the data matrix then it is scaled through dividing by the standard deviation).

The significance of the variance of the resolved NA isomers was tested using one-way ANOVA and T-test. One-way ANOVA tests for the variation between 3 or more means whereas these variations are considered significant if they have a P-value of $<0.05$. The one-way ANOVA test was followed by a Tukey test to determine what specific pairs had the significant variance. On the other hand, T-test variations were considered significant if the P-value is $\leq 0.05$, and marginally significant if $\leq 0.1$. These tests were also performed using MetaboAnalyst 4.0.

| Isomer no | Isomer-name | NA species | Isomer no | Isomer-name | NA species | Isomer no | Isomer-name | NA species |
|---|---|---|---|---|---|---|---|---|
| 1 | 208-A | C12-adamntane | 32 | 168-E | C-9 bicyclic | 63 | 196-L | C-11 bicyclic |
| 2 | 208-H | C12-adamntane | 33 | 168-F | C-9 bicyclic | 64 | 196-M | C-11 bicyclic |
| 3 | 208-I | C12-adamntane | 34 | 168-G | C-9 bicyclic | 65 | 196-N | C-11 bicyclic |
| 4 | 208-J | C12-adamntane | 35 | 168-H | C-9 bicyclic | 66 | 196-O | C-11 bicyclic |
| 5 | 208-K | C12-adamntane | 36 | 168-I | C-9 bicyclic | 67 | 196 k-1 | C-11 bicyclic |
| 6 | 208-C | C12-adamntane | 37 | 168-J | C-9 bicyclic | 68 | 184-1 | C-10 monocyclic |
| 7 | 208-D | C12-adamntane | 38 | 168-K | C-9 bicyclic | 69 | 184-2 | C-10 monocyclic |
| 8 | 208-E | C12-adamntane | 39 | 168-L | C-9 bicyclic | 70 | 184-3 | C-10 monocyclic |
| 9 | 208-F | C12-adamntane | 40 | 168-M | C-9 bicyclic | 71 | 184-4 | C-10 monocyclic |
| 10 | 208-G | C12-adamntane | 41 | 168-N | C-9 bicyclic | 72 | 184-5 | C-10 monocyclic |
| 11 | 194-A | C11-adamntane | 42 | 182-A | C-10 bicyclic | 73 | 184-6 | C-10 monocyclic |
| 12 | 194-B | C11-adamntane | 43 | 182-B | C-10 bicyclic | 74 | 184-7 | C-10 monocyclic |
| 13 | 194-1 | C11-adamntane | 44 | 182-D | C-10 bicyclic | 75 | 184-8 | C-10 monocyclic |
| 14 | 194-2 | C11-adamntane | 45 | 182-D2 | C-10 bicyclic | 76 | 184-1B | C-10 monocyclic |
| 15 | 170-1 | C7-thiophene | 46 | 182-E | C-10 bicyclic | 77 | 184-2B | C-10 monocyclic |
| 16 | 170-2 | C7-thiophene | 47 | 182-F | C-10 bicyclic | 78 | 184-3B | C-10 monocyclic |
| 17 | 170-3 | C7-thiophene | 48 | 182-G | C-10 bicyclic | 79 | 184-4B | C-10 monocyclic |
| 18 | 170-4 | C7-thiophene | 49 | 182-H | C-10 bicyclic | 80 | 184-5B | C-10 monocyclic |
| 19 | 170-B | C7-thiophene | 50 | 182-I | C-10 bicyclic | 81 | 184-1C | C-10 monocyclic |
| 20 | 170-C | C7-thiophene | 51 | 182-M | C-10 bicyclic | 82 | 184-2C | C-10 monocyclic |
| 21 | 170-A | C7-thiophene | 52 | 182-N | C-10 bicyclic | 83 | 184-3C | C-10 monocyclic |
| 22 | 170-D | C7-thiophene | 53 | 196-B | C-11 bicyclic | 84 | 184-4C | C-10 monocyclic |
| 23 | 154-E | C-8 bicyclic | 54 | 196-C | C-11 bicyclic | 85 | 184-5C | C-10 monocyclic |
| 24 | 154-1 | C-8 bicyclic | 55 | 196-D | C-11 bicyclic | 86 | 184-6C | C-10 monocyclic |
| 25 | 154-2 | C-8 bicyclic | 56 | 196-E | C-11 bicyclic | 87 | 184-F | C-10 monocyclic |
| 26 | 168-1 | C-9 bicyclic | 57 | 196-F | C-11 bicyclic | 88 | 184-G | C-10 monocyclic |
| 27 | 168-2 | C-9 bicyclic | 58 | 196-G | C-11 bicyclic | 89 | 184-H | C-10 monocyclic |
| 28 | 168-3 | C-9 bicyclic | 59 | 196-H | C-11 bicyclic | 90 | 184-I | C-10 monocyclic |
| 29 | 168-4 | C-9 bicyclic | 60 | 196-I | C-11 bicyclic | 91 | 184-J | C-10 monocyclic |
| 30 | 168-5 | C-9 bicyclic | 61 | 196-J | C-11 bicyclic | 92 | 184-K | C-10 monocyclic |
| 31 | 168-D | C-9 bicyclic | 62 | 196-K | C-11 bicyclic | | | |

Table 1: List of NAs isomers identified in water column, FFT BML, OSPW, and bitumen samples.

## 3-Results and discussion

### 3.1 Stability of NAs in the water column of BML:

For this study, a set of 92 individual NA compounds, adapted from (Bowman et al., 2020), were identified using the GC×GC. The relative abundances of these compounds (calculated by normalizing peak areas to internal standard then multiplying by 1000 ) were used as an analog for their concentration following the method of (Bowman et al., 2020). This set of compounds was made up of groups of isomers of the following NA species: C11 adamantane; C12 adamantane, C8 bicyclic, C9 bicyclic, C10 bicyclic, C11 bicyclic, C10 monocyclic, and C7 thiophene.

The relative abundance for all NA species in the water column, (determined by the summation of all isomers of each species) was highest for the thiophanate species (C-7 thiophene), followed by the higher ring moieties such as adamantanes, and higher alkyl branching species. The abundances followed this order of decreasing abundance: C-7 thiophene > C12 adamantane ≥ C11 bicyclic > C 10 bicyclic ≥ C 11 adamantane > C9 bicyclic ≥ C8 bicyclic > C10 monocyclic. This pattern was consistent with the study by (Bowman et al., 2020) that found that BML water column samples also exhibited elevated abundances for the higher alkyl branching and ring moieties NA species.

The NA species abundances were consistent across the three time points (2015, 2017, 2019) within both the epilimnion and hypolimnion (Figure 3). Minor variations were observed for each NA species between the time points, in particular the C10 monocyclic and C8 bicyclic species, but were not statistically significant (One-way ANOVA: P-value > 0.05). The previous study by (Bowman et al., 2020) reported also no significant variation in the epilimnion while they observed minor variations in the C-8 bicyclic and C-10 monocyclic species in the hypolimnion. Comparison of the NAs species between the epilimnion and the hypolimnion revealed no statistically significant variation for most species. The C7 thiophene was the only species to show a significant variation between zones as a result of the elevated abundances in the hypolimnion. The study by (Bowman et al., 2020), also reported that the C7 thiophene was the only species to significantly vary between zones due to the elevated abundances in the hypolimnion.

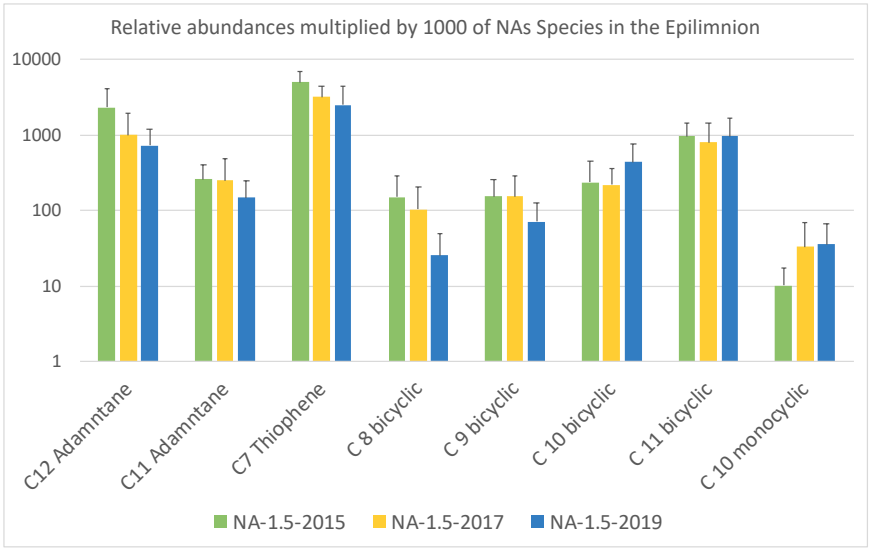


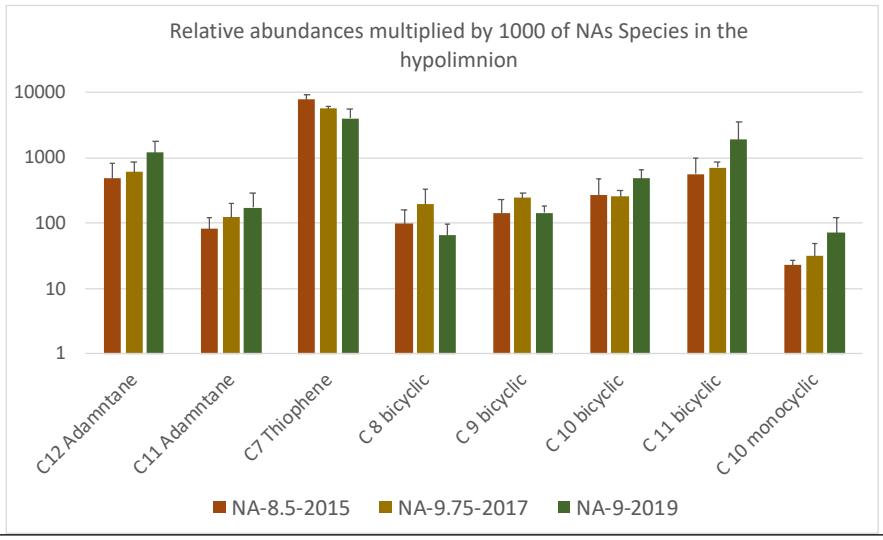


Figure 3: Relative abundances for each NA species calculated by the summation of all NAs isomers within each species multiplied by 1000. Each bar represents the average of all triplicate analysis for 2015, 2017, 2019 time points in the epilimnion and the hypolimnion of BML.

The distributions of individual isomers of each NA species were also consistent across the three time points 2015, 2017, 2019. A PCA plot (Figure 4) of the relative abundances of all the 92 individual NAs isomers in the water column show all three-time points cluster in one zone except two outliers for one replicate from 2015 and 2019 samples. A one-way ANOVA analysis revealed that there wasn't any statistically significant variability between all the NA isomers. The study by (Bowman et al., 2020) also reported that most NAs isomers didn't show a

significant change except for a few isomers mostly in the hypolimnion. Comparison of the NAs isomers relative abundances between epilimnion and hypolimnion show no statistically significant variation except for two isomers for the C-7 thiophene, and one isomer from C-9 bicyclic and C11 bicyclic. All these four isomers showed a significant variation due to their enrichment at the hypolimnion.

Ongoing inputs of FFT porewater and associated NAs to the BML water column are expected to be occurring based on the elevated abundances of NA species within the FFT observed by (Bowman et al., 2020), and the modelling of ( Dompierre and Barbour, 2016) that showed exchange between the upper 1m of the FFT and the water column. Similarly, biodegradation of NA within the water column is expected based on aerobic microcosm studies for NAs biodegradation (Clemente and Mackinnon, 2004; Gervais, 2004). The temporal stability of the monitored NAs in the water column in addition to the depletion of the least alkylated/cyclic species that are preferentially degraded(Han et al., 2008b; Smith et al., 2008) , and the slight elevation of some species in the hypolimnion relative to the epilimnion suggest that if such ongoing inputs are occurring, degradation is balancing them such that the observed NA distributions remain relatively constant.

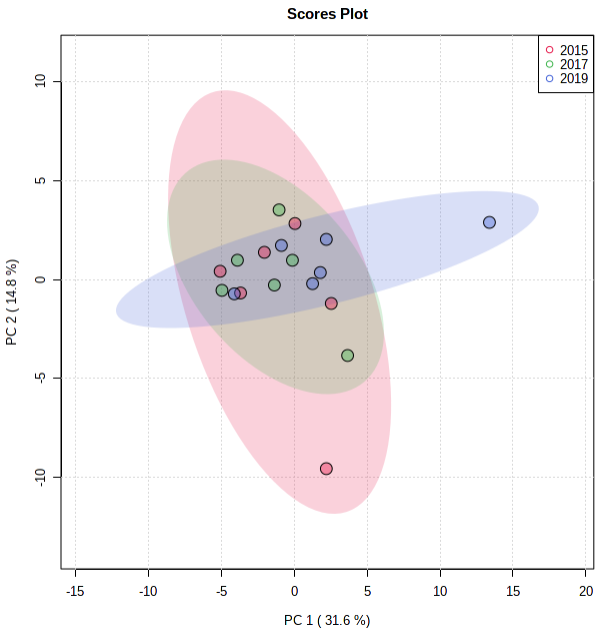


Figure 4: PCA plot for the relative abundances of the NAs individual isomers in the water column of BML for the average of 2015, 2017, 2019 samples.

### 3.2 Assessment of Potential sources of NAs input to the water column of BML:

To evaluate the contribution of potential sources of NAs observed in the water column of BML, the NA distributions within the water column were compared to FFT porewater that is hypothesized to represent an ongoing source, the OSPW that was originally used to fill the lake, and bitumen which is the original source of the NAs within the BML system.

#### *3.2.1 Comparison of NAs species relative abundances between the water column and FFT of BML*

A comparison of NA distribution fingerprints between the FFT and water column indicated that the FFT and particularly the deeper FFT was a potential source of NAs to the water column. The NA distribution fingerprint in the shallow FFT sample (1 m from FFT water interface and 10 m from water surface) showed no statistically significant difference for most NA species to the average of water column samples (Figure 5), though the C-7 thiophene and the C-10 bicyclic NAs species showed a marginally significant variation due to enrichment in the water column (P-values= 0.07, 0.08). The similarity observed in the abundances for most NAs species between the shallow FFT and water column is consistent with the proposed exchange between these intervals proposed by ( Dompierre and Barbour, 2016).

In contrast, the two deeper FFT samples showed elevated NA species abundances and distinct distributions as compared to the water column samples (Figure 5). The enrichment of the deep FFT was statistically significant (P-value $\leq 0.05$) for the C9 bicyclic, and C10 monocyclic, while marginally significant (P-value $\leq 0.1$) for the C8 bicyclic, and C11-adamnatne, and C-7 thiophene. These observations are consistent with (Bowman et al., 2020) who found elevated FFT NA species abundances relative to the water column. The previous study by (Dompierre and Barbour, 2016) using isotope and heat tracers showed that advective diffusive mass transport occurs vertically from the FFT pore water upon consolidation into the water column. The observed overall elevated NAs species and isomers abundances in deep FFT suggest that the upwards transport of NA from the FFT porewater to the water column/shallow FFT can occur as demonstrated by (Dompierre and Barbour, 2016) through advection of porewater during FFT

compaction, in addition to inputs associated with water transport during ebullition and by molecular diffusion.

It's worthy to note that the FFT didn't show a preferential depletion signature for the more biodegradable low alkylated/cyclic species that was obvious in the water column. This may be due to the fact that effective microbial metabolism and removal of NAs occurs under aerobic conditions, similar to the water column of BML, in comparison to the anaerobic FFT (Clemente and Mackinnon, 2004; Scott et al., 2005). For instance, (Gervais, 2004) studied the effect of aerobic vs anaerobic degradation in a microcosm prepared from groundwater aquifers adjacent to tailing ponds that contained NAs. The study found that 60% of the acyclic, bicyclic and tricyclic NAs were degradable in aerobic culture while anaerobic culture didn't show any evidence for biodegradation during a period of 6 months. Thus, the elevation of the abundances of low alkylated/cyclic species in the FFT in comparison to the water column further supports that the depletion of these species in the water column was a result of biodegradation.

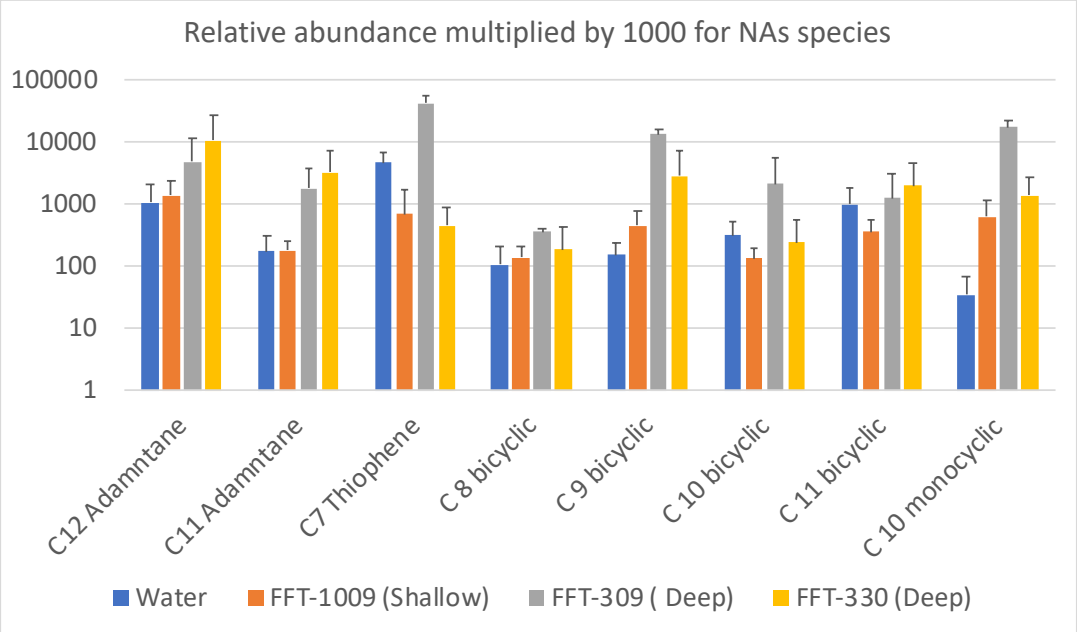


Figure 5: Relative abundance of NAs species in average of water column samples in comparison to the average of triplicate analysis for shallow and deep FFT samples.

*3.2.2 Comparison of NAs species relative abundances between the water column and OSPW*

As BML was originally filled with OSPW that was subsequently diluted with freshwater inputs, the NA present in the water column could represent diluted remnants of the original OSPW inputs. To assess this, the relative abundances of the NAs species observed within the water column were compared between the water column and OSPW samples. The triplicate analysis for the two OSPW samples from the MLSB and SWIP sites showed no statistically significant difference for their NAs species abundances, and thus the average of all OSPW samples was compared to that of the water column (Figure 6). The comparison revealed that the relative abundances of the NAs in the water column and OSPW were not significantly different for the C8 bicyclic and C11 and C12 adamantanes. However, the relative abundances were distinct for the other NA species. There was a statistically significant (P-value $< 0.05$) enrichment of C 10 monocyclic and C 9 bicyclic NAs species in the OSPW. Also, there was a statistically significant enrichment of C7 thiophene and C 10 bicyclic species and a marginally significant enrichment of C 11 bicyclic in the water column.

Recognizing that the OSPW analyzed was not the same as that used to fill BML in 2012 it is possible that the differences in NAs species abundances compared to the water column are due to variations in OSPW NA distributions over time. However, since the OSPW in BML has been diluted by the addition of freshwater it would be expected that the BML NA abundances would be less than in OSPW. The observation of similar abundances between the water column and OSPW for three NAs species and enrichment of two species in the water column suggests that ongoing inputs of these species have been occurring into the water column.

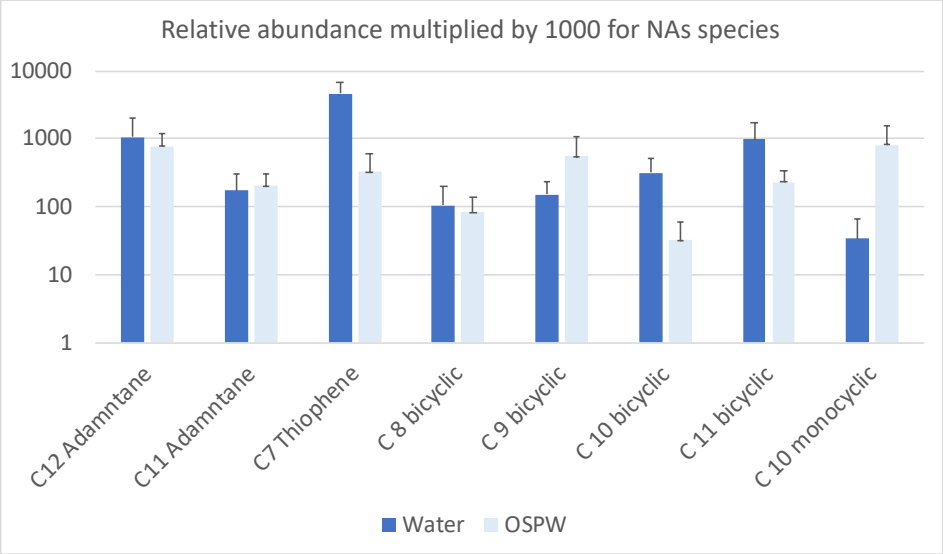


Figure 6: Relative abundances of NAs species in average of all water column samples in comparison to the average of two OSPW samples (MLSB and SWIP) in triplicates.

*3.2.3 Comparison of NAs species relative abundances between the water column and bitumen*

The NA observed within the BML systems originated either as a component of the bitumen ore or due to degradation of the hydrocarbon components of this ore during processing tailings storage or within BML. To assess the contributions of the original ore, NA distribution fingerprints from unrefined bitumen samples, representing a pre-processing time point, were compared to the water column, FFT, and OSPW samples. The bitumen samples were extracted in water in order to mimic the scenario at BML and OSPW sites where the NAs within the residual bitumen in the tailings partition into the aqueous phase.

The first notable observation was that the C-8 bicyclic NAs species were not detected in any of the bitumen samples. The absence of the C-8 bicyclic NAs in the bitumen indicates that generation of these compounds occurred at a time point post extraction from the subsurface. While, all other NAs species were present in the bitumen, implying that they are an original component of the deposit as well as potentially being produced post-extraction during in situ

biodegradation. These C-8 bicyclics could be generated as a transformative product of bicyclanes(Wilde et al., 2015b). Hydrocarbons analysis in the FFT (Chapter 2) didn't resolve any of the cycloalkanes as they eluted within the UCM region. The absence of C-8 bicyclic NAs in the bitumen implies that the biological processing of hydrocarbons is a source of NAs input into the tailing sites or BML.

A second notable observation was that the relative abundances of NA species were variable between the water column and bitumen samples. Bitumen samples (13:30) and (15:30), were comparable to each other, and consistently higher in NAs species abundances than the water column (Figure 7). The enrichment of the C-12 adamantane, C-11- adamantane, C-9 bicyclic, C-11 bicyclic, C-10 monocyclic, and C-7 thiophene at the bitumen compared to the water column were statistically significant (P-value= 0.02, 0.02, 0.03, 0.03, 0.04 respectively), while the enrichment for the C-10 bicyclic was marginally significant (P-value= 0.08). However, the bitumen sample (17:30) NA species abundances were distinct from the other two samples and comparable to the water sample. The variability observed for the bitumen samples illustrates that this is a heterogeneous system. And while such heterogeneity over time would be expected to contribute to variations in NA distributions in the OSPW, FFT and water column, the strong elevation NAs species in the bitumen relative to these other pools, indicates that biological processing has likely depleted NAs post-extraction.

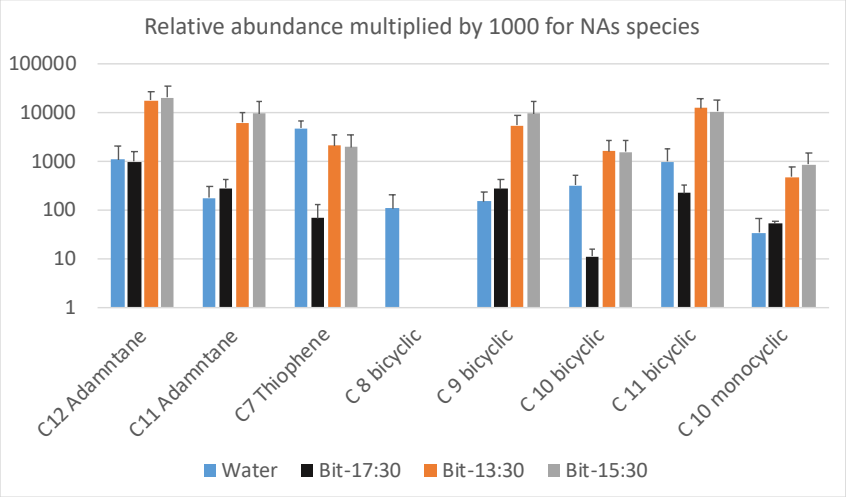


Figure 7: Relative abundances of NAs species in average of all water column samples in comparison to the average of triplicate analysis for bitumen samples.

*3.2.4 Comparison of NA isomers relative abundances across all samples using PCA plots*

The relative abundance of individual NA isomers identified by GC× GC was used to further explore the drivers of the variability across water column, FFT, OSPW, and bitumen samples NA species and to evaluate the evidence for biodegradation. The relative abundance of individual isomers across all samples was characterized using the PCA plot shown in figure 8. Each circle in the plot represents one out of 3 triplicates for each FFT, OSPW, and bitumen sample, while the water column circle symbols represent the average of triplicate analysis for 2015, 2017, 2019 time points.

Figure 8 shows that the water column and bitumen samples had the most distinct NAs isomer distributions and that the OSPW and FFT samples clustered together near the origin of the plot. In fact, in PC1, which explained the majority of the variation (37%), the water, OSPW, and FFT all clustered together. However, one replicate of two deep FFT samples was separated from the cluster of all the other samples on PC1. These samples plotted along a line consistent with the two bitumen samples that had the highest abundances of NAs species. The following 8 isomers drove this variability in the FFT samples: **C8 bicyclic:** 154-1/ **C9 bicyclic:** 168-4, 168-5, **C10 monocyclic:**184-1, 184-1B/ **C7 thiophene** 170-1, 170-3, 170-B, while the following 16 isomers were driving this variability at the two bitumen samples (**C10 bicyclic**: 182-F, 182-G, 182-A/ **C11- bicyclic:** 196-K, 196-B, 196-O, 196-H, 196-M, 196-E, 196-D, 196-C/ **C10 monocyclic:** 184-8/ **C7 thiophene:** 170-4, 170-A, 170-C, 170-D). Since we don't know the specific structural configuration of each isomer, we couldn't assess whether the elevated abundances of the isomers in the deep FFT and bitumen samples are related to biodegradation.

While the water column plotted closely with FFT and OSPW in PC1, the variation observed in PC2 (14%) was entirely driven by distinct isomers present in the water column (Figure 9). The isomers driving this distinction were the following 14 isomers: **C8 bicyclic:** 154-2 / **C9 bicyclic:**168-D, 168-J, 168-E, 168-I, 168-G, 168-H, 168-N/ C**10 bicyclic:** 182-H, 182-N, 182-M/ **C10 monocyclic:**184-I,184-H/ **C11 adamntane:**194-2. The absence of these 14 isomers in the

FFT, OSPW, and bitumen could imply that they have been preferentially biodegraded in these samples. However, the unique presence of these isomers only in water samples suggests that they could be recently produced as a metabolic intermediate through aerobic biodegradation in the water column. These newly generated NAs isomers can be produced through a series of oxidations of the parent hydrocarbons (Rojo, 2009). The bicyclic NAs isomers would be produced from the bicyclic alkanes, the monocyclic would be products of cycloalkanes, and the adamantane NAs would be generated from adamantane hydrocarbons ( Rowland et al., 2011; Wilde and Rowland, 2015). Thus, studying the isomer distribution of NAs in all samples enabled the detection of a biological cycling signature that was not observed through the NAs species analysis.

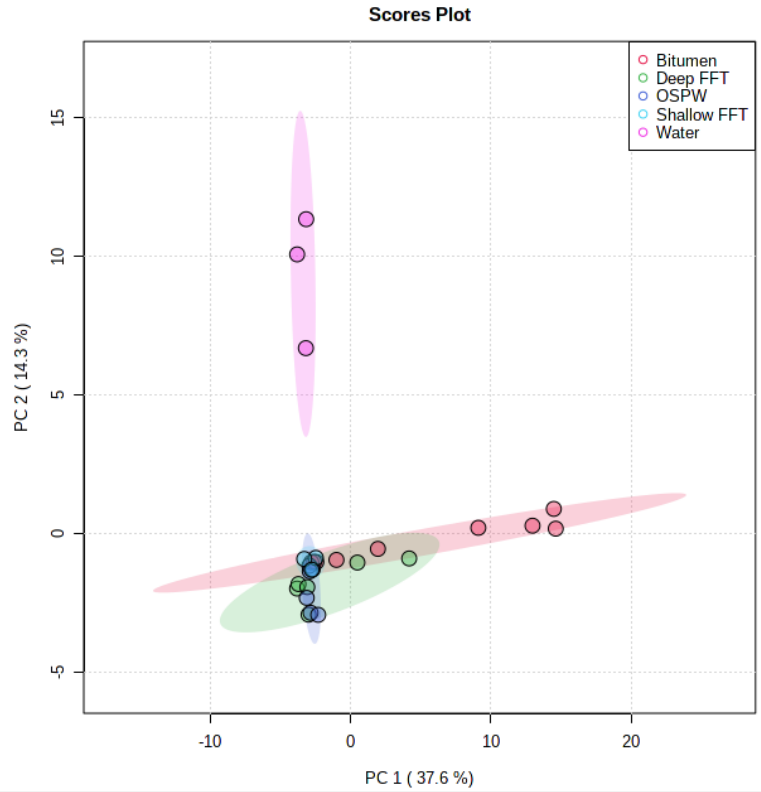


Figure 8: PCA plot for the relative abundances of NAs individual isomers in the water column, FFT, OSPW, Bitumen samples. Water sample 3 circles represent the average of all 2015, 2017, 2019 time points analyzed in triplicates. All other samples, each circle represent one sample of triplicates for 3 bitumen, 2 OSPW, 2 deep FFT, and 1 shallow FFT sample.

## 4-Summary/ implications

The relative abundances of selected, GC×GC resolved adamantane, bicyclic, monocyclic, and thiophene NA species were used as a proxy to elucidate the sources of input and the biodegradation potential of NAs into the water column. Integrating the observations of NAs species and isomers relative abundances between the FFT, OSPW, bitumen, and water column of BML showed that additional inputs of NA are occurring into the water column through advection from FFT and biodegradation in BML. The elevated abundances of NAs in the FFT and their comparability in OSPW relative to the water column suggested that advective diffusive inputs should result in increasing concentration of NAs in the water column. Evidence of NAs input through hydrocarbons biodegradation was based on the observations of 14 unique NAs isomers in the water column and the absence of the C8 bicyclic in the bitumen. The temporal stability of NAs in the water column in addition to the depletion of least alkylated/cyclic species in the water column in concordance with their elevation in the FFT, and the minor elevation of NAs species in the hypolimnion compared to the epilimnion indicate that if such ongoing inputs are occurring they must be consumed by ongoing biodegradation in the water column. Thus, the GC×GC analysis of NAs distributions in the water column, FFT, OSPW, and bitumen suggests that biodegradation in the water column of BML is balancing out and managing the release of additional NAs input into the system.

## 5-References


Bataineh, M., Scott, A.C., Fedorak, P.M., Martin, J.W., 2006. Capillary HPLC/QTOF-MS for characterizing complex naphthenic acid mixtures and their microbial transformation. Anal. Chem. 78, 8354–8361. https://doi.org/10.1021/ac061562p

Bennett, B., Abbott, G., 1998. A natural pyrolysis experiment—hopanes from hopanoic acids? Org. Geochem. 30, 1509–1516.

Bowman, D.T., Slater, G.F., Warren, L.A., McCarry, B.E., 2014. Identification of individual thiophene-, indane-, tetralin-, cyclohexane-, and adamantane-type carboxylic acids in composite tailings pore water from Alberta oil sands. Rapid Commun. Mass Spectrom. 28, 2075–2083. https://doi.org/10.1002/rcm.6996

Bowman, D.T., Warren, L.A., Slater, G.F., 2020. Isomer-specific monitoring of naphthenic acids at an oil sands pit lake by comprehensive two-dimensional gas chromatography–mass spectrometry. Sci. Total Environ. 746, 140985. https://doi.org/10.1016/j.scitotenv.2020.140985

Brown, L.D., Ulrich, A.C., 2015. Oil sands naphthenic acids: A review of properties, measurement, and treatment. Chemosphere 127, 276–290. https://doi.org/10.1016/j.chemosphere.2015.02.003

Clemente, J.S., Mackinnon, M.D., 2004. Aerobic Biodegradation of Two Commercial Naphthenic Acids Preparations 38, 1009–1016. https://doi.org/10.1021/es030543j

Dompierre, K.A., Barbour, S.L., 2016. Characterization of physical mass transport through oil sands fluid fine tailings in an end pit lake: A multi-tracer study. J. Contam. Hydrol. 189, 12–26. https://doi.org/10.1016/j.jconhyd.2016.03.006

Eickhoff, C., Laroulandie, J., 2010. A Review of the Nature of Naphthenic Acid Occurrence, Toxicity, and Fate in Refinery and Oil Sands Extraction Wastewaters. Presentation.

Frank, R.A., Fischer, K., Kavanagh, R., Kent Burnison, B., Arsenault, G., Headley, J. V., Peru, K.M., Van Glen Kraak, D.E.R., Solomon, K.R., 2009. Effect of carboxylic acid content on the acute toxicity of oil sands naphthenic acids. Environ. Sci. Technol. 43, 266–271. https://doi.org/10.1021/es8021057

Frank, R.A., Kavanagh, R., Kent Burnison, B., Arsenault, G., Headley, J. V., Peru, K.M., Van Der Kraak, G., Solomon, K.R., 2008. Toxicity assessment of collected fractions from an extracted naphthenic acid mixture. Chemosphere 72, 1309–1314. https://doi.org/10.1016/j.chemosphere.2008.04.078

Frysinger, G., 2002. GC×GC—A New Analytical Tool For Environmental Forensics. Environ. Forensics 3, 27–34. https://doi.org/10.1006/enfo.2002.0077

Gervais, J.J.., 2004. Fate and Transport of Naphthenic Acids in a Glacial Aquifer by 1–566.

Han, X., Scott, A.C., Fedorak, P.M., Bataineh, M., Martin, J.W., 2008a. Influence of molecular structure on the biodegradability of naphthenic acids. Environ. Sci. Technol. 42, 1290–1295. https://doi.org/10.1021/es702220c

Han, X., Scott, A.C., Fedorak, P.M., Bataineh, M., Martin, J.W., 2008b. Influence of molecular structure on the biodegradability of naphthenic acids. Environ. Sci. Technol. 42, 1290–1295. https://doi.org/10.1021/es702220c

Heider, J., Spormann, A.M., Beller, H.R., Widdel, F., 1998. Anaerobic bacterial metabolism of hydrocarbons. FEMS Microbiol. Rev. 22, 459–473. https://doi.org/10.1016/S0168-6445(98)00025-4

Herman, D.C., Fedorak, P.M., MacKinnon, M.D., Costerton, J.W., 1994. Biodegradation of naphthenic acids by microbial populations indigenous to oil sands tailings. Can. J. Microbiol. 40, 467–477. https://doi.org/10.1139/m94-076

Holowenko, F.M., MacKinnon, M.D., Fedorak, P.M., 2002. Characterization of naphthenic acids in oil sands wastewaters by gas chromatography-mass spectrometry. Water Res. 36, 2843–2855. https://doi.org/10.1016/S0043-1354(01)00492-4

Holowenko, F.M., MacKinnon, M.D., Fedorak, P.M., 2001. Naphthenic acids and surrogate naphthenic acids in methanogenic microcosms. Water Res. 35, 2595–2606. https://doi.org/10.1016/S0043-1354(00)00558-3

Hsu, C.S., Dechert, G.J., Robbins, W.K., Fukuda, E.K., 2000. Naphthenic acids in crude oils characterized by mass spectrometry. Energy and Fuels 14, 217–223. https://doi.org/10.1021/ef9901746

Jaffé, R., Gallardo, M.T., 1993. Application of carboxylic acid biomarkers as indicators of biodegradation and migration of crude oils from the Maracaibo Basin, Western Venezuela. Org. Geochem. 20, 973–984. https://doi.org/10.1016/0146-6380(93)90107-M

Kindzierski, W., Jin, J., Gamal El-Din, M., 2012. Review of Health Effects of Naphthenic Acids: Data Gaps and Implications for Understanding Human Health Risk.

Meredith, W., Kelland, S., Jones, D.M., 2000. Influence of biodegradation on crude oil acidity and carboxylic acid composition 31.

Ong, R.C.Y., Marriott, P.J., 2002. A Review of Basic Concepts in Comprehensive Two-Dimensional Gas Chromatography. J. Chromatogr. Sci. 40, 276–291. https://doi.org/10.1093/chromsci/40.5.276

Rojo, F., 2009. Degradation of alkanes by bacteria: Minireview. Environ. Microbiol. 11, 2477–2490. https://doi.org/10.1111/j.1462-2920.2009.01948.x

Ross, M.S., Pereira, A.D.S., Fennell, J., Davies, M., Johnson, J., Sliva, L., Martin, J.W., 2012. Quantitative and qualitative analysis of naphthenic acids in natural waters surrounding the canadian oil sands industry. Environ. Sci. Technol. 46. https://doi.org/10.1021/es303432u

Rowland, Steven J, Scarlett, A.G., Jones, D., West, C.E., Frank, R.A., 2011. Diamonds in the rough: Identification of individual naphthenic acids in oil sands process water. Environ. Sci. Technol. 45, 3154–3159. https://doi.org/10.1021/es103721b

Rowland, Steven J., West, C.E., Scarlett, A.G., Jones, D., 2011. Identification of individual acids in a commercial sample of naphthenic acids from petroleum by two-dimensional comprehensive gas chromatography/mass spectrometry. Rapid Commun. Mass Spectrom. 25, 1741–1751. https://doi.org/10.1002/rcm.5040

Scott, A.C., MacKinnon, M.D., Fedorak, P.M., 2005. Naphthenic acids in athabasca oil sands tailings waters are less biodegradable than commercial naphthenic acids. Environ. Sci. Technol. 39, 8388–8394. https://doi.org/10.1021/es051003k

Seifert, W.K., 1975. Carboxylic acids in petroleum and sediments[J]. Progress in the Chemistry of Organic Natural Products, Phytochemistry. https://doi.org/10.1016/S0031-9422(00)98679-5

Smith, B.E., Lewis, C.A., Belt, S.T., Whitby, C., Rowland, S.J., 2008. Effects of alkyl chain branching on the biotransformation of naphthenic acids. Supporting information. Environ. Sci. Technol. 42, 9323–8.

Stauffer, E., Dolan, J.A., Newman, R., Stauffer, E., Dolan, J.A., Newman, R., 2008. Gas Chromatography and Gas Chromatography—Mass Spectrometry, in: Fire Debris Analysis. Elsevier, pp. 235–293. https://doi.org/10.1016/B978-012663971-1.50012-9

Tissot, B.P., Welte, D.H., 1985. Petroleum Formation and Occurrence, Eos, Transactions American Geophysical Union. https://doi.org/10.1029/EO066i037p00643
Vazquez-Roig, P., Pico, Y., 2012. Gas chromatography and mass spectroscopy techniques for the detection of chemical contaminants and residues in foods, in: Chemical Contaminants and Residues in Food. Elsevier, pp. 17–61. https://doi.org/10.1533/9780857095794.1.17
Watson, J.S., Jones, D.M., Swannell, R.P.J., Van Duin, A.C.T., 2002. Formation of carboxylic acids during aerobic biodegradation of crude oil and evidence of microbial oxidation of hopanes. Org. Geochem. 33, 1153–1169. https://doi.org/10.1016/S0146-6380(02)00086-4
Whitby, C., 2010. Microbial naphthenic Acid degradation., 1st ed, Advances in applied microbiology. Elsevier Inc. https://doi.org/10.1016/S0065-2164(10)70003-4
Widdel, F., Rabus, R., 2001. Anaerobic biodegradation of saturated and aromatic hydrocarbons. Curr. Opin. Biotechnol. 12, 259–276. https://doi.org/10.1016/S0958-1669(00)00209-3
Wilde, M.J., Rowland, S.J., 2015. Structural Identification of Petroleum Acids by Conversion to Hydrocarbons and Multidimensional Gas Chromatography-Mass Spectrometry. Anal. Chem. 87, 8457–8465. https://doi.org/10.1021/acs.analchem.5b01865
Wilde, M.J., West, C.E., Scarlett, A.G., Jones, D., Frank, R.A., Hewitt, L.M., Rowland, S.J., 2015. Bicyclic naphthenic acids in oil sands process water: Identification by comprehensive multidimensional gas chromatography-mass spectrometry. J. Chromatogr. A 1378, 74–87. https://doi.org/10.1016/j.chroma.2014.12.008

# Appendix

| Sample name | Location | Depth from surface | Coordinates | Replicate number | Date |
|---|---|---|---|---|---|
| NA-1.5-2015 | BML water column-platform 1 | 1.5m | N6318912, E462178 | 3 | 2015 |
| NA-8.5-2015 | BML water column-platform 1 | 8.5m | N6319575, E461990 | 3 | 2015 |
| NA-1.5-2017 | BML water column-platform 1 | 1.5m | N6319575, E461990 | 3 | 2017 |
| NA-9.75-2017 | BML water column-platform 1 | 9.75m | N6319575, E461990 | 3 | 2017 |
| NA-1.5-2019 | BML water column-platform 1 | 1.5m | N6319575, E461990 | 3 | 2019 |
| NA-9-2019 | BML water column-platform 1 | 9m | N6319575, E461990 | 3 | 2019 |
| FFT-1009 | BML FFT-3C | 10m | N6317590, E461311 | 3 | 2019 |
| FFT-309 | BML FFT-19-06 | 15m | N6320352, E463112 | 3 | 2019 |
| FFT-330 | BML FFT-19-01 | 15m | N6319575, E461990 | 3 | 2019 |
| MLSB-OSPW | MLSB-tailing pond | | | 3 | 2019 |
| SWIP-OSPW | SWIP-tailing pond | | | 3 | 2019 |
| Bit-17:30 | Oil sands | | | 3 | 2019 |
| Bit-13:30 | Oil sands | | | 3 | 2019 |
| Bit-15:30 | Oil sands | | | 3 | 2019 |

Table A1: List of all samples in the study.

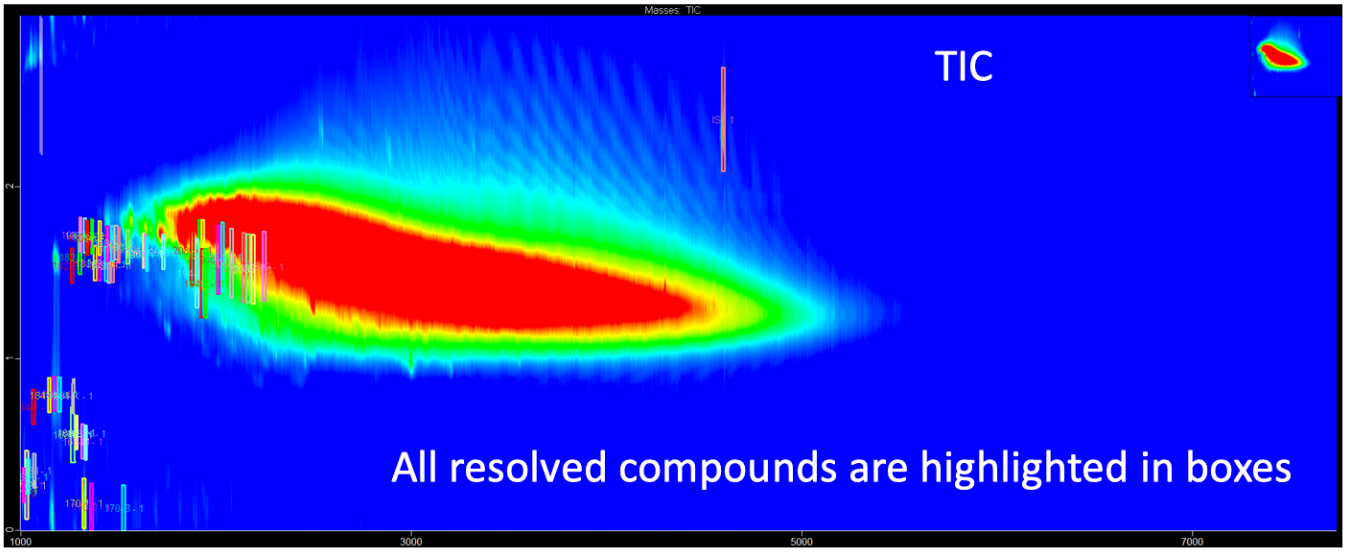

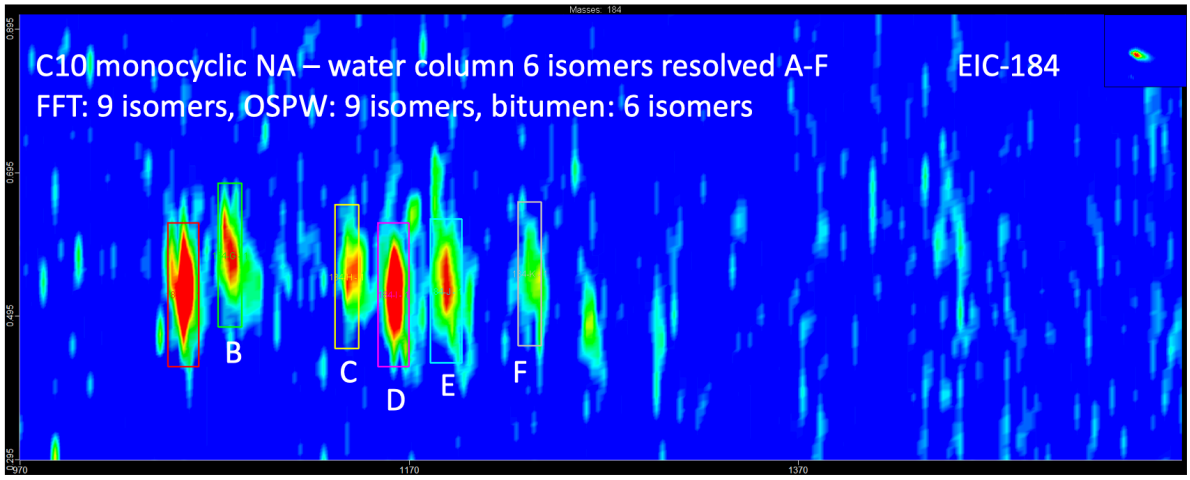
Masses: 184
C10 monocyclic NA – water column 6 isomers resolved A-F
FFT: 9 isomers, OSPW: 9 isomers, bitumen: 6 isomers
EIC-184
B
C
D
E
F
970
1170
1370

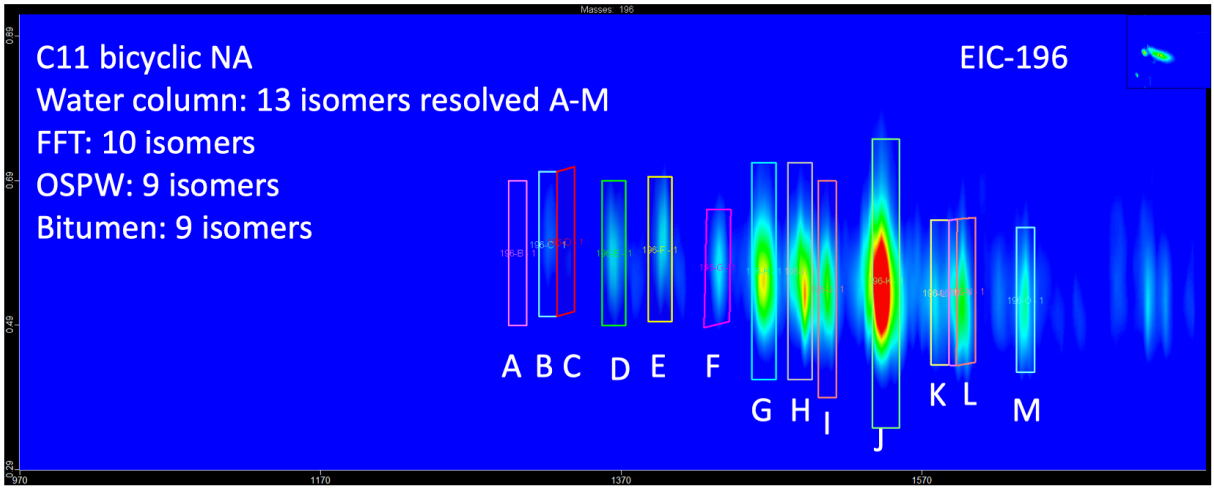
Masses: 196
C11 bicyclic NA
Water column: 13 isomers resolved A-M
FFT: 10 isomers
OSPW: 9 isomers
Bitumen: 9 isomers
EIC-196
A B C D E F G H I J K L M
970
1170
1370
1570

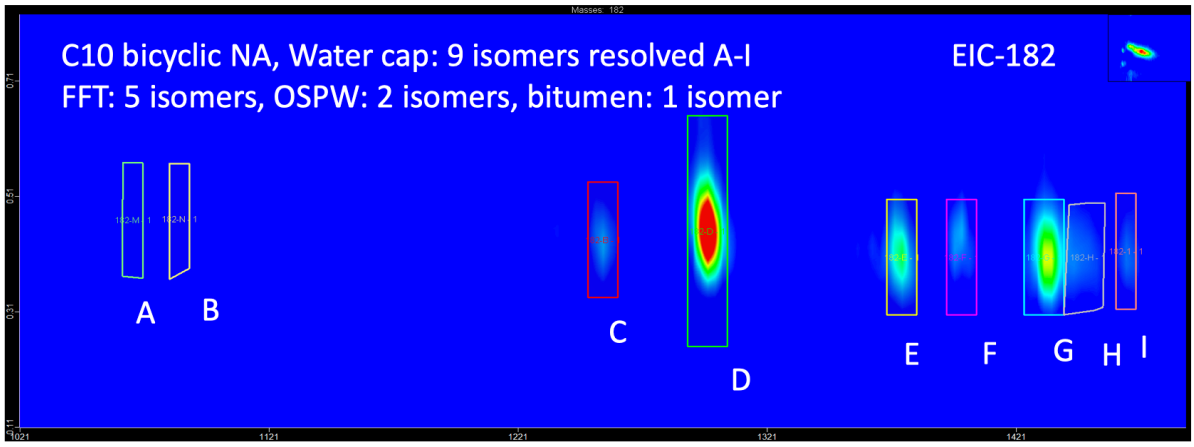
C10 bicyclic NA, Water cap: 9 isomers resolved A-I
FFT: 5 isomers, OSPW: 2 isomers, bitumen: 1 isomer
EIC-182
A
B
C
D
E
F
G
H
I

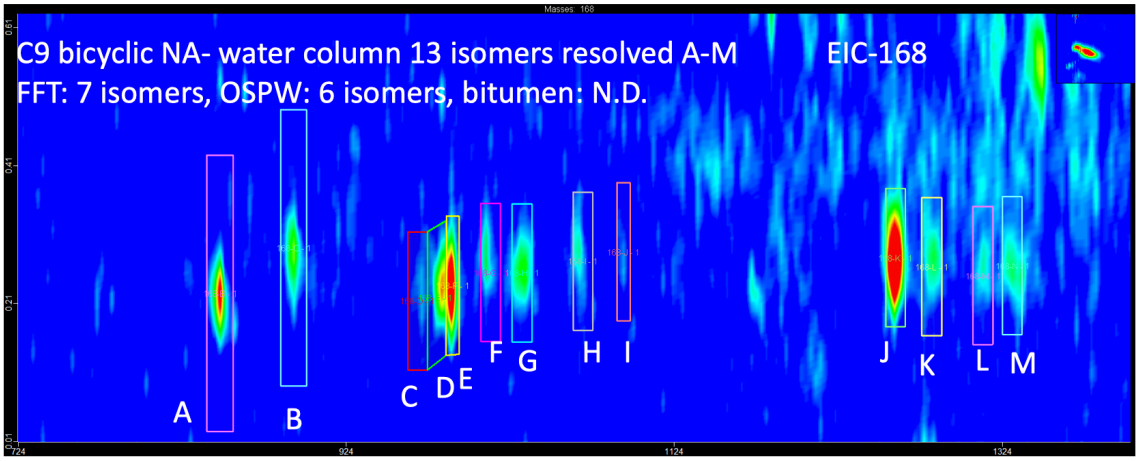
C9 bicyclic NA- water column 13 isomers resolved A-M
FFT: 7 isomers, OSPW: 6 isomers, bitumen: N.D.
EIC-168
A
B
C
D
E
F
G
H
I
J
K
L
M

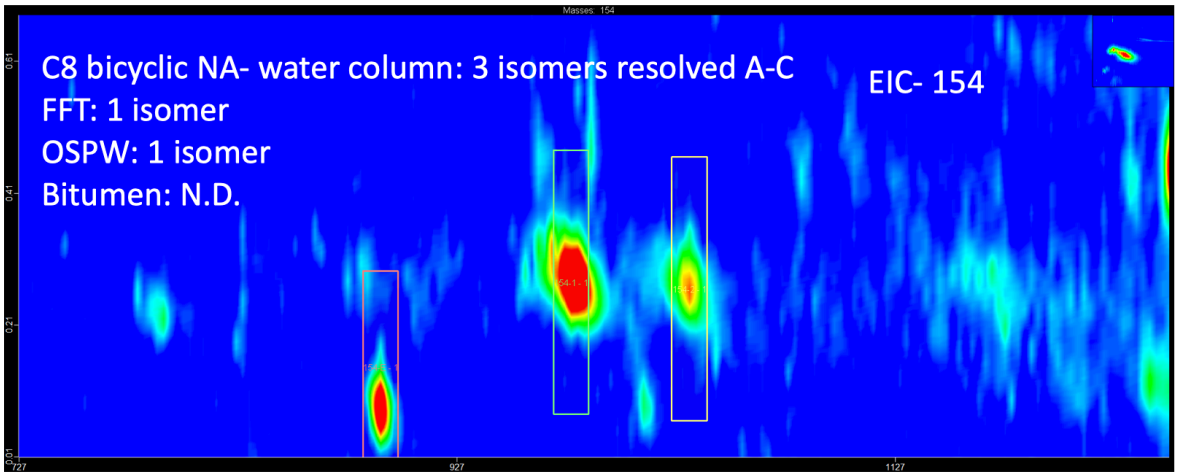
C8 bicyclic NA- water column: 3 isomers resolved A-C
FFT: 1 isomer
OSPW: 1 isomer
Bitumen: N.D.
EIC- 154

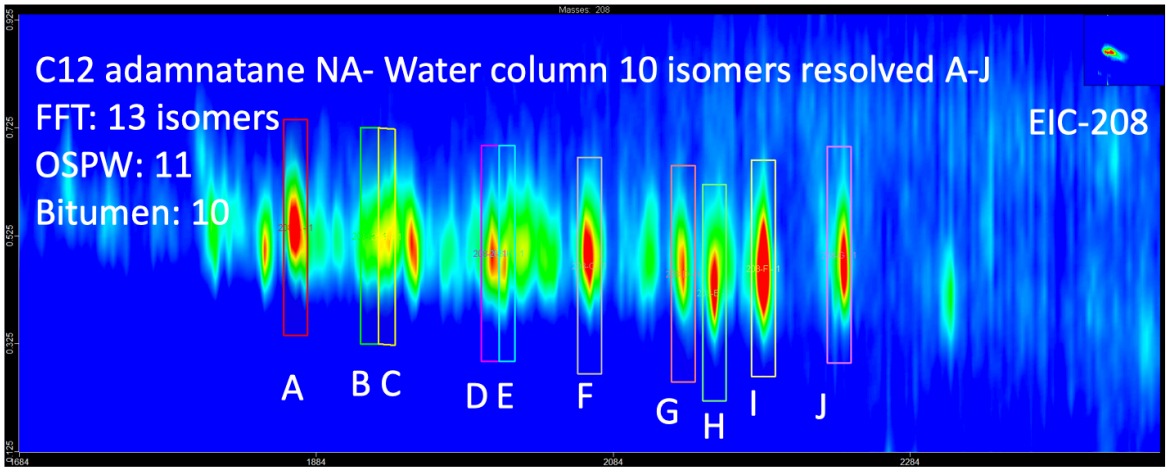


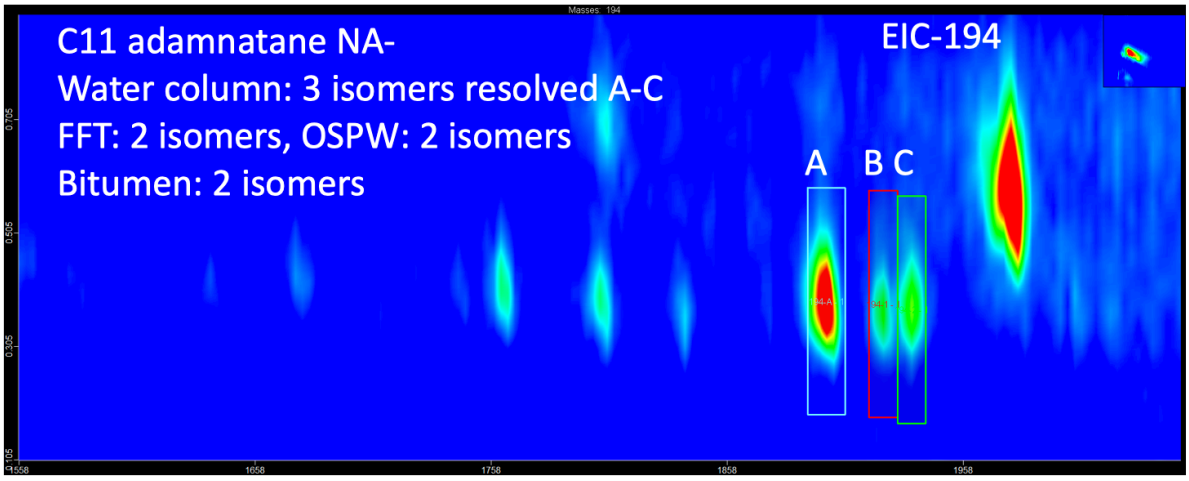


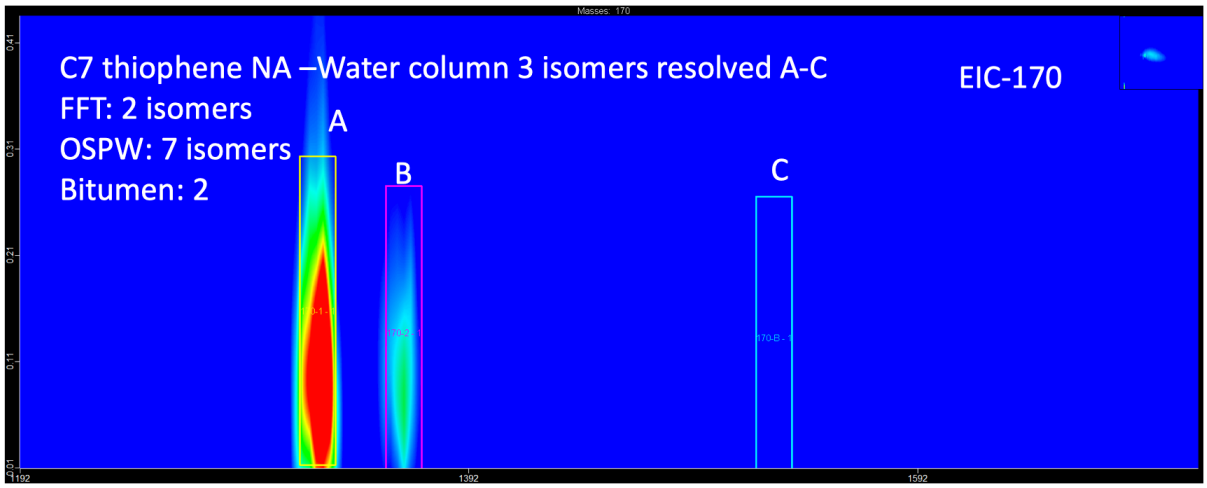


Figure A1: GC×GC chromatographs of resolved NAs.

**Evaluation of biodegradation in an oil sand end pit lake using oxygenated metabolic intermediates**

*Mohamed El-Waraky, David Bowman, Robert Nelson, Christopher Reddy, Lesley Warren, Greg Slater*

## Abstract

Intrinsic microbial biodegradation is considered an effective mechanism for the removal of organic contaminants and their associated toxicity in environmental systems. In the Alberta oil sands regions, petroleum hydrocarbons and Naphthenic acids (NAs) are the primary chemicals of concern associated with oil sands tailings. As part of ongoing efforts to develop reclamation mechanisms for oil sands sites, Syncrude commissioned an end pit lake known as Base Mine Lake (BML) in 2012 by capping the fluid fine tailings (FFT) with a water column. An important component of confirming that hazardous chemicals are effectively sequestered beneath the lake is to confirm that biodegradation is occurring within the water column. The detection of metabolites generated during biodegradation can directly demonstrate the occurrence of biodegradation. Metabolic pathways involved can also be inferred from the type of metabolites detected. In this study, the high resolving power for the GC×GC was used to search for signature metabolites indicative of in-situ biodegradation of hydrocarbons and NAs in the water column and FFT of BML. While hydroxylated intermediates were not able to be detected, here we report the first tentative identification, using chromatographic and mass spectral evidence, of alkylated cyclohexane and bicyclic succinates. These compounds were only detected in the FFT, implying their in-situ production as a result of anaerobic biodegradation. We postulate these succinates as being metabolic intermediates between monocyclanes and bicyclanes parent hydrocarbons, and downstream metabolites of cyclohexane and bicyclic NAs identified previously in oil sands process water (OSPW) and BML. Furthermore, naphthoic acids and tetrahydro ethanoic metabolites indicative of the anaerobic biodegradation of naphthalene and alkylated naphthalene were identified in the FFT through comparison with published mass spectra further supporting the occurrence of anaerobic biodegradation in the FFT. In the water column, the NAs metabolites, $C_{12}$ and $C_{13}$ adamantane diacids were identified by comparison with the previously published mass spectrum of these diacids. The $C_{13}$ adamantane diacid metabolites are speculated to be downstream metabolites of the $C_{12}$ adamantane monoacids previously reported in OSPW and BML and are found to be less toxic than their monoacid precursor. While the $C_{12}$ adamantane diacid metabolites are speculated to be produced from the further biodegradation of the $C_{13}$ adamantane diacids. The presence of the $C_{12}$ and $C_{13}$ adamantane diacids only in the water column implied that they are generated in situ as a result of the aerobic microbial processing within the water column. Tracking the relative abundance of these metabolites temporally showed a significant increase in their abundance from 2015 to 2018. The fold change in relative abundances from 2015 till 2018 for the $C_{13}$ adamantane diacids was greater than the $C_{12}$ adamantane diacids implying that the rate of production of the $C_{13}$ adamantane diacids is slightly greater than their further downstream processing into $C_{12}$ adamantane diacids. This research demonstrated that the identifications of succinates, naphthoic acids, and diacids

metabolites provided evidence for the anaerobic biodegradation of hydrocarbons in the FFT and the aerobic biodegradation of NAs in BML. Thus, biodegradation in BML can mitigate the release of hazardous compounds and help achieve reclamation certification.

## 1-Introduction

Water capped tailing technology is currently being demonstrated as a promising reclamation strategy in the Alberta oil sands region for restoration of mined landscapes and mitigating the environmental risks associated with oil sands tailing ponds. The first application to this technology was implemented by overlaying a volume of fluid fine tailings (FFT) at Syncrude's West In-pit (WIP) with a water column, thus commissioning an artificial lake known as Base Mine Lake (BML) in 2012. One of the requirements for certification of this technology is to demonstrate that it will not release hazardous contaminants such as petroleum hydrocarbons or Naphthenic acids (NAs), that are known to be the most toxic in the tailings (Brown and Ulrich, 2015). Previous lab-based studies have shown that biodegradation was found to be able to deplete hydrocarbons or NAs substrates extracted from the tailings(Johnson et al., 2012; Siddique et al., 2007, 2006). However, the effectiveness of biodegradation as a control on contaminants release, particularly NAs, has not yet been directly demonstrated in BML.

Demonstration of the occurrence of biodegradation in the environmental system can be accomplished through tracking the temporal change in substrate concentrations or through the detection of signature metabolites generated as a byproduct of biodegradation. Tracking the temporal change in substrates concentrations to demonstrate biodegradation can be confounded in complex systems where the rates of source inputs are not well constrained and where there are multiple potential sinks. In such cases, detection of metabolites produced during biodegradation can provide direct evidence for its occurrence.

The biodegradation of hydrocarbons generates oxygenated compounds as metabolic intermediates that include alcohols, aldehydes, ketones, and carboxylic acids also known as Naphthenic acids (NAs). This process occurs along aerobic and anaerobic pathways (1-6) as summarized in figure 1. Aerobic biodegradation of hydrocarbons occurs mainly along pathway 1 and involves the oxidation of a terminal methyl group to produce primary alcohol that is

oxidized to aldehyde, ketones and finally converted to NAs with a monocarboxylic acid moiety (Das and Chandran, 2011; Olajire and Essien, 2014; Rojo, 2009; Sierra-Garcia and de Oliveira, 2013; van der Heul, 2009). However, an anaerobic pathway for the biodegradation of hydrocarbons along pathway 1 was proposed by (Heider and Schule, 2013) that entails an oxygen-independent hydroxylation for hydrocarbons substrate with water as the donor for the hydroxyl group, followed by further oxidation to produce ketones, then NAs metabolites.

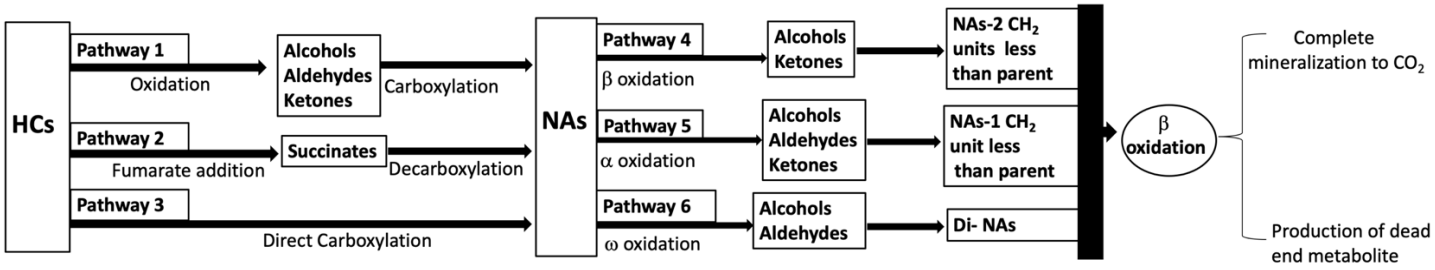


Figure 1: A sketch that shows the routes for the biodegradation of hydrocarbons (HCs) and NAs.

The biodegradation of hydrocarbons along pathways 2 and 3 (Figure 1) occurs exclusively via anaerobic routes. Biodegradation along pathway 2 entails the conversion of the hydrocarbon substrate to succinate intermediates via the fumarate addition pathway (Gray et al., 2010; Head et al., 2003; Kendall et al., 2003; Magot et al., 2000; Rojo, 2009; Widdel and Rabus, 2001). In this reaction, the hydrocarbon substrates are activated through the addition of fumarate at the terminal or subterminal carbon to yield alkyl succinate that retains the hydrocarbon skeleton (Figure 2) (Matthias Boll et al., 2002; Das and Chandran, 2011; Rojo, 2009; Widdel and Rabus, 2001). Alkyl or cycloalkyl succinate derivatives have been detected as metabolic intermediates from the anaerobic biodegradation of alkanes and cycloalkanes in several studies(M Boll et al., 2002; Gruner et al., 2017; Jarling et al., 2015; Kropp et al., 2000; Widdel and Rabus, 2001; Wilkes et al., 2003, 2002). Succinate derivatives have also been detected in aromatic compounds such as 2- Napthyl methyl succinate that is produced from the activation of alkyl naphthalene (Widdel and Rabus, 2001). The further metabolization of the succinate derivatives occurs through rearrangement of the carbon skeleton through an exchange of hydrogen with a carboxyl

group to yield an alkyl malonate intermediate, which is followed by a decarboxylation reaction generating carboxylic acids compounds also referred to as NAs (Wilkes et al., 2003) (Figure 2).

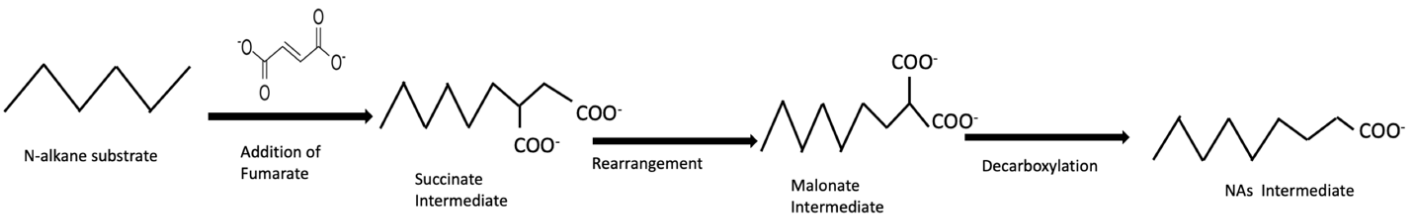


Figure 2: Metabolic pathway of fumarate addition (Wilkes et al., 2003).

Another pathway for the anaerobic biodegradation of alkanes was proposed through direct carboxylation (Pathway 3, figure 1) based on (So et al., 2003) lab findings that reported the generation of fatty acids metabolites, with an odd number of carbons, in a culture medium that contains even carbon numbered n-alkanes and vice versa. The study suggested that an explanation for this transformation would be first the activation of the substrate through carboxylation with inorganic carbon at the $C_3$ position followed by the removal of two subterminal carbon atoms from the alkane chain to yield a fatty acid one carbon atom shorter than the parent alkane. Direct carboxylation pathways have also been reported for the anaerobic biodegradation of aromatics followed by a stepwise reduction of the aromatic ring (Widdel and Rabus, 2001). For instance, naphthalene is initially activated to 2-naphthoate via carboxylation(Widdel and Rabus, 2001), which is followed by the reduction of one ring to yield tetrahydro naphthoic acid then the other ring to yield 2-carboxylate(Widdel and Rabus, 2001).

The oxygenated metabolites, including NAs, generated from the biodegradation of hydrocarbons through pathways (1-3) can be further metabolized through pathways (4-6) as shown in figure 1. These pathways were postulated mainly from studies that tracked surrogate NAs (single ring NAs) under aerobic conditions. The biodegradation of NAs through pathway 4 proceeds through beta (β)-oxidation pathway that entails a sequence of oxidations at the β-Carbon that forms oxygenated NAs (alcohols, and ketones) as an intermediary metabolite. The product of the β-

oxidation sequence is a NAs with two fewer carbon units ($CH_2$) than its parent (Quagraine et al., 2005). NAs biodegradation was also found to proceed through α pathway (pathway 5), although not as common as β-oxidation pathway (Quagraine et al., 2005). The alpha (α) oxidation pathway also produces oxygenated NAs intermediates (alcohols, aldehydes, ketones), then eventually a new NAs is produced with one carbon unit less than the parent. Another pathway was postulated to occur through the omega (ω) oxidation sequence (route 6) that produces oxygenated NAs intermediates (alcohols, aldehydes), that are further metabolized to a dicarboxylic acid moiety NAs ( Di NAs) (Johnson et al., 2012). The Di NAs have also been reported previously to occur in oil sand tailings (Frank et al., 2009; Headley et al., 2011; Lengger et al., 2013), and are found to be less toxic than their monocarboxylic acid precursor (Frank et al., 2009). NAs metabolites generated through pathways (4-6) can be subsequently oxidized through β-oxidations sequence opening the ring structure and producing linear chain fatty acids. The β-oxidations sequence can continue till complete mineralization of the substrate or the production of dead-end metabolites that hinder the progress of the β-oxidations sequence.

Few studies have investigated the biodegradation of NAs under anaerobic conditions, and thus the metabolic pathway under these conditions is not well defined. Long-chain carboxylic acids were found to degrade with anaerobic sewage digestors through β-oxidation (Jeris and Perry L. McCarty, 1965). Surrogate NAs (single ringed NAs) were found to be biodegradable in anaerobic microcosm with sewage sludge (Holowenko et al., 2001), and tailings from OSPW under nitrate, sulfate, iron-reducing, and methanogenesis(Clothier and Gieg, 2016). While, ( Folwell et al., 2016) have found that NAs extracted from OSPW are recalcitrant to biodegradation under sulfate reducing and methanogenic conditions similar to that of the FFT. Thus, additional research is still needed to elucidate the biodegradation extent of NAs and the metabolic pathway under anaerobic conditions.

Previous lab studies have demonstrated that biodegradation can deplete hydrocarbons or NAs substrates from oil sand tailings through anaerobic pathways (Clothier and Gieg, 2016; Folwell et al., 2016; Siddique et al., 2006) or aerobic pathways (Clemente and Mackinnon, 2004; Gervais, 2004). Nonetheless, the effect of biodegradation on the removal of hazardous contaminants in BML hasn't been directly assessed. Thus, in this study, we used the high

resolving power of the GC×GC to assess the presence of signature metabolites in both the water column and underlying FFT in BML that would provide direct evidence for the occurrence of biodegradation. To achieve this, we searched for potential metabolites generated from hydrocarbons biodegradation along pathways (1-3), in addition to metabolites generated from NAs biodegradation along pathways (4-6). To ascertain whether the identified metabolites were produced in BML, and thereby demonstrate in situ biodegradation, we searched for the observed metabolites in OSPW from neighbouring tailing ponds and in unrefined bitumen samples. The confirmation of biodegradation occurrence would indicate that the BML system is functioning as planned in maintaining the release of hazardous chemicals as NAs.

## 2-Methods

### 2.1 Study area and sampling

Samples were collected from Base Mine Lake (BML), mine site, north of Fort McMurray, Alberta, Canada (Figure 3). A total of 9 water samples were collected by van dorn sampler from the Epilimnion (1.5m), Metalimnion (5m), and Hypolimnion (9-10m) at platform 1 of BML during the summer of 2015, 2017, and 2018. One FFT sample located at platform 2 was collected at a depth of 16 m from the surface or 6 m from FFT- water interface (FWI) during the summer 2015 sampling campaign. Additionally, one FFT sample was collected from the shallow FFT interval at a depth of 10m (1m from FFT-water interface and two deeper FFT (16m) from 3 locations (BML01, BML06, BML3C) in 2019 (Figure 2). The two OSPW samples were collected from MLSB (Mildred lake settling basin) and SWIP (Southwest end- pit) sites in 2019. Additionally, 3 raw unrefined bitumen from the production lines were collected in 2019. Water and OSPW samples were collected in Nalgene bottles previously shown to have no NA blank, while FFT was collected into pails and subsamples taken away from the pail sides were then transferred into Nalgene bottles. Bitumen samples were collected in glass jars. All samples were kept frozen before extraction.

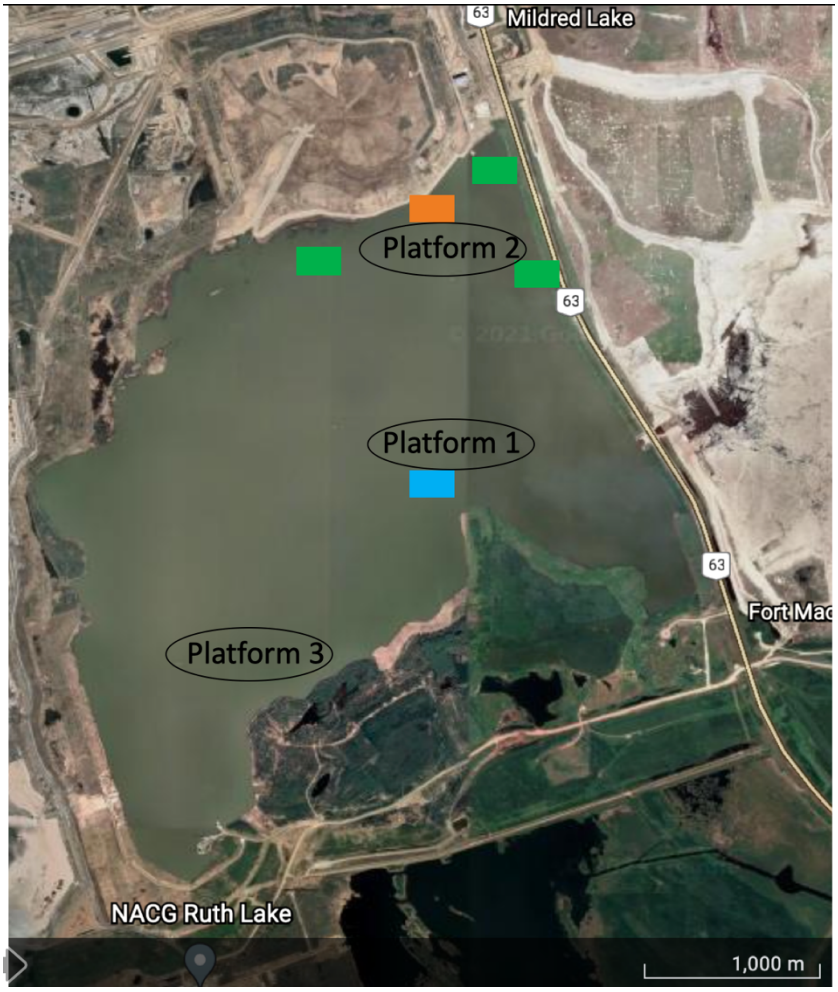


Figure 3: (A) A satellite image of BML that shows Water column samples (blue circle) collected from platform 1 in BML over 2015, 2017, 2018. 1 FFT sample in orange circle collected from 2015 at P2. Additional, 3 FFT samples (green circles) collected from platforms BML-1901, BML-19-06, BML-3C in BML.

### 2.2 Sample extraction

The water column samples were extracted using the method outlined by (Bowman et al., 2014). Briefly, 20 ml water samples were filtered through a 0.45 µm syringe filter, then acidified to PH< 2, extracted with dichloromethane ( 15 ml× 4) using liquid-liquid chromatography. The extract was blown down with inert $N_2$ gas to 30 µl then derivatized by adding a freshly prepared

diazomethane. The diazomethane is prepared by adding Diazold, Dimethylester, Carbitol in an inner tube surrounded by an outer tube that contains DCM. Then the diazomethane generation is initiated by the addition of 1.5 ml of 37% KOH aqueous solution dropwise to the contents of the inner tube via the septum using a plastic syringe with a narrow-gauge (no.22) needle. Then, the diazomethane generated is added to the samples dropwise until the yellow colour persisted to methyl any carboxylic acid groups into methyl esters. Finally, 5∝-cholestane is added as an internal standard, and the extract ran on the GC×GC MS. FFT samples were centrifuged at 3600 RPM for 90 minutes, and then the supernatant was collected, then extracted as the water samples mentioned above (Bowman et al., 2020). The bitumen samples were first extracted by adding 100 ml water, left to partition for 24 hours, then the aqueous phase was collected, and extracted as mentioned above for the water samples.

**2.3 Instrumental analysis**

Water column samples were analyzed on a LECO Pegasus 4D GC×GC–TOFMS, that used a primary column Restek Rtx-1 column (60 m, 0.25mm ID, 0.25 μm film thickness), and a secondary column SGE BPX-50 column (1.25 m, 0.10mm ID, 0.10 μm film thickness). While FFT, OSPW, and bitumen samples were analyzed using another Pegasus 4D system that used an Rtx-17sil ms (30 m x 0.25 mm x 0.15 μm) as the primary column and DB-5ms (1 m x 0.25mm x 0.1 μm) as the secondary column. The oven temperature program was the same for the two 4D Pegasus systems as follows: the primary oven temperature was initiated at 80 °C (held for 15 minutes), then the temperature was ramped up to 335 °C with a rate of 1.66 °C /min. Whereas the secondary oven temperature was offset by +5 °C. The modulation period used was 7.5s. The TOFMS data acquisition rate was 100 HZ, the detector voltage was 1425 V, and the mass spectrometer used voltage energy of -70 eV.

**2.5 Statistical testing**

The significance of the variance for the resolved diacid NA isomers were tested using one-way ANOVA and T-test. One-way ANOVA tests for the variation between 3 or more means whereas these variations are considered significant if they have a P-value of <0.05. The one-way ANOVA

test was followed by a Tukey test to determine what specific pairs had the significant variance. On the other hand, T-test variations were considered significant if the P-value is ≤ 0.05, and marginally significant if ≤ 0.1. Statistical tests were performed using MetaboAnalyst 4.0.

## 3-Results

### 3.1 Identification of metabolites indicative of hydrocarbons biodegradation

Using the GC×GC we looked for signature metabolites of hydrocarbons biodegradation along pathways (1-3) in all samples through chromatographic and mass spectral analysis. Functional groups associated with metabolites produced along each metabolic pathway were searched for using characteristic fragments produced in the mass spectrum. Once such fragments were identified, the mass spectrum of the compounds was compared to the library and published mass spectrum. Alternatively, the mass spectrum was interpreted based on known fragmentation patterns.

#### 3.1.1 Oxygenated metabolites

Oxygenated metabolic intermediates (alcohols, aldehydes, ketones) of hydrocarbon biodegradation along pathway 1 (Figure 1) were searched for using diagnostic m/z fragments in the spectrum. For instance, alcohols were searched for using m/z 31, associated with a (CH2OH) group that is formed due to cleavage of the C-C bond next to the OH group, m/z 18 due to loss of water, and m/z 33 due to the loss of a methyl group and water. However, we couldn't detect any of these oxygenated intermediates using diagnostic fragments in mass spectrums of all the samples.

### 3.1.2 Succinates

Succinates formed pathway 2 (Figure 1) were specifically targeted as they have been widely reported as a signature metabolite for anaerobic biodegradation of hydrocarbons(Aitken et al., 2018; Wilkes et al., 2003, 2002). Succinate metabolites were only detected in the 2015 FFT samples from BML. We report here, the tentative identification of cyclohexane and bicyclic succinates (as their dimethyl esters) that has never been previously reported. The cyclohexane and bicyclic NAs downstream metabolites for the succinates have been previously detected in 2015 FFT samples from BML(Bowman et al., 2020). No authentic standards were available for these compounds; therefore, identifications were based on chromatographic evidence and mass spectral interpretations using first-hand principles. Previously identified alkyl and cycloalkyl succinates exhibit a diagnostic m/z 114 and 116 (Bian et al., 2014; Jarling et al., 2015; Wilkes et al., 2003). The m/z at 146 is associated with a fragment of $CH_3OOC\text{-}CH_2\text{-}CH_2\text{-}COOCH_3$ as a result of McCafferty arrangements where either the alkyl or cyclohexyl moiety can provide a δ-H for this rearrangement (Figure 4). The m/z 114 ion is associated with a loss of $CH_3OH$ as a result of a secondary fragmentation of the 146 ion fragment due to α-cleavage (Bian et al., 2014). These fragments occur independent of the alkyl or cycloalkyl chain, thus they occur in all compounds that exhibit a succinate moiety.

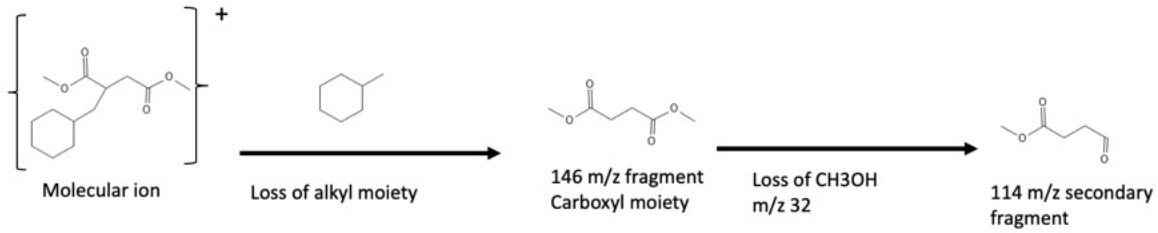


Figure 4: Fragmentation mechanism for the succinates (Bian et al., 2014).

Accordingly, we searched for the presence of succinates in the FFT samples using m/z 146. The EIC at 146 m/z of the FFT sample revealed a series of well resolved peaks eluting between 2577s and 3577s (RT 1, Figure 5). As the succinates exhibit a dicarboxylic acids moiety, they appeared at a later retention time than the monocarboxylic acid moiety compounds (cyclohexane

and bicyclic NA) (Figure 5). All identified peaks showed a molecular ion with approximately 1-5% abundance of the base peak. No illogical fragment losses were observed for all identified molecular ions further supporting that the identified succinates exhibit a molecular ion. The absence of [M+2] $^{34}S$ isotope peak from the mass spectra of the identified compounds implies that they do not contain sulphur.

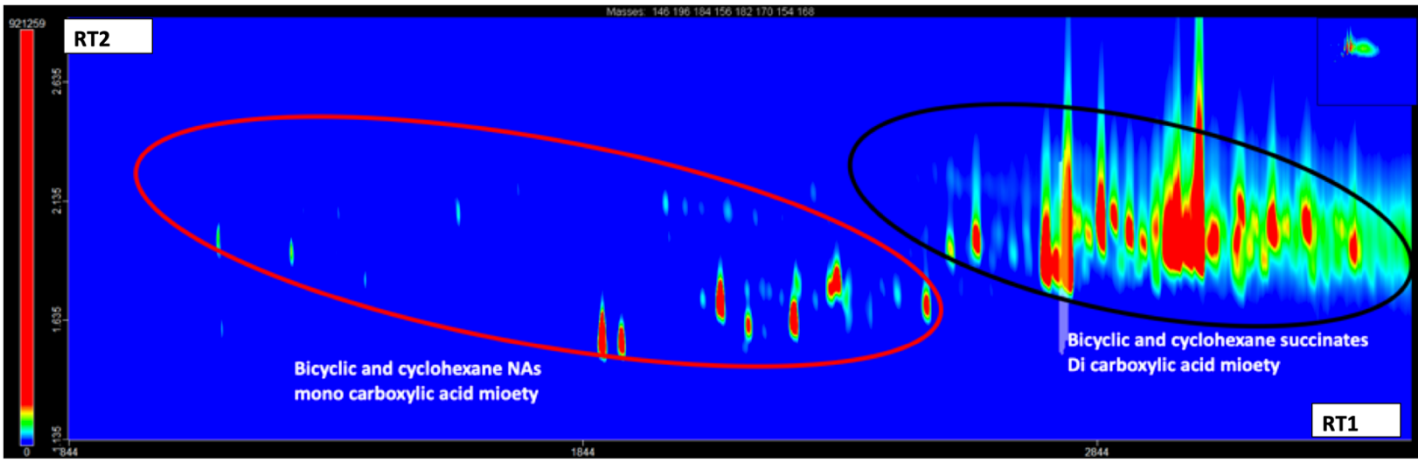


Figure 5: GC×GC chromatograph of succinates vs NAs (TIC).

Three Cyclohexane and three bicyclic succinates (Figure 6) were identified as homologues series due to a sequential increase of 14 amu from the molecular ion (Cyclohexanes – Groups 1,2,3: 242, 256, 270/ Bicyclics – Groups 4,5,6: 240,254,268) in addition to other fragments in the spectrum. Isomers (A, B) from C11 cyclohexane succinates, (G, H) from C12 cyclohexane succinates, (C, E) from C11 bicyclic succinates, and (J, K) from C12 bicyclic succinates, and ( M, N) from C13 bicyclic succinates, had an identical mass spectrum implying that they are stereoisomers. Succinates reported in previous studies (Jarling et al., 2015; Wilkes et al., 2003) were also preset as double peaks representing diastereomers. Thus, the detection of the diastereomers for compounds mentioned above further supports their identification as succinate derivatives.

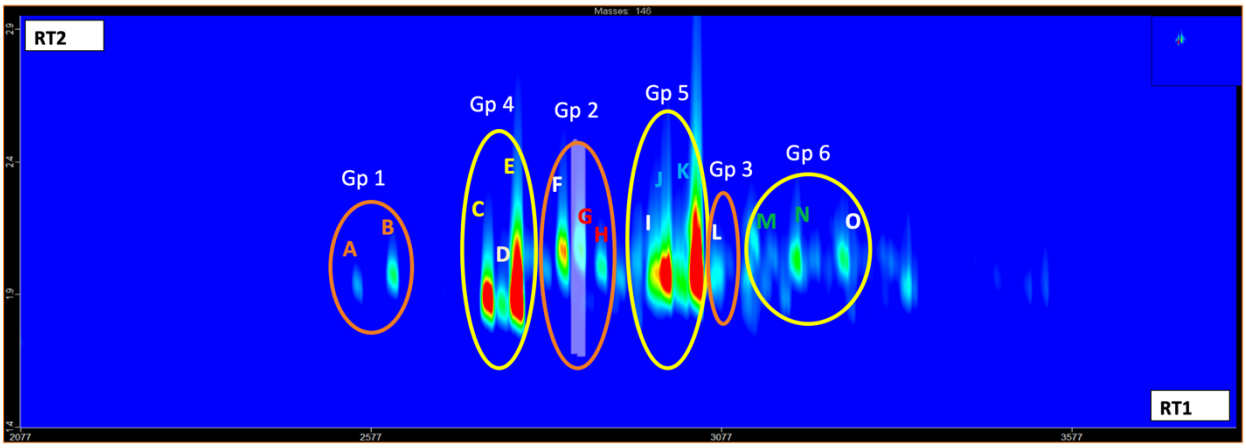


Figure 6: GC×GC chromatograph of resolved peaks tentatively identified as cyclohexane and bicyclic succinate isomers. Compounds identified are denoted with letters A to O. Compounds that are stereoisomers are denoted with the same color. Cyclohexane succinate compounds are grouped in orange circles as follow: Group (Gp) 1: C11 cyclohexane succinate, Gp 2: C12 cyclohexane succinate, Gp 3: C13 cyclohexane succinate. Bicyclic succinate compounds are grouped in yellow circles as follow: Gp 4: C11 bicyclic succinate, Gp 5: C12 bicyclic succinate, Gp: 6: C13 bicyclic succinate.

### 3.1.2.1 Cyclohexane succinates

The EI mass spectra of the Group 1 compounds (see Figure 7 and Table 1) (2 isomers) possess a low abundance molecular ion ( <1% of the base peak) at m/z 242, consistent with their proposed chemical formula ($C_{13}H_{22}O_4$). The diagnostic succinate fragment ion ($CH_3OOC\text{-}CH_2\text{-}CH_2\text{-}COOCH_3$) at m/z 146 was present and was observed as the base peak ion. The second most prominent ion, present at m/z 114, was formed by the further loss of a $CH_3OH$ (32 amu) from the 146 m/z fragment. The cycloalkyl moiety fragment (M-146) was detected at m/z 96 and m/z 97 following a hydrogen transfer. Fragment ions generated by losses from the cycloalkyl moiety were observed at m/z 41, 55, 69 associated with $C_3H_5^+$, $C_4H_7^+$ and $C_5H_9^+$ groups, respectively. While a fragment of a $CH_3COO^{\bullet}$ group, lost from the carboxyl moiety, was observed at m/z 59. Other smaller fragments were observed at 211 m/z due to a loss of a $CH_3OH$ (32 amu) group from the molecular ion, and at 179 m/z due to a further loss of a $CH3O^{\bullet}$ (31 amu) from the 211m/z fragment. Accordingly, the proposed formula for unknowns in group 1 is $C_{13}H_{22}O_4$, and

thus we tentatively identify the compounds as cyclohexyl methyl succinate ($C_{11}$- Cyclohexane succinates).

The EI spectra of group 2 (Figure 7) compounds ( 3 isomers) also showed a low abundance molecular ion at m/z 256. A fragment associated with a $CH_3O^{\bullet}$ (31 amu) loss from the molecular ion at m/z 225 and its secondary fragment at m/z 193 due to the additional $CH_3OH$ (32 amu) loss was observed at all 3 isomers. While another fragment due to a $CH_3COOCH_2$ (73 amu) loss from the molecular ion at m/z 183 was observed at only one isomer. The base peak was detected at the diagnostic 146 m/z peak associated with carboxyl moiety, while the second most common peak was its secondary fragment due to the $CH_3O^{\bullet}$ (31 amu) loss at m/z 114. The fragment of $CH_3COO$, due to a loss from the carboxyl moiety, was detected at m/z 59. The cycloalkyl moiety ( M-146) was observed at m/z 110 and 111 following a hydrogen transfer. Common fragments of 41, 55, and 69 m/z due to the alkyl group losses from the cycloalkyl moiety were also detected. Therefore, our interpretation implies that the formula of these compounds is $C_{14}H_{24}O_4$, and can be tentatively identified as a cyclohexyl dimethyl succinate ($C_{12}$-cyclohexane succinate).

Only one isomer was identified in group 3 (Figure 5) possessing a molecular ion at m/z 270. Fragments observed due to losses from the molecular ion at m/z 239 was due to a $CH_3O^{\bullet}$ (31 amu) loss, its secondary fragment due to a further $CH_3OH$ (32 amu) loss and at 197 m/z due to a $CH_3COOCH_2$ (73 amu) group loss. The diagnostic 146 m/z and 114 m/z were detected as the base peak and second most prominent ions respectively. The cycloalkyl moiety fragment (M-146) was observed at m/z 124 and 125 following a hydrogen transfer. Accordingly, the analysis of the spectrum implies that the compound formula is $C_{15}H_{26}O_4$, and can be tentatively identified as a cyclohexyl ethyl methyl succinate ($C_{13}$-cyclohexane succinate).

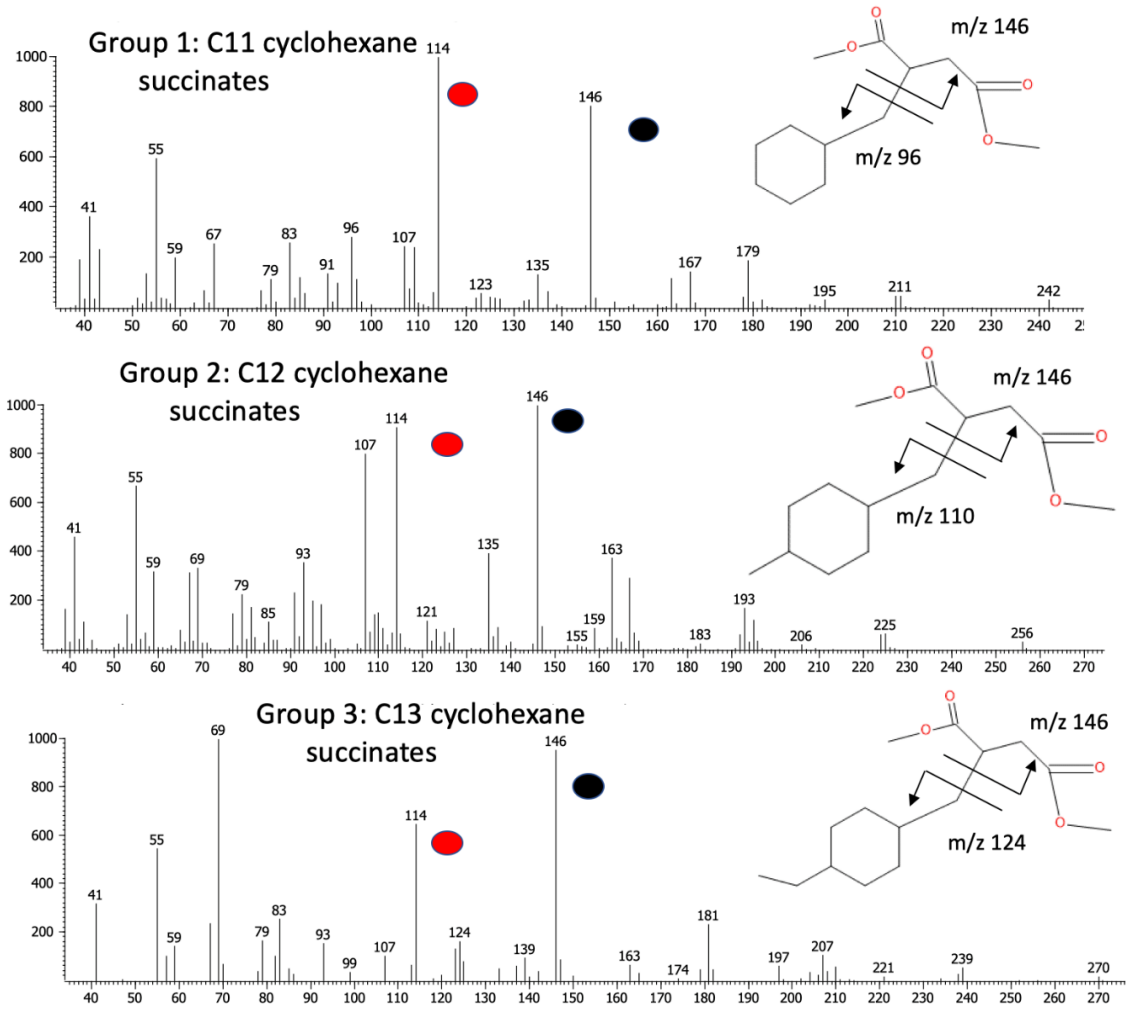


Figure 7: Mass spectrum for $C_{11}$, $C_{12}$, $C_{13}$ cyclohexane succinates detected in the FFT. Diagnostic succinates fragments 146m/z and 114 m/z are labelled with black and red circles respectively.

| Group | Isomers | $M^+$ | 146 m/z Carboxyl moiety | 114 m/z 146 m/z -32 m/z CH3OH | $M^+$ - 146/145 Cyclo alkyl moiety | $M^+$- 31m/z CH3O | $M^+$ -63 m/z CH30 + CH3OH | $M^+$-73 CH3CH 2COOH | 41 m/z C3H5, 55 m/z C4H7, 69 m/z C5H9 59 m/z CH3COO | Formula | Identification |
|---|---|---|---|---|---|---|---|---|---|---|---|
| 1 | A,B | 242 | √ | √ | 96/97 | 211 | 179 | | √, √, √, √ | C13H22O4 | C11 cyclohexane succinates |
| 2 | F,G,H | 256 | √ | √ | 110/111 | 225 | 193 | 183 | √, √, √, √ | C14H24O4 | C12 cyclohexane succinates |
| 3 | L | 270 | √ | √ | 124/125 | 239 | 207 | 197 | √, √, √, √ | C15H26O4 | C13 cyclohexane succinates |

Table 1: Fragmentation of cyclohexane succinates.

### 3.1.2.2 Bicyclic succinates

The EI mass spectra of group 4 (Figure 8, Table 2) compounds (3 isomers) contained a weak molecular ion (<1% of the base peak) at m/z 240. The second most prominent peak was observed at m/z 146 suggesting that it's the carboxyl moiety fragment commonly detected in succinates. The base peak observed at m/z 114 as a result of a secondary fragmentation of the 146-ion due to α-cleavage was detected in all isomers. Other prominent ions in the spectrum at m/z 209 associated with a loss of $CH_3O^{\bullet}$ (31 amu) from the molecular ion, 180 m/z due to a loss of $CH_3COOH$ (60 amu), and a fragment at m/z 167 due to a loss of the methylated ethanoic acid moiety ($CH_3COOCH_2$, 73 amu). The cycloalkyl moiety fragment was observed at m/z 94 and 95 following hydrogen transfer. Fragments due to losses from the cycloalkyl moiety were observed at m/z 41, 55, and 69 associated with $C_3H_5^+$, $C_4H_7^+$, and $C_5H_9^+$ groups. Accordingly, the proposed formula for the unknown is $C_{13}H_{22}O_4$, and thus tentatively identified as bicyclic succinate with a $C_7$ ring structure ($C_{11}$ bicyclic succinate).

The EI mass spectrum of group 5 (Figure 8) compounds (3 isomers) also shows a molecular ion with a small abundance at m/z 254. The base peak is apparent at m/z 146 representing the carboxyl moiety, and the second most prominent ion at 114 indicating that the group has a succinate structure. The cycloalkyl moiety fragments ( M-146) were observed at m/z 108 and 109 following hydrogen transfer. The common cyclo alkyl fragments at m/z 41, 55, and 69 were also detected. Additionally, losses from the molecular ion were detected at 223m/z, 194 m/z, and 181 m/z due to a loss of a $CH_3O^{\bullet}$ (31amu), $CH_3COOH$ (60 amu), and a $CH_3COOCH_2$ (73 amu) groups respectively. We propose the formula for this group to be $C_{14}H_{22}O_4$, and thus tentatively identified as bicyclic succinate with a $C_8$ ring structure or a $C_7$ ring with a methyl substituent ($C_{12}$ bicyclic succinate).

Finally, the mass spectrum of group 6 (Figure 8) compounds (3 isomers) also showed a low abundance of the molecular ion at m/z 268. Diagnostic 146 m/z for the carboxyl moiety and its 114 /z secondary fragment were observed for all isomers as the base peak and second most

prominent ions respectively. Ion observed at 237 was due to a loss of $CH_3O^{\bullet}$ (31 amu) from the molecular ion, as well as 208 m/z due to $CH_3COOH$ (60 amu) loss, and at 195 m/z due to $CH_3COOCH_2$ (73 amu) loss. The cycloalkyl moiety fragment was observed at m/z 122 and 123 following a hydrogen transfer. Accordingly, we propose the formula for this group as $C_{15}H_{24}O_4$, and thus tentatively identified as bicyclic succinate with a $C_9$ ring structure or a $C_8$ ring with a methyl substituent or a $C_7$ with an ethyl substituent ($C_{13}$ bicyclic succinate).

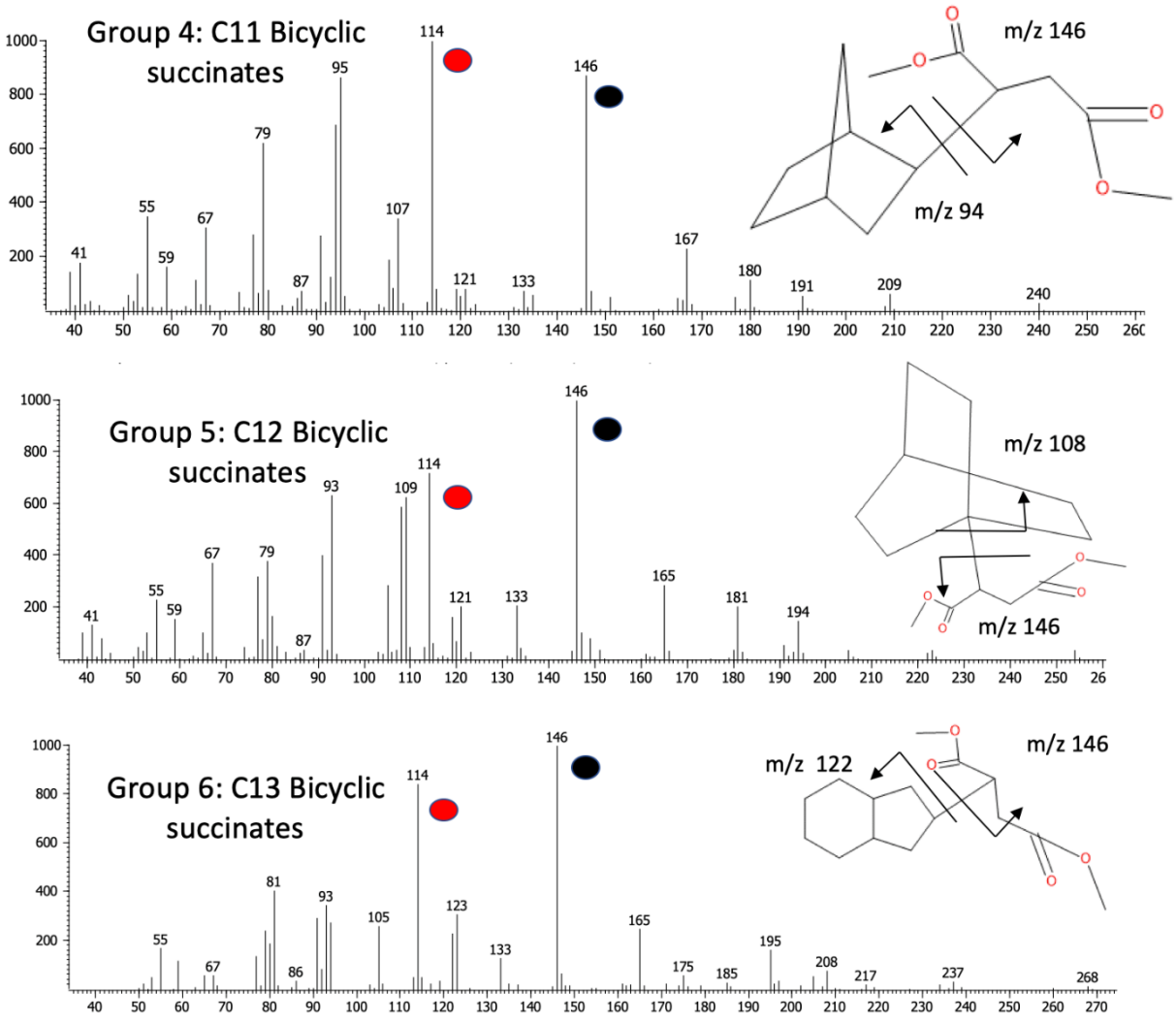


Figure 8: Mass spectrum for $C_{11}$, $C_{12}$, $C_{13}$ bicyclic succinates detected in the FFT. Diagnostic succinates fragments 146m/z and 114 m/z are labelled with black and red circles respectively.

| Group | Isomers | $M^+$ | 146 m/z Carboxyl moiety | 114 m/z 146 m/z -32 m/z CH3OH | $M^+$ - 146/145 Cyclo alkyl moiety | $M^+$- 31m/z CH3O | $M^+$ -60 m/z CH3COOH | $M^+$-73 CH3CH2COOH | 41 m/z C3H5, 55 m/z C4H7, 59 m/z CH3COO | Formula | Identification |
|---|---|---|---|---|---|---|---|---|---|---|---|
| 4 | C,D,E | 240 | √ | √ | 94/95 | 209 | 180 | 167 | √, √, √ | C13H20O4 | C11 Bicyclic succinates |
| 5 | I,J,K | 254 | √ | √ | 108/109 | 223 | 194 | 181 | √, √, √ | C14H22O4 | C12 Bicyclic succinates |
| 6 | M,N,O | 268 | √ | √ | 122/123 | 237 | 208 | 195 | √ | C15H24O4 | C13 Bicyclic succinates |

Table 2: Fragmentation of bicyclic succinates.

### 3.1.3 Aromatic acids

Additionally, since aromatic acids have been previously reported as signature metabolites during the anaerobic biodegradation of hydrocarbons (Aitken et al., 2017; Gruner et al., 2017), we extended our metabolite search to include these compounds. The aromatic acids would be downstream metabolites from the biodegradation of aromatic hydrocarbons, detected previously in the FFT of BML (Chapter 1), through direct carboxylation (Aitken et al., 2017; Gruner et al., 2017) (pathway3, Figure 1). Indeed, we were able to identify bicyclic aromatic metabolites naphthoic acids and tetrahydro naphthoic acids in the FFT and water column samples. These compounds were identified through a comparison with the mass spectrum of previously reported bicyclic aromatic acids extracted from commercial NAs from petroleum (West et al., 2014) (Figure 9).

The spectra of the naphthoic acids reported by (West et al., 2014) closely resembled that identified in the 2015 FFT sample herein. The mass spectrum of the methyl esters of naphthoic acid identified in the FFT, and that reported by (West et al., 2014), was characterized by a molecular ion at 186 m/z, a base peak at 127m/z due to a loss of a methylated carboxy group (COOCH3, 59 amu) from the molecular ion, and a peak at 155 m/z due to a loss of methoxy group ( CH3OH, 32 amu), commonly reported for the spectra of carboxylic acid methyl esters. Thus, we tentatively assign the compound as either naphthalene-1-carboxylic acids or naphthalene-2-carboxylic acids.

Additionally, 2 isomers of the tetrahydro ethanoic acids were identified only in the 2015 FFT sample by comparison with previously reported mass spectrum (West et al., 2014) ( Figure 9). The spectrum in the FFT matched that in (West et al., 2014), with a molecular ion at m/z 204, a base peak at 144 m/z corresponding to a loss of CH3COOH (60 amu) and m/z of 131 as a result of a loss of CH3COOCH2 (73 amu). Thus, we tentatively assign the two compounds identified in the FFT as 1,2,3,4 tetrahydro-2-ethanoic acid and 5,6,7,8 tetrahydro-2-ethanoic acid. Another isomer of the tetrahydro ethanoic acids were identified in the 2019 FFT sample and 2015-2018 water column samples. The mass spectrum of the ethanoic acids closely matched the previously reported spectrum in(West et al., 2014) ( Figure 9). The spectrum was characterized by a molecular ion at m/z 204, m/z of 130 as a result of a loss of CH3CH2COOH (74 amu), and a smaller fragment at m/z 115 as a result of a loss of CH3 (15 amu) from the 130 m/z fragments. Thus, the compound is tentatively assigned as 1,2,3,4 tetrahydro-1-ethanoic acid.

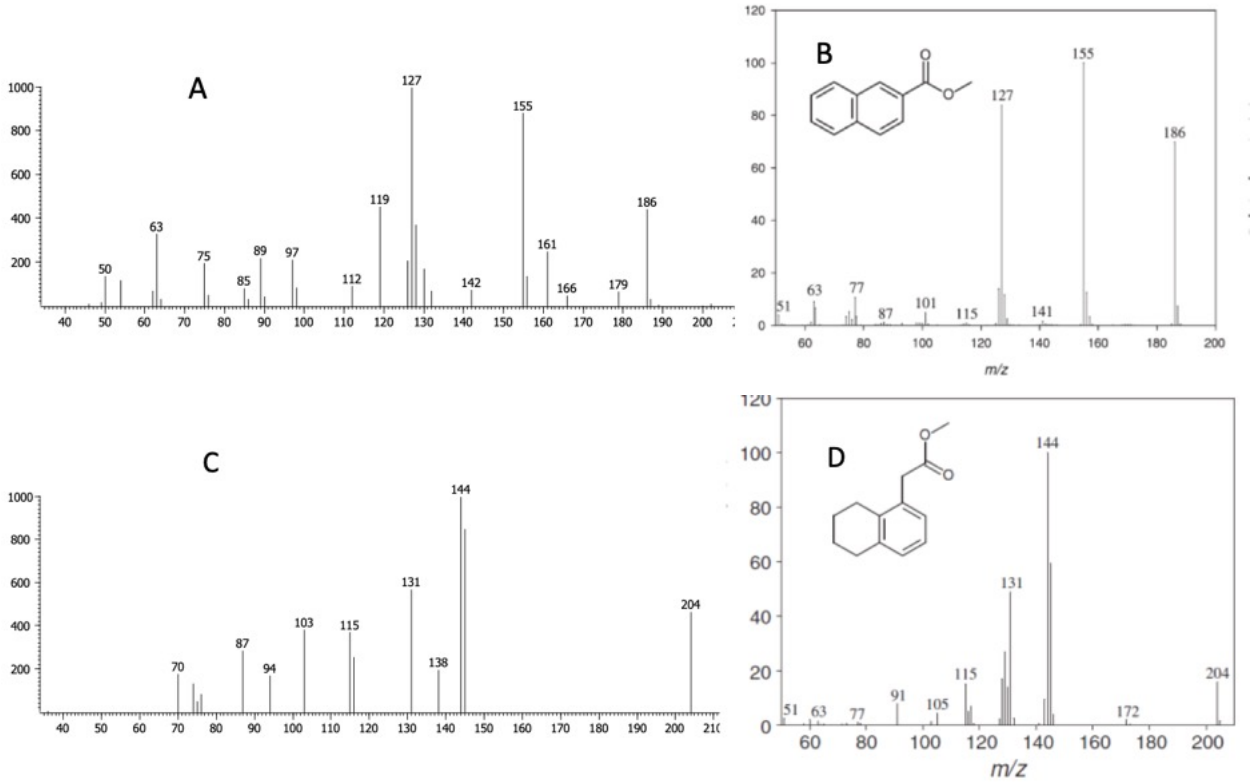

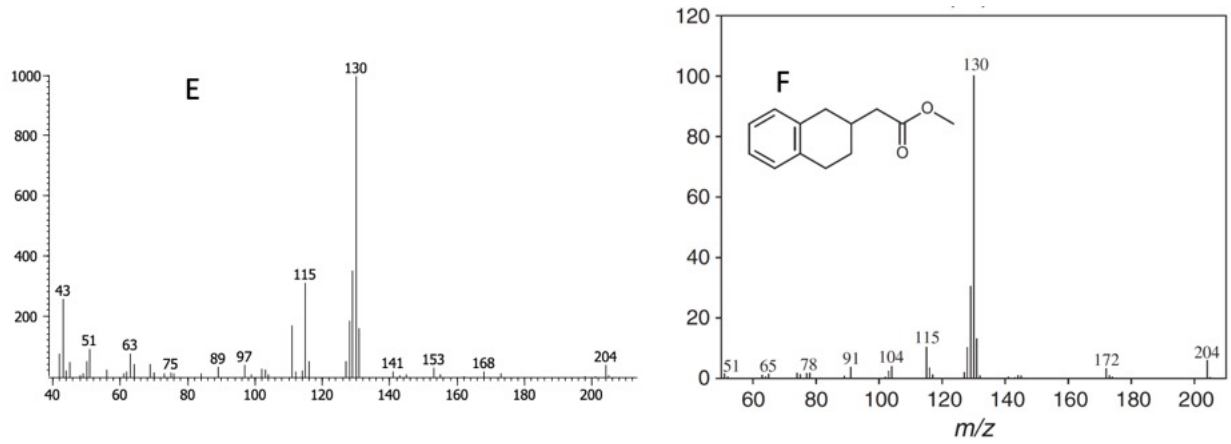


Figure 9: Comparison of the Identification of naphthoic acids in the FFT (A) with previously published spectrum (B) (West et al., 2014), Identification of 1,2,3,4 tetrahydro-2-ethanoic acid or 5,6,7,8 tetrahydro-2-ethanoic acid in the FFT (C) with spectrum published in (West et al., 2014) (D), Identification of 1,2,3,4 tetrahydro-1-ethanoic acid in the water column (E) with spectrum published in (West et al., 2014) (F).

### 3.2 Identification of metabolites indicative of NAs biodegradation

As NAs are considered the most toxic organic compounds in BML, (Bowman et al., 2020), we searched for their downstream metabolites along pathways (4-6) that could directly demonstrate their biological processing. All potential oxidative metabolites produced from the biodegradation of the previously identified monocyclic, bicyclic, and adamantane NAs (Bowman et al., 2020), along pathways (4-6), were searched for by replacing the exposed methyl group with OH, CHO, CO, and COOH groups representing their respective alcohol, aldehyde, ketone, and diacid metabolites. Each potential metabolite was searched for in all samples using their molecular ion and diagnostic fragments.

This analysis only detected the $C_{12}$ and $C_{13}$ adamantane diacid downstream metabolites for the $C_{12}$ adamantane NAs previously identified in BML(Bowman et al., 2020). The metabolites were only present in water column samples comprising a time range from 2015-2018. We were able to identify four isomers of the $C_{12}$ adamantane diacids through comparison with the mass spectrum of the diacids previously reported by (Lengger et al., 2013). The mass spectrum of the C12

adamantane diacids were characterized by a molecular ion at 252 m/z, and an ion at m/z 220 associated with a loss of CH3OH (32 amu) from the molecular ion. The base peak was observed at 193 m/z associated with a COOCH3 (59 amu) loss from the molecular ion or at 192 m/z due to H transfer following the COOCH3 loss. The peak at m/z 161 was due to further loss of CH3OH (32 amu) from the 193 m/z fragment. The fragment detected at 133 m/z was associated with a retained adamantane core after the loss of both methylated carboxy groups and hydrogen from the molecular ion.

Additionally, we detected six isomers from the $C_{13}$ dicarboxylic acids adamantane also reported by (Lengger et al., 2013) in OSPW. The mass spectrum in agreement with that published in (Lengger et al., 2013) , was characterized by a molecular ion at m/z 266, and a fragment at 252 m/z associated with a CH2 (14 amu) loss, and a fragment at 234 m/z due to a loss of CH3OH (32 amu) from the molecular ion, further confirming its assignment. The base peak was observed at 207 m/z due to a COOCH3 (59 amu) loss or at 206 m/z due to an additional hydrogen transfer, and a fragment at 175 m/z due to further loss of CH3OH (32 amu) from the 207 m/z fragment. The 133 m/z associated with the retained adamantane core was only observed at 3 isomers for the $C_{13}$ adamantane diacids.

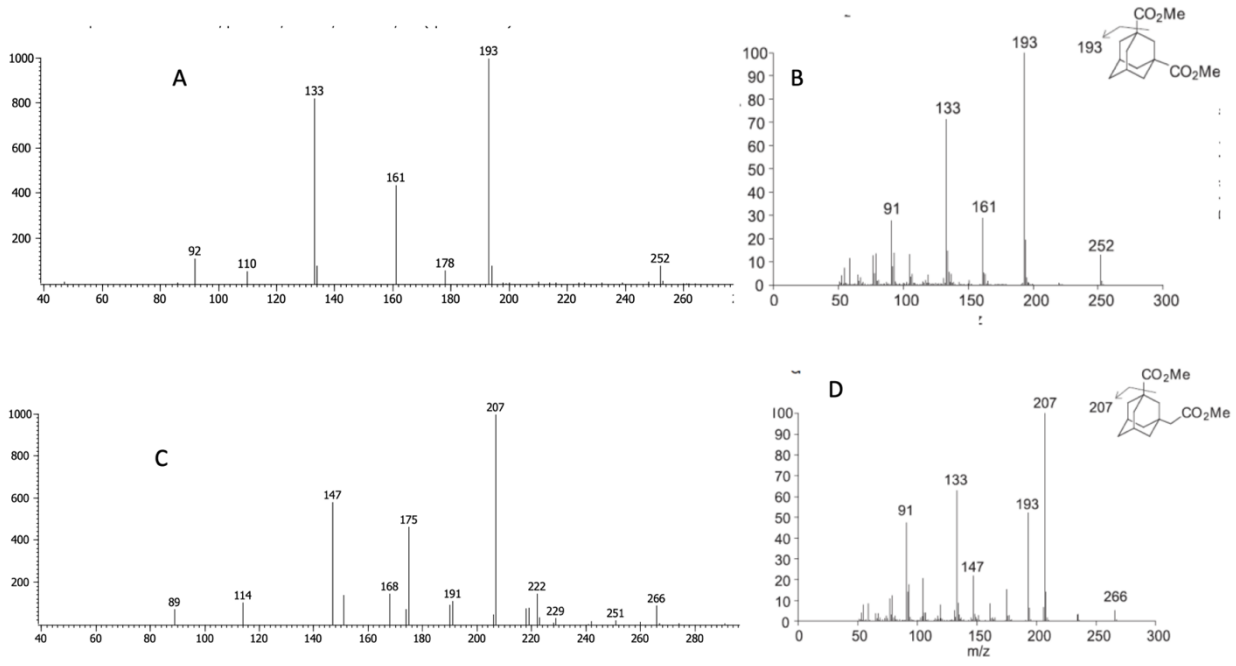


Figure 10: Comparison of the Identification of $C_{12}$ diacids adamantane in the water column (A) with previously published spectrum (B) (Lengger et al., 2013), $C_{13}$ diacids adamantane in the water column (C) with previously published spectrum (Lengger et al., 2013) (D).

# 4-Discussion

## 4.1 Anaerobic biodegradation of hydrocarbons in the FFT of BML

Succinate derivatives have been previously identified as signature metabolites exclusively for the anaerobic biodegradation of hydrocarbons (Aitken et al., 2018; Rabus et al., 2001). We report in the study, the identifications for cyclohexane and bicyclic succinates anaerobic biodegradation metabolites. The succinates metabolites were only present in 2015 FFT samples. However, the lack of detection of these succinates in the 2019 samples may well be due to a decrease in instrument sensitivity from 2015 to 2019. Notably, the succinates metabolites concentrations produced from alkyl benzene biodegradation in a controlled field study (Beller et al., 1995) were found to sharply decrease after reaching the concentration maximum implying their transient nature. Thus, it would be expected to detect succinates in settings with recent biological activity. The unique presence of the succinates in 2015 FFT samples would imply their intrinsic production in the FFT as a result of the anaerobic biodegradation of hydrocarbons.

Cyclohexane succinates were previously identified as metabolites produced from the anaerobic microbial incubations of cycloalkanes under denitrifying conditions(Wilkes et al., 2003), and through synthesis (Bian et al., 2014). However, cyclohexane succinates with methyl substituents, identified herein, have not been previously identified. We postulate that the possible precursor for $C_{11}$, $C_{12}$, $C_{13}$ cyclohexane succinates are methyl, dimethyl or ethyl, and ethyl methyl cyclohexane alkanes. Under anaerobic conditions in the FFT, the alkylated cyclohexanes would be activated to yield the succinate intermediates (pathway 2) (Figure 11). Further metabolism can occur through carbon skeleton rearrangement and decarboxylation to yield a downstream metabolite with a single carboxylic acid moiety. Such metabolites structure would match cyclohexane NAs previously identified in OSPW and BML (Bowman et al., 2020; Rowland et al., 2011). Bicyclic succinates have also never been identified previously. The possible precursor for the bicyclic succinates would be the $C_8$, $C_9$, $C_{10}$ bicyclanes never previously reported in oil sand tailings. The analysis of hydrocarbons in the FFT of BML couldn't resolve any of the cyclic

alkanes as they eluted within the UCM (unresolved complex mixture) region. However, $C_9$ and $C_{10}$ bicyclanes have been previously reported in West Siberian oils (Sokolova et al., 1989). They would be expected to follow the same metabolic pathway as the cyclohexane succinates generating NAs metabolites through rearrangement then decarboxylation. Their potential downstream metabolites would be bicyclic NAs that have been previously identified in OSPW (Wilde et al., 2015) and BML (Bowman et al., 2020). Thus, these succinates represent metabolic intermediates between the parent hydrocarbons and NAs acid downstream metabolites.

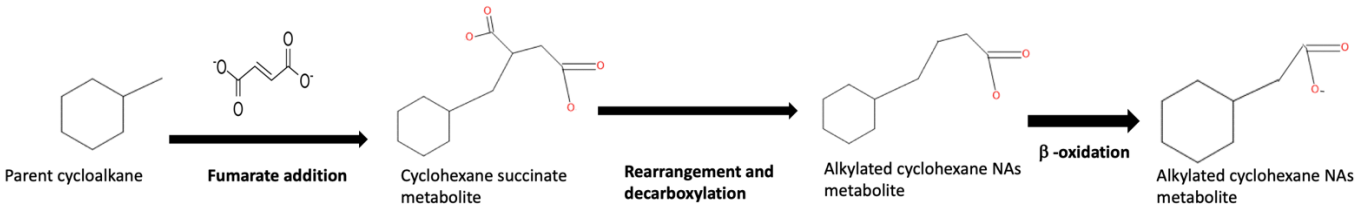


Figure 11: Postulated Metabolic pathway for the cyclohexane derivative showing the precursor parent cycloalkane and downstream metabolite cyclohexane NAs.

The detection of the succinate metabolites herein provides a direct indication for the occurrence of biodegradation that could be more sensitive than tracking the change in concentration of the parent substrate. Previous lab studies of oil sand tailings under methanogenic conditions that included methyl and ethyl cyclohexane didn't show any signs of depletion during incubation (Faidz et al., 2017; Siddique et al., 2020). The reason for this conclusion may be that there wasn't sufficient transformation of the parent cycloalkanes due to the slow biodegradation rates under anaerobic conditions and their less favorability for biodegradation compared to the other branched alkane substrates used in the experiment. This limitation is overcome by the detection of the succinates that provides a direct indication for the occurrence of anaerobic biodegradation in the FFT of BML.

Aromatic acids, naphthoic acids and tetrahydro naphthoic acids, were also detected in both 2015 and 2019 FFT samples as well as 2015-2018 water samples of BML. Naphthoic acids have been reported as a metabolite from the degradation of naphthalene through direct carboxylation (pathway 3) or methyl naphthalene through decarboxylation of its succinic derivative ( pathway

2) ( Aitken et al., 2004). Tetrahydro naphthoic acids are formed as a result of further degradation of 2-napthoic acid via a series of hydrogenation steps (Widdel and Rabus, 2001). Previous studies detected the tetrahydro naphthoic acids metabolite only in anaerobically degraded oils (Meckenstock et al., 2000; Phelps and Young, 2002). Even though naphthoic acid has been detected also in aerobic settings (Seo et al., 2009), their detection in the anaerobic FFT in the presence of tetrahydro naphthoic acid would indicate that the naphthoic acids have been generated through the anaerobic pathways(Aitken et al., 2004). Thus, the detection of the aromatic acids in the FFT directly indicates the occurrence of anaerobic biodegradation. While the observation of naphthoic acids in the water column could have been due to aerobic biodegradation, the detection of the tetrahydro ethanoic isomers in the aerobic water column indicates that they have been upwardly transported from the FFT through advection. Accordingly, the detection of the aromatic acids in BML suggests that hydrocarbons in the FFT are biodegraded anaerobically then transported upward into the water column of BML.

**4.2 Aerobic biodegradation of NAs in the water column**

Hydroxylated NAs and diacids have been reported in aerobic lab studies to be generated as further metabolites for NAs biodegradation through the α,β, or ω oxidation pathways (pathways 4-6) (Johnson et al., 2012; Whitby, 2010). Here we report the presence of C12, C13 diacids in the water column of BML that are postulated to be further downstream metabolites of C12 adamantane monoacidic NAs previously identified in OSPW and water column of BML(Bowman et al., 2020; Rowland et al., 2011).

A metabolic pathway for the diacids production ( Figure 12) proposed by(Lengger et al., 2013) entails carboxylation of the methyl substituent of the $C_{12}$ adamantane monoacid to form $C_{13}$ diacid adamantane through ω oxidation process(Johnson et al., 2012). This is followed by further metabolization through α the oxidation process (Quagraine et al., 2005; Whitby, 2010), to form the $C_{12}$ diacid adamantane which could be further processed through β-oxidation (Quagraine et al., 2005; Whitby, 2010). It's worthy to note that no other metabolites for NAs biodegradation were detected in the water column. This could be due to analytical limitations in identifying these compounds as UCM still comprised most of the chromatogram. But, it could also indicate

the transient nature of other metabolites generated in the water column of BML in comparison to the recalcitrance of the adamantane.

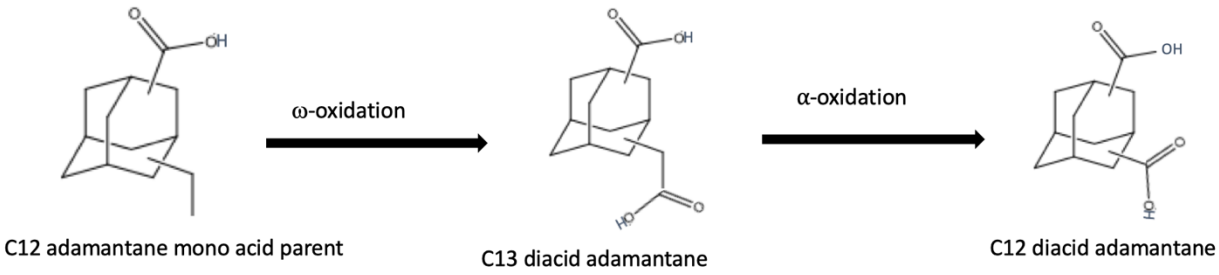


Figure 12: Postulated metabolic pathway for $C_{12}$ and $C_{13}$ diacids metabolites, modified from (Lengger et al., 2013).

The $C_{12}$ and $C_{13}$ adamantane diacids were previously reported in stored OSPW collected from WIP in 2011(Lengger et al., 2013), while they were not detected in fresh OSPW taken from the inlet pipe into WIP (Rowland et al., 2011) implying that they are only generated as a result of the intrinsic biodegradation in WIP. Laboratory studies confirmed that the generation of diacids metabolites from NAs biodegradation only occurs under aerobic conditions(Johnson et al., 2012), while there are no reports yet of their production under anaerobic conditions. In this study, we didn't detect these diacids in two OSPW samples from other tailing pond sites (SWIP and MLSB), FFT samples from 2015-2019, and bitumen, consistent with the fact that these environments are anaerobic. This lack of anaerobic production implies that the diacids previously identified in OSPW collected from WIP (Lengger et al., 2013) were generated as a result of aerobic biodegradation that occurred either near the surface of WIP or prior to the development of fully anoxic conditions. The detection of the diacids in this study only in the aerobic water column from 2015-2018 suggests that they are produced as a result of intrinsic aerobic biodegradation in the water column of BML.

To access the temporal changes of the identified $C_{12}$ and $C_{13}$ adamantane diacids in the water column, their relative abundance (calculated by multiplying peak areas by 1000, normalizing to internal standard 5 α cholestane, then adding up all isomers within each species) was compared

across 2015, 2017, 2018 samples in platform 1 from the epilimnion, metalimnion, and hypolimnion. There wasn't any significant change in abundance with depth across the epilimnion, metalimnion, and hypolimnion for any given year in 2015, 2017, 2018 samples. The stability in the depth profile for the $C_{12}$ and $C_{13}$ adamantane diacid metabolites indicates that aerobic biodegradation rates are consistent throughout the water column.

The relative abundances for the average of the $C_{12}$ and $C_{13}$ adamantane diacids in the epilimnion, metalimnion, and hypolimnion at each year were highest in 2018 (Figure 13). And indeed, the relative abundances of the $C_{13}$ adamantane diacids showed a statistically significant (P-value < 0.05) increase from 2015 to 2018, while $C_{12}$ adamantane diacids showed a marginally significant increase (p-value = 0.06) from 2017 to 2018. The relative abundances of the $C_{13}$ adamantane diacids showed ~ a 2-fold increase from 2015 to 2018 while the abundances of $C_{12}$ adamantane diacids decreased slightly from 2015 to 2017, then increased by ~ 1.8-fold from 2017 to 2018. The imbalance between the temporal change of the $C_{13}$ and $C_{12}$ adamantane diacids implies that the rate of production of the $C_{13}$ adamantane diacids, from the monoacid precursor, exceeds the rate of their further transformation to $C_{12}$ adamantane diacids through the α oxidation pathway.

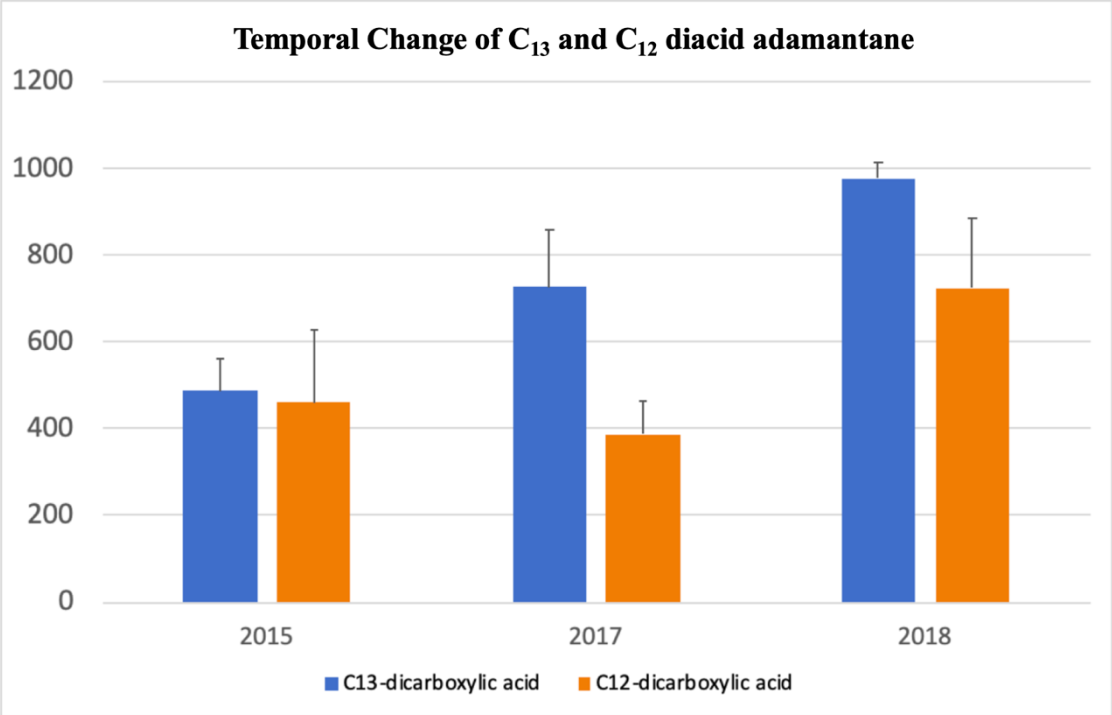


Figure 13: Bar graph for the relative abundances for the $C_{12}$ and $C_{13}$ adamantane diacids metabolites in the water column from 2015 to 2018. Error bars represent the average of the abundances at the epilimnion, metalimnion, and hypolimnion at each year.

## 5-Summary/implications

The GC×GC TOFMS analysis of the methylated extracts from the FFT and water column of BML revealed the presence of signature metabolic intermediates indicative of the occurrence of in-situ biodegradation. In the FFT, we tentatively identified the cyclohexane and bicyclic succinates metabolic intermediates between their parent hydrocarbons and downstream NAs. Additionally, signature naphthoic acid and tetrahydro ethanoic acids metabolites of naphthalene and alkylated naphthalene were also identified in the FFT through comparison with published mass spectrum, further supporting the occurrence of in-situ anaerobic biodegradation in the FFT. We also identified $C_{12}$, $C_{13}$ adamantane diacid metabolites for the aerobic biodegradation of $C_{12}$ monoacid adamantane in the water column. Tracking the relative abundance of these metabolites temporally from 2015 to 2018 revealed a significant increase implying that their rate of production is greater than further processing. The identification of the metabolites reported herein provided evidence that the anaerobic biodegradation in the FFT generates metabolic intermediates that are released upward into the water column, and are then subjected to active aerobic biodegradation in the water column. Thus, biodegradation can be considered a natural mitigation process for contaminants in BML. Further tracking of these metabolites and others temporally in future studies can delineate the significance of biodegradation towards establishing reclamation certification in BML.

**References**


Aitken, C.M., Head, I.M., Jones, D.M., Rowland, S.J., Scarlett, A.G., West, C.E., 2018. Comprehensive two-dimensional gas chromatography-mass spectrometry of complex mixtures of anaerobic bacterial metabolites of petroleum hydrocarbons. J. Chromatogr. A 1536, 96–109. https://doi.org/10.1016/j.chroma.2017.06.027

Aitken, C.M., Head, I.M., Jones, D.M., Rowland, S.J., Scarlett, A.G., West, C.E., 2017. Comprehensive two-dimensional gas chromatography-mass spectrometry of complex mixtures of anaerobic bacterial metabolites of petroleum hydrocarbons. J. Chromatogr. A. https://doi.org/10.1016/j.chroma.2017.06.027

Aitken, Carolyn M., Jones, D.M., Larter, S.R., 2004. Anaerobic hydrocarbon biodegradation in deep subsurface oil reservoirs. Nature 431, 291–294. https://doi.org/10.1038/nature02922

Aitken, Carolyn M, Jones, D.M., Larter, S.R., 2004. Anaerobic hydrocarbon biodegradation in deep subsurface oil reservoirs. Nature 431, 291–294. https://doi.org/10.1038/nature02922

Beller, H.R., Ding, W.H., Reinhard, M., 1995. Byproducts of Anaerobic Alkylbenzene Metabolism Useful as Indicators of in Situ Bioremediation. Environ. Sci. Technol. 29, 2864–2870. https://doi.org/10.1021/es00011a024

Bian, X.Y., Mbadinga, S.M., Yang, S.Z., Gu, J.D., Ye, R.Q., Mu, B.Z., 2014. Synthesis of anaerobic degradation biomarkers alkyl-, aryl- and cycloalkylsuccinic acids and their mass spectral characteristics. Eur. J. Mass Spectrom. 20, 287–297. https://doi.org/10.1255/ejms.1280

Boll, Matthias, Fuchs, G., Heider, J., 2002. Anaerobic oxidation of aromatic compounds and hydrocarbons. Curr. Opin. Chem. Biol. 6, 604–611. https://doi.org/10.1016/S1367-5931(02)00375-7

Boll, M, Fuchs, G., Heider, J., 2002. Anaerobic oxidation of aromatic compounds and hydrocarbons. Curr. Opin. Chem. Biol. 6, 604–611. https://doi.org/10.1016/s1367-5931(02)00375-7

Bowman, D.T., Slater, G.F., Warren, L.A., McCarry, B.E., 2014. Identification of individual thiophene-, indane-, tetralin-, cyclohexane-, and adamantane-type carboxylic acids in composite tailings pore water from Alberta oil sands. Rapid Commun. Mass Spectrom. 28, 2075–2083. https://doi.org/10.1002/rcm.6996

Bowman, D.T., Warren, L.A., Slater, G.F., 2020. Isomer-specific monitoring of naphthenic acids at an oil sands pit lake by comprehensive two-dimensional gas chromatography–mass spectrometry. Sci. Total Environ. 746, 140985. https://doi.org/10.1016/j.scitotenv.2020.140985

Brown, L.D., Ulrich, A.C., 2015. Oil sands naphthenic acids: A review of properties, measurement, and treatment. Chemosphere 127, 276–290. https://doi.org/10.1016/j.chemosphere.2015.02.003

Clemente, J.S., Mackinnon, M.D., 2004. Aerobic Biodegradation of Two Commercial Naphthenic Acids Preparations 38, 1009–1016. https://doi.org/10.1021/es030543j

Clothier, L.N., Gieg, L.M., 2016. Anaerobic biodegradation of surrogate naphthenic acids. Water Res. 90, 156–166. https://doi.org/10.1016/j.watres.2015.12.019

Das, N., Chandran, P., 2011. Microbial degradation of petroleum hydrocarbon contaminants: an overview. Biotechnol. Res. Int. 2011, 941810. https://doi.org/10.4061/2011/941810

Faidz, M., Shahimin, M., Siddique, T., 2017. Sequential biodegradation of complex naphtha

hydrocarbons under methanogenic conditions in two different oil sands tailings * 221.
Folwell, Benjamin D, Mcgenity, T.J., Price, A., Johnson, R.J., Whitby, C., 2016. International Biodeterioration & Biodegradation Exploring the capacity for anaerobic biodegradation of polycyclic aromatic hydrocarbons and naphthenic acids by microbes from. Int. Biodeterior. Biodegradation 108, 214–221. https://doi.org/10.1016/j.ibiod.2014.12.016
Folwell, Benjamin D., McGenity, T.J., Price, A., Johnson, R.J., Whitby, C., 2016. Exploring the capacity for anaerobic biodegradation of polycyclic aromatic hydrocarbons and naphthenic acids by microbes from oil-sands-process-affected waters. Int. Biodeterior. Biodegrad. 108, 214–221. https://doi.org/10.1016/j.ibiod.2014.12.016
Frank, R.A., Fischer, K., Kavanagh, R., Kent Burnison, B., Arsenault, G., Headley, J. V., Peru, K.M., Van Glen Kraak, D.E.R., Solomon, K.R., 2009. Effect of carboxylic acid content on the acute toxicity of oil sands naphthenic acids. Environ. Sci. Technol. 43, 266–271. https://doi.org/10.1021/es8021057
Gervais, J.J.., 2004. Fate and Transport of Naphthenic Acids in a Glacial Aquifer by 1–566.
Gray, N.D., Sherry, A., Hubert, C., Dolfing, J., Head, I.M., 2010. Methanogenic degradation of petroleum hydrocarbons in subsurface environments: Remediation, heavy oil formation, and energy recovery, 1st ed, Advances in Applied Microbiology. Elsevier Inc. https://doi.org/10.1016/S0065-2164(10)72005-0
Gruner, A., Jarling, R., Vieth-Hillebrand, A., Mangelsdorf, K., Janka, C., van der Kraan, G.M., Köhler, T., Morris, B.E.L., Wilkes, H., 2017. Tracing microbial hydrocarbon transformation processes in a high temperature petroleum reservoir using signature metabolites. Org. Geochem. 108, 82–93. https://doi.org/10.1016/j.orggeochem.2017.03.003
Head, I.M., Jones, D.M., Larter, S.R., 2003. Biological activity in the deep subsurface and the origin of heavy oil. Nature 426, 344–352. https://doi.org/10.1038/nature02134
Headley, J. V., Barrow, M.P., Peru, K.M., Fahlman, B., Frank, R.A., Bickerton, G., McMaster, M.E., Parrott, J., Hewitt, L.M., 2011. Preliminary fingerprinting of Athabasca oil sands polar organics in environmental samples using electrospray ionization Fourier transform ion cyclotron resonance mass spectrometry. Rapid Commun. Mass Spectrom. 25, 1899–1909. https://doi.org/10.1002/rcm.5062
Heider, J., Schule, K., 2013. Anaerobic Biodegradation of Hydrocarbons Including Methane, In: Rosenberg E., DeLong E.F., Lory S., Stackebrandt E., Thompson F. (eds) The Prokaryotes - Prokaryotic Biology and Symbiotic.
Holowenko, F.M., MacKinnon, M.D., Fedorak, P.M., 2001. Naphthenic acids and surrogate naphthenic acids in methanogenic microcosms. Water Res. 35, 2595–2606. https://doi.org/10.1016/S0043-1354(00)00558-3
Jarling, R., Kühner, S., Janke, E.B., Gruner, A., Drozdowska, M., Golding, B.T., Rabus, R., Wilkes, H., 2015. Versatile transformations of hydrocarbons in anaerobic bacteria: Substrate ranges and regio- and stereo-chemistry of activation reactions. Front. Microbiol. 6, 1–14. https://doi.org/10.3389/fmicb.2015.00880
Jeris, J.S., Perry L. McCarty, 1965. The Biochemistry of Methane Fermentation Using C14 Tracers. Water Pollut. Control Fed. 37, 178–192.
Johnson, R.J., West, C.E., Swaih, A.M., Folwell, B.D., Smith, B.E., Rowland, S.J., Whitby, C., 2012. Aerobic biotransformation of alkyl branched aromatic alkanoic naphthenic acids via two different pathways by a new isolate of Mycobacterium. Environ. Microbiol. 14, 872–882. https://doi.org/10.1111/j.1462-2920.2011.02649.x
Kendall, M.M., Jeanthon, C., Corre, E., Reysenbach, A.L., 2003. Microbial diversity of

petroleum reservoirs. Encycl. Environ. Microbiol. https://doi.org/10.1002/0471263397.env080
Kropp, K.G., Davidova, I. a, Suflita, J.M., 2000. Anaerobic Oxidation of n -Dodecane by an Addition Reaction in a Sulfate-Reducing Bacterial Enrichment Culture. Appl. Environ. Microbiol. 66, 5393–8. https://doi.org/10.1128/AEM.66.12.5393-5398.2000.Updated
Lengger, S.K., Scarlett, A.G., West, C.E., Rowland, S.J., 2013. Diamondoid diacids ("O4" species) in oil sands process-affected water. Rapid Commun. Mass Spectrom. 27, 2648–2654. https://doi.org/10.1002/rcm.6729
Magot, M., Ollivier, B., Patel, B.K.C., 2000. Microbiology of petroleum reservoirs [Review]. Antonie van Leeuwenhoek Int. J. Gen. Mol. Microbiol. 77, 103–116.
Meckenstock, R.U., Annweiler, E., Michaelis, W., Richnow, H.H., Schink, B., 2000. Anaerobic naphthalene degradation by a sulfate-reducing enrichment culture. Appl. Environ. Microbiol. 66, 2743–2747. https://doi.org/10.1128/AEM.66.7.2743-2747.2000
Olajire, A.A., Essien, J.P., 2014. Aerobic Degradation of Petroleum Components by Microbial Consortia. J. Pet. Environ. Biotechnol. 5, 1–22. https://doi.org/10.4172/2157-7463.1000195
Phelps, C.D., Young, L.Y., 2002. Metabolic biomarkers for detecting anaerobic PAH biodegradation in groundwater and sediments. Soil Sediment Contam. 11, 1023.
Quagraine, E.K., Headley, J. V., Peterson, H.G., 2005. Is biodegradation of bitumen a source of recalcitrant naphthenic acid mixtures in oil sands tailing pond waters? J. Environ. Sci. Heal. - Part A Toxic/Hazardous Subst. Environ. Eng. 40, 671–684. https://doi.org/10.1081/ESE-200046637
Rabus, R., Wilkes, H., Behrends, A., Armstroff, A., Fischer, T., Pierik, A.J., Widdel, F., 2001. Anaerobic Initial Reaction of n -Alkanes in a Denitrifying Bacterium : Evidence for ( 1-Methylpentyl ) succinate as Initial Product and for Involvement of an Organic Radical in n -Hexane Metabolism Anaerobic Initial Reaction of n -Alkanes in a Denitrifyin. J. Bacteriol. 183, 1707–15. https://doi.org/10.1128/JB.183.5.1707
Rojo, F., 2009. Degradation of alkanes by bacteria: Minireview. Environ. Microbiol. 11, 2477–2490. https://doi.org/10.1111/j.1462-2920.2009.01948.x
Rowland, S.J., Scarlett, A.G., Jones, D., West, C.E., Frank, R.A., 2011. Diamonds in the rough: Identification of individual naphthenic acids in oil sands process water. Environ. Sci. Technol. 45, 3154–3159. https://doi.org/10.1021/es103721b
Seo, J.S., Keum, Y.S., Li, Q.X., 2009. Bacterial degradation of aromatic compounds, International Journal of Environmental Research and Public Health. https://doi.org/10.3390/ijerph6010278
Siddique, T., Fedorak, P.M., Foght, J.M., 2006. Biodegradation of short-chain n -alkanes in oil sands tailings under methanogenic conditions 40, 5459–5464.
Siddique, T., Phillip, M., Mackinnon, M.D., 2007. Metabolism of BTEX and Naphtha Compounds to Methane in Oil Sands Tailings 41, 2350–2356.
Siddique, T., Semple, K., Li, C., Foght, J.M., 2020. Methanogenic biodegradation of iso-alkanes and cycloalkanes during long-term incubation with oil sands tailings. Environ. Pollut. 258, 113768. https://doi.org/10.1016/j.envpol.2019.113768
Sierra-Garcia, I.N., de Oliveira, V.M., 2013. Microbial Hydrocarbon Degradation: Efforts to Understand Biodegradation in Petroleum Reservoirs. Biodegrad. Eng. Technol. 47–82. https://doi.org/10.5772/55920
So, C.M., Phelps, C.D., Young, L.Y., 2003. Anaerobic transformation of alkanes to fatty acids by a sulfate-reducing bacterium, strain Hxd3. Appl. Environ. Microbiol. 69, 3892–3900.

https://doi.org/10.1128/AEM.69.7.3892-3900.2003
Sokolova, I.M., Berman, S.S., Abryutina, N.., Petrov, A.A., 1989. Natrual concentrates of bi and tricyclic naphthenes. Chem. Technol. Fuels oils 233–235.
van der Heul, R., 2009. Environmental Degradation of petroleum hydrocarbons. Presentation.
West, C.E., Pureveen, J., Scarlett, A.G., Lengger, S.K., Wilde, M.J., Korndorffer, F., Tegelaar, E.W., Rowland, S.J., 2014. Can two-dimensional gas chromatography/mass spectrometric identification of bicyclic aromatic acids in petroleum fractions help to reveal further details of aromatic hydrocarbon biotransformation pathways? Rapid Commun. Mass Spectrom. 28, 1023–1032. https://doi.org/10.1002/rcm.6876
Whitby, C., 2010. Microbial naphthenic Acid degradation., 1st ed, Advances in applied microbiology. Elsevier Inc. https://doi.org/10.1016/S0065-2164(10)70003-4
Widdel, F., Rabus, R., 2001. Anaerobic biodegradation of saturated and aromatic hydrocarbons. Curr. Opin. Biotechnol. 12, 259–276. https://doi.org/10.1016/S0958-1669(00)00209-3
Wilde, M.J., West, C.E., Scarlett, A.G., Jones, D., Frank, R.A., Hewitt, L.M., Rowland, S.J., 2015. Bicyclic naphthenic acids in oil sands process water: Identification by comprehensive multidimensional gas chromatography-mass spectrometry. J. Chromatogr. A 1378, 74–87. https://doi.org/10.1016/j.chroma.2014.12.008
Wilkes, H., Kühner, S., Bolm, C., Fischer, T., Classen, A., Widdel, F., Rabus, R., 2003. Formation of n-alkane- and cycloalkane-derived organic acids during anaerobic growth of a denitrifying bacterium with crude oil. Org. Geochem. 34, 1313–1323. https://doi.org/10.1016/S0146-6380(03)00099-8
Wilkes, H., Rabus, R., Fischer, T., Armstroff, A., Behrends, A., Widdel, F., 2002. Anaerobic degradation of n-hexane in a denitrifying bacterium: Further degradation of the initial intermediate (1-methylpentyl)succinate via C-skeleton rearrangement. Arch. Microbiol. 177, 235–243. https://doi.org/10.1007/s00203-001-0381-3

**Chapter five: Conclusions and recommendations for future work:**

The studies in this dissertation are part of an integrated project that assesses the effectiveness of the water capped tailings technology (WCTT) implemented by Syncrude Canada Ltd. as a reclamation solution for managing the oil sand tailings and the mined-out pits in the BaseMine lake (BML) demonstration. In order to validate WCTT in the BML demonstration, the water quality of the lake should continue to improve with time. The oxygen levels in the water column of BML in addition to the toxicity of residual organic matter, particularly naphthenic acids (NAs), released from the fluid fine tailings (FFT) are the key parameters that control the water quality of BML. Assessment of the water quality through these parameters would help inform future managerial decisions towards the reclamation of BML and potentially other tailing sites. This dissertation demonstrated that utilizing fingerprinting of organic compounds resolved by multidimensional chromatography (GC×GC) can help understand the identity of residual organic matter in BML, their biological cycling, and their potential release into the water column.

**Chapter two:**

Methane generation in oil sand tailing sites presents an environmental concern due to its effect on depleting oxygen levels upon oxidation(Arriaga et al., 2019; Risacher et al., 2018b) in addition to its role as a component of greenhouse gas emissions. Maintaining aerobic conditions in end pit lake demonstrations as BML is crucial to facilitate the biodegradation of toxic contaminates and establish natural ecosystems. Thus, characterizing the hydrocarbons that are capable of generating methane can help predict future methane generation potential from BML or other tailing sites. In addition, these insights will be able to be transferred to other sites where high concentrations of complex petroleum hydrocarbons are present within sediments such as harbors, and spill sites.

In chapter two, the objective of the study was to identify the hydrocarbons capable of methane generation within the fluid fine tailings (FFT) of BML and evaluate their biodegradation potential. This study was the first study to directly characterize the hydrocarbons from the FFT in

BML. A suite of FFT samples from platforms one, two, and three (P1, P2, P3) were extracted and analyzed for bulk parameters as the TOC (total organic carbon), TLE (total lipid extract), saturates, aromatics, and polar fractions. Additionally, hydrocarbon compounds such as alkylated PAHs, low molecular weight alkanes, and biomarkers compounds were resolved using multi-dimensional chromatography. The overall depletion of the high biodegradable compounds in addition to the enrichment of the polars relative to the saturate and aromatics implied that the samples exhibit a biodegradation signature as expected for oil sand bitumen that is known to be heavily biodegraded. Identifying the occurrence of in situ biodegradation, within the biodegraded hydrocarbons in the FFT, was further complicated by the spatial heterogeneity observed across platforms in the shallow and deep intervals. Despite this heterogeneity, an intrinsic biodegradation signature was detected at shallow intervals at P2 and P3 as a result of the depletion of the low molecular weight compounds/high biodegradable compounds that didn't show a variation spatially across the two platforms. The occurrence of biodegradation was further confirmed by the greater initial loading of organic matter at the shallow interval at P2 and P3 that was inferred from the high concentrations of TOC and low biodegradable/ higher molecular weight compounds.

Future research can focus on optimizing methods for higher extraction efficiency and detection of the low molecular weight compounds in particular the naphtha components that have a higher potential to biodegrade and eventually generate methane(Siddique et al., 2007, 2006). Our ability to resolve the low molecular weight compounds was limited in this study due to low instrument sensitivity and also because they eluted within the unresolved complex mixture (UCM) observed in the GC×GC chromatographs of the FFT samples. The extraction of the low molecular weight compounds through fractionation prior to GC analysis can enhance their resolving in future studies. Also, the utilization of high-resolution mass spectrometry techniques can enhance the identification of these compounds.

A limitation of this study was the lack of temporal tracking of the resolved hydrocarbons. Continuous temporal tracking of these compounds in future studies can determine their biodegradation rate and potential to generate methane. However, as the low molecular weight compounds can also be transported from the FFT into the water column through gas stripping or

movement on the bubble surface associated with methane ebullition, future studies should also focus on identifying the hydrocarbons present on the bubble surface to differentiate between the impacts of biodegradation and ebullition on depleting these compounds.

**Chapter three:**

As a result of the toxicity associated with NAs (Frank et al., 2008; Holowenko et al., 2002), efforts to elucidate their molecular fingerprint, sources, and biodegradation potential have been ongoing in order to manage their release into the environment (Bowman et al., 2020, 2014; Johnson et al., 2012; Steven J. Rowland et al., 2011d, 2011c; Wilde et al., 2015a). For instance, deciphering the molecular fingerprint and sources of NAs in oil sand tailing ponds would help assess their potential contamination for nearby groundwater aquifers and the Athabasca River through the leakage of oil sands process water from the ponds. In the context of this study, evaluating the sources of input of NAs into the water column of BML and their biodegradation potential helped validate water cap tailing technology towards managing the release of NAs from the FFT and allowing future water release from BML.

The study used the GC×GC to identify and monitor the relative abundances of a suite of monocyclic, bicyclic, adamantane, and thiophene NAs across water column, FFT, OSPW, and bitumen samples. The occurrence of NAs inputs into the water column through advection from the FFT was indicated by the elevated abundances of the NAs species and isomers in the FFT and their similar concentrations in OSPW relative to the water column. The unique presence of 14 NAs isomers in the water column implied their production from intrinsic hydrocarbons biodegradation in BML. Further evidence of NAs input from hydrocarbons biodegradation was indicated by the absence of the C8 bicyclic in the bitumen implying their production post extraction from the subsurface as a result of biodegradation of their bicyclanes precursor. The stability of NAs in the water column, observed from tracking their abundances temporally over four years, implied that active biological cycling must be occurring in the water column to balance out additional inputs of NAs from FFT advection or hydrocarbon biodegradation. The occurrence of biodegradation in the water column was further confirmed by the preferential depletion of the least alkylated/cyclic NA species in the water column relative to the FFT in

addition to the slight enrichment of NA species in the hypolimnion. Thus, this study demonstrated that biodegradation in the water column can manage the release of ongoing NAs inputs.

As this study only analyzed FFT for one-year, future studies can focus on the addition of FFT samples from subsequent years to track their temporal variations. The comparison of temporal variations between the FFT and water column can better elucidate the extent of NAs input from the FFT into the water column. Also, since the one shallow FFT sample analyzed in this study showed a significant depletion of NAs relative to deep FFT samples, the analysis of additional FFT samples could help constrain this spatial variability. The analysis of additional shallow FFT samples could help determine if the depletion relative to the deep FFT samples was due to heterogeneity within the FFT or as a result of other processes such as mixing with the water column.

**Chapter Four:**

Determining the occurrence of hydrocarbons and NAs biodegradation, in chapters two and three, through tracking the spatial and temporal change in the concentration of reactants was perplexed by the heterogeneity of their distribution in addition to advection and/or ebullition from the FFT. Thus, to overcome this limitation, identifying the signature metabolites in chapter four, provided a direct indication for the occurrence of biodegradation in BML. Through the utilization of the GC×GC, we searched for all possible metabolites that could be generated from the biodegradation of hydrocarbons or NAs through aerobic or anaerobic pathways. The identification of cyclohexane and bicyclic succinates metabolites in the FFT implied that they have been generated as a result of the anaerobic biodegradation of their cyclane and bicyclane hydrocarbon precursors in the FFT. Evidence for the occurrence of anaerobic biodegradation in the FFT was further supported by the identification of aromatic acids metabolites, naphthoic acids and tetrahydronaphthoic acids, that are generated as intermediates for the biodegradation of naphthalene and alkylated naphthalene.

While the identification of C12 and C13 diacid adamantane metabolites only in the water column

implied that they have been generated as a result of the aerobic biodegradation of their C12 adamantane monoacids precursor. Tracking the relative abundance of the diacids temporally revealed that the fold change of C13 diacid was greater than its C12 diacid downstream metabolites, thus implying that the rate of C13 diacid production is greater than its subsequent transformation to C12 diacids. This study demonstrated that the anaerobic biodegradation of hydrocarbons in the FFT and the aerobic biodegradation of NAs in the water column could help manage their release and achieve reclamation certification in BML.

As this study proved that metabolites indicative of the biodegradation of hydrocarbons and NAs occur in BML, future studies can focus on optimizing extraction and analytical techniques that facilitate the resolving and identification of these compounds. For instance, successful derivatization can aid in resolving the hydroxylated intermediates that we failed to detect in this study as they often don't show a molecular ion in their mass spectrum. Furthermore, the utilization of high-resolution mass spectrometry could aid in the firm identification of these metabolites compared to the nominal mass spectrometry used in this study. Also, the synthesis of compounds that have never been previously identified, as succinates, could further support their mass spectral assignments.

**Outlook**:

The occurrence of biodegradation in environmental systems are assessed through laboratory microcosm studies, for example, (Clemente and Mackinnon, 2004; Fedorak et al., 2002; Holowenko et al., 2001a; Mohamad Shahimin and Siddique, 2017; Siddique et al., 2008, 2007) or directly through characterizing the distribution of the organic in the field, for example, (Gros et al., 2014; Hall et al., 2013; Wardlaw et al., 2008). In this dissertation, the analysis of hydrocarbons and NAs biodegradation potential in BML assessed the biodegradation from oil sand tailings directly through field analysis. Previous studies that analyzed the biodegradation of hydrocarbons from oil sand tailings mainly utilized laboratory microsome analysis (Holowenko et al., 2001b; Siddique et al., 2020, 2011, 2008, 2007). These studies have successfully proved that methane can be generated from the anaerobic biodegradation of low molecular weight organic carbon, however, the extent of hydrocarbons biodegradation and methane production

rates that are estimated in these laboratory incubation studies are probably not representable to the generation that occur in the subsurface. This is due to the following reasons: First, laboratory incubation experiments are grown in a medium that favors the growth of specific microorganisms, thus they can fail to re-create the same environmental conditions in the field that is controlled by temperature, PH, salinity, substrates, and nutrients. Second, the anaerobic biodegradation of organic matter in the field is believed to occur through a consortium of microorganisms that could encompass several processes such as fermentation, sulfate reduction, and methanogens whereas laboratory studies only focus on the enrichment of a specific microbial process or microorganisms. Thus, the direct analysis of the hydrocarbon in the field within environmental systems can provide a more accurate assessment for biodegradation occurrence than laboratory studies.

Through field analysis, the results of chapters two and four directly demonstrated the occurrence of anaerobic biodegradation of hydrocarbons in the FFT of BML. The evidence of anaerobic biodegradation of hydrocarbons was demonstrated through the preferential depletion of the low molecular weight/ high biodegradable at shallow depths in the FFT BML (Chapter two). More conclusive evidence for the occurrence of anaerobic biodegradation was demonstrated through the identification of the anaerobic signature metabolites (succinates and aromatics acids) in the FFT (Chapter four). These studies provided evidence that anaerobic biodegradation is a viable process for reclamation of contaminates from oil sand tailings. The demonstration of anaerobic biodegradation in these studies expanded our knowledge on the environmental systems of anaerobic biodegradation that are not widely studied. These results can inform future biodegradation studies in other anaerobic environments such as petroleum reservoirs.

Aerobic biodegradation in the water column of BML was demonstrated as a reclamation solution to manage the release of the toxic NAs compounds in chapters three and four. The results of chapter three implied that active biodegradation of NAs in the water column is managing the release of additional NAs inputs. Direct evidence for the biodegradation of NAs in the water column of BML was inferred from the identification of the diacids metabolites in the water column (chapter four). Since biodegradation can either completely mineralize NAs (Clemente and Mackinnon, 2004) or convert them to diacid metabolites (Johnson et al., 2012) that are found

to be less toxic than their monoacids precursor(Frank et al., 2009), the process would be a natural cost-effective reclamation solution towards mitigating the toxicity associated with NAs in oil sand tailing ponds.

**References:**


Arriaga D., Nelson T. C., Risacher F. F., Morris P. K., Goad C., Slater G. F. and Warren L. A. (2019) The co-importance of physical mixing and biogeochemical consumption in controlling water cap oxygen levels in Base Mine Lake. *Appl. Geochemistry* **111**, 104442. Available at: https://doi.org/10.1016/j.apgeochem.2019.104442.

Bowman D. T., Slater G. F., Warren L. A. and McCarry B. E. (2014) Identification of individual thiophene-, indane-, tetralin-, cyclohexane-, and adamantane-type carboxylic acids in composite tailings pore water from Alberta oil sands. *Rapid Commun. Mass Spectrom.* **28**, 2075–2083. Available at: http://doi.wiley.com/10.1002/rcm.6996 [Accessed March 13, 2018].

Bowman D. T., Warren L. A. and Slater G. F. (2020) Isomer-specific monitoring of naphthenic acids at an oil sands pit lake by comprehensive two-dimensional gas chromatography–mass spectrometry. *Sci. Total Environ.* **746**, 140985. Available at: https://doi.org/10.1016/j.scitotenv.2020.140985.

Clemente J. S. and Mackinnon M. D. (2004) Aerobic Biodegradation of Two Commercial Naphthenic Acids Preparations. **38**, 1009–1016.

Fedorak P. M., Coy D. L., Salloum M. J. and Dudas M. J. (2002) Methanogenic potential of tailings samples from oil sands extraction plants. *Can. J. Microbiol.* **48**, 21–33.

Frank R. A., Fischer K., Kavanagh R., Kent Burnison B., Arsenault G., Headley J. V., Peru K. M., Van Glen Kraak D. E. R. and Solomon K. R. (2009) Effect of carboxylic acid content on the acute toxicity of oil sands naphthenic acids. *Environ. Sci. Technol.* **43**, 266–271.

Frank R. A., Kavanagh R., Kent Burnison B., Arsenault G., Headley J. V., Peru K. M., Van Der Kraak G. and Solomon K. R. (2008) Toxicity assessment of collected fractions from an extracted naphthenic acid mixture. *Chemosphere* **72**, 1309–1314.

Gros J., Reddy C. M., Aeppli C., Nelson R. K., Carmichael C. A. and Arey J. S. (2014) Resolving biodegradation patterns of persistent saturated hydrocarbons in weathered oil samples from the Deepwater Horizon disaster. *Environ. Sci. Technol.* **48**, 1628–1637.

Hall G. J., Frysinger G. S., Aeppli C., Carmichael C. A., Gros J., Lemkau K. L., Nelson R. K. and Reddy C. M. (2013) Oxygenated weathering products of Deepwater Horizon oil come from surprising precursors. *Mar. Pollut. Bull.* **75**, 140–149.

Holowenko F. M., MacKinnon M. D. and Fedorak P. M. (2002) Characterization of naphthenic acids in oil sands wastewaters by gas chromatography-mass spectrometry. *Water Res.* **36**, 2843–2855.

Holowenko F. M., MacKinnon M. D. and Fedorak P. M. (2001a) Naphthenic acids and surrogate naphthenic acids in methanogenic microcosms. *Water Res.* **35**, 2595–2606.

Holowenko F. M., MacKinnon M. D. and Fedorak P. M. (2001b) Naphthenic acids and surrogate naphthenic acids in methanogenic microcosms. *Water Res.* **35**, 2595–2606.

Johnson R. J., West C. E., Swaih A. M., Folwell B. D., Smith B. E., Rowland S. J. and Whitby C. (2012) Aerobic biotransformation of alkyl branched aromatic alkanoic naphthenic acids via two different pathways by a new isolate of Mycobacterium. *Environ. Microbiol.* **14**, 872–882.

Mohamad Shahimin M. F. and Siddique T. (2017) Sequential biodegradation of complex naphtha hydrocarbons under methanogenic conditions in two different oil sands tailings. *Environ. Pollut.* **221**, 398–406. Available at: http://dx.doi.org/10.1016/j.envpol.2016.12.002.

Risacher F. F., Morris P. K., Arriaga D., Goad C., Nelson T. C., Slater G. F. and Warren L. A. (2018) The interplay of methane and ammonia as key oxygen consuming constituents in early stage development of Base Mine Lake, the first demonstration oil sands pit lake. *Appl. Geochemistry* **93**, 49–59. Available at: https://doi.org/10.1016/j.apgeochem.2018.03.013.

Rowland S. J., West C. E., Scarlett A. G. and Jones D. (2011a) Identification of individual acids in a commercial sample of naphthenic acids from petroleum by two-dimensional comprehensive gas chromatography/mass spectrometry. *Rapid Commun. Mass Spectrom.* **25**, 1741–1751. Available at: http://doi.wiley.com/10.1002/rcm.5040 [Accessed March 13, 2018].

Rowland S. J., West C. E., Scarlett A. G. and Jones D. (2011b) Identification of individual acids in a commercial sample of naphthenic acids from petroleum by two-dimensional comprehensive gas chromatography/mass spectrometry. *Rapid Commun. Mass Spectrom.* **25**, 1741–1751.

Siddique T., Fedorak P. M. and Foght J. M. (2006) Biodegradation of short-chain n -alkanes in oil sands tailings under methanogenic conditions. **40**, 5459–5464.

Siddique T., Gupta R., Fedorak P. M., Mackinnon M. D. and Foght J. M. (2008) Chemosphere A first approximation kinetic model to predict methane generation from an oil sands tailings settling basin. **72**, 1573–1580.

Siddique T., Penner T., Semple K. and Foght J. M. (2011) Anaerobic biodegradation of longer-chain n -alkanes coupled to methane production in oil sands tailings. , 5892–5899.

Siddique T., Phillip M. and Mackinnon M. D. (2007) Metabolism of BTEX and Naphtha Compounds to Methane in Oil Sands Tailings. **41**, 2350–2356.

Siddique T., Semple K., Li C. and Foght J. M. (2020) Methanogenic biodegradation of iso-alkanes and cycloalkanes during long-term incubation with oil sands tailings. *Environ. Pollut.* **258**, 113768. Available at: https://doi.org/10.1016/j.envpol.2019.113768.

Wardlaw G. D., Arey J. S., Reddy C. M., Nelson R. K., Ventura G. T. and Valentine D. L. (2008) Disentangling oil weathering at a marine seep using GCxGC: Broad metabolic specificity accompanies subsurface petroleum biodegradation. *Environ. Sci. Technol.* **42**, 7166–7173.

Wilde M. J., West C. E., Scarlett A. G., Jones D., Frank R. A., Hewitt L. M. and Rowland S. J. (2015) Bicyclic naphthenic acids in oil sands process water: Identification by comprehensive multidimensional gas chromatography-mass spectrometry. *J. Chromatogr. A* **1378**, 74–87.